OPTICAL BLACK HOLES AND SOLITONS

by

SHAWN MICHAEL WESTMORELAND

B.S., University of Texas, Austin, 2001
M.A., University of Texas, Austin, 2004

AN ABSTRACT OF A DISSERTATION

submitted in partial fulfillment of the
requirements for the degree

DOCTOR OF PHILOSOPHY

Department of Mathematics
College of Arts and Sciences

KANSAS STATE UNIVERSITY
Manhattan, Kansas
2010

Abstract

We exhibit a static, cylindrically symmetric, exact solution to the Euler-Heisenberg field equations (EHFE) and prove that its effective geometry contains (optical) black holes. It is conjectured that there are also soliton solutions to the EHFE which contain black hole geometries.

OPTICAL BLACK HOLES AND SOLITONS

by

Shawn Michael Westmoreland

B.S., University of Texas, Austin, 2001
M.A., University of Texas, Austin, 2004

A DISSERTATION

submitted in partial fulfillment of the
requirements for the degree

DOCTOR OF PHILOSOPHY

Department of Mathematics
College of Arts and Sciences

KANSAS STATE UNIVERSITY
Manhattan, Kansas
2010

Approved by:

Major Professor
Louis Crane

Copyright

Abstract

We exhibit a static, cylindrically symmetric, exact solution to the Euler-Heisenberg field equations (EHFE) and prove that its effective geometry contains (optical) black holes. It is conjectured that there are also soliton solutions to the EHFE which contain black hole geometries.

Table of Contents

List of Figures

List of Tables

Acknowledgments

I thank my advisor Louis Crane for his guidance and for many exploratory conversations which, in particular, lead him to suggest the present topic as a thesis. Working with him has taught me valuable lessons about perseverance and creative thinking in research.

I also wish to thank the following people for their input: Lei Cao, Renaud Gauthier, IkJae Lee, Dany Majard, Charles Moore, Virginia Naibo, James Neill, Larry Weaver, and David Yetter.

Special loving thanks to my mother.

Dedication

I dedicate this thesis in loving memory to my father, Michael Eugene Westmoreland; my brother, John Kamin Stewart; and friends Josh Watson, Chad Hunter, Ricky Valenzuela.

Chapter 1

Introduction and overview

The underlying motivation of the present thesis is the idea of a mathematical connection between solitons and black holes. Connections of this sort have been considered elsewhere, though not in the same context as the present thesis.[1] We will study a particular system of nonlinear PDEs, arising from the Euler-Heisenberg field equations (EHFE), which we conjecture has solutions uniting solitonic and black hole-like properties. The EHFE derive from the Euler-Heisenberg effective Lagrangian for quantum electrodynamics; the solutions that we are interested in are optical black holes.

1.1 Solitons

The theory of solitons arises from the study of wave phenomena in nonlinear PDEs. A soliton is a solitary traveling wave that maintains its shape through time. Of particular importance for us is the nonlinear Schrödinger equation (NSE). In 1-dimension, for a complex wave amplitude $\psi(t, x)$ with coupling constant γ, the NSE has the canonical form (e.g., Sulem and Sulem[2] pp. 5, 20, Drazin and Johnson[3] pp. 34 - 35):

$$i\partial_t\psi + \partial_x^2\psi + \gamma|\psi|^2\psi = 0. \tag{1.1}$$

1.2 General relativity

A *spacetime* is a 4-dimensional pseudo-Riemannian manifold. The key equation in general relativity is the Einstein field equation (EFE), which unfolds to give a system of nonlinear PDEs. Solving these PDEs allows one to express the metric coefficients $g_{\mu\nu}$ of spacetime in terms of the stress-energy tensor $T_{\mu\nu}$. With the cosmological constant Λ included, the EFE reads (Hawking and Ellis[4] p. 74):

$$G_{\mu\nu} + \Lambda g_{\mu\nu} = 8\pi\mathcal{G}T_{\mu\nu}, \tag{1.2}$$

where $\mathcal{G}$ is Newton's gravitational constant and the speed of light is set equal to 1. The Einstein tensor $G_{\mu\nu}$ can be expressed in terms of the Ricci tensor $R_{\mu\nu}$, the scalar $R = R_\mu{}^\mu$, and the metric $g_{\mu\nu}$:

$$G_{\mu\nu} = R_{\mu\nu} - \frac{R}{2}g_{\mu\nu}. \tag{1.3}$$

Among the known exact solutions to (1.2) are those describing black holes.

Definition 1. *A black hole is a region of spacetime where future-directed outgoing null geodesics cannot escape.*

Definition 2. *A white hole is a region of spacetime where future-directed ingoing null geodesics cannot enter.*

Definition 3. *The boundary of a black (or white) hole is called an event horizon.*

We use these definitions even outside the context of general relativity. For us, any pseudo-Riemannian manifold will be called a spacetime whether it satisfies the EFE or not, and one can ask whether or not a given spacetime has black holes.

1.3 The Euler-Heisenberg field equations

Quantum electrodynamics can be approximated as an effective field theory governed by the Euler-Heisenberg Lagrangian (cf. Euler and Heisenberg,[5] Schwinger,[6] Novello[7] p. 292, Boer

and van Holten[8]):

$$L \;=\; -\frac{1}{4}F + \frac{\alpha^2}{90}\left(F^2 + \frac{7}{4}G^2\right), \tag{1.4}$$

where α is the fine structure constant, and F and G are the Poincaré invariants of the electromagnetic field. The speed of light, the reduced Planck constant, the mass of the electron, and the permittivity of free space are here set equal to 1. Applying the principle of least action to (1.4) leads to the Euler-Heisenberg field equation (EHFE):

$$\nabla_\mu F^{\mu\nu} \;=\; \frac{\alpha^2}{45}\nabla_\mu\left(4FF^{\mu\nu} + 7GF^{*\mu\nu}\right). \tag{1.5}$$

Here, $F^{\mu\nu}$ is the electromagnetic field tensor, $F^{*\mu\nu}$ is its dual, and ∇_μ represents the covariant derivative with respect to the coordinate x^μ, using the connection determined by the background spacetime metric. Note that (1.5) is, in general, yet another system of nonlinear PDEs.

According to the Euler-Heisenberg effective field theory, the vacuum behaves like a nonlinear physical medium. Light rays passing through electromagnetic fields are bent as if they were passing through water, thus affecting the apparent geometry of objects. This motivates the idea that the effective field theory can be interpreted geometrically. Indeed, Novello[7] has shown in a seminal work that light rays (small disturbances traveling through the field) follow null geodesics with respect to a spacetime metric $\widetilde{g}_{\mu\nu}$ distinct from the background metric $g_{\mu\nu}$. This is called the effective metric. The inverse (or cometric) $\widetilde{g}^{\mu\nu}$ can be expressed in terms of the stress-energy tensor of the electromagnetic field:

$$\widetilde{g}^{\mu\nu} \;=\; \mathcal{A}g^{\mu\nu} + \mathcal{B}T^{\mu\nu}, \tag{1.6}$$

where $\mathcal{A}$ and $\mathcal{B}$ are special functions of the Poincaré invariants F and G (see Equation (3.57)). This geometrical interpretation of effective field theory demonstrates an analogy between nonlinear optics and general relativity, with Equation (1.6) playing the role of the Einstein field equation (1.2).[7] Let us note two subtleties. (1) The effective metric is uniquely determined only up to a conformal factor. (2) Since light in the nonlinear vacuum

experiences birefringence, a given electromagnetic field actually carries two distinct effective metrics; one for each polarization state.

1.4 The idea

Our main proposal is that the EHFE (1.5) has soliton solutions with a corresponding effective geometry containing a black hole. In this sense, the EHFE would be somewhat in between the NSE (1.1) and the EFE (1.2). We have a theorem and a conjecture:

Theorem 1. *There is an exact static solution to the Euler-Heisenberg field equations where the effective geometries of each polarization state have black holes.*

Conjecture 1. *There is an exact solution to the Euler-Heisenberg field equations which is a soliton and whose effective geometries have black holes.*

The theorem is proven in Section 5.3.1. The soliton of the conjecture is, we believe, an imploding solitonic wave. Evidence for this belief is discussed in the section below. The purist will note that the hypothetical "imploding soliton" cannot strictly be a soliton as a soliton does not change its shape. As the soliton in the conjecture implodes, it will become more concentrated and lose its initial shape. However, in cylindrical coordinates (t, r, θ, z), for a cylindrically symmetric wave approaching the axis $r = 0$, we conjecture that its radial cross section will keep its shape if multiplied by r.

1.5 Evidence for the conjecture

Evidence in support of the conjecture comes from nonlinear optics.[9] In particular, Soljačić and Segev[10] have examined the behavior of a beam resulting from the perpendicular collision of two plane waves in the Euler-Heisenberg vacuum. Using approximations, they determined that the amplitude of the resulting beam satisfies the NSE (1.1). Since an imploding wave can be thought of as a limiting case of infinitely many colliding plane waves, it seems reasonable to expect that the NSE should be obtained in the case of an imploding wave.

In the work of Brodin *et al.*,[11] which nicely complements Soljačić and Segev's paper, a beam guided between two parallel conducting planes is studied. It was found that the amplitude of this beam satisfies a 2-dimensional cylindrically symmetric NSE. According to Brodin *et al.*,[11] for a beam with a certain critical intensity I_c, the dispersive and self-focusing effects exactly balance and the beam forms an optical soliton of constant width. If the intensity I of the beam is less than I_c, then the beam width diffracts without bound. If $I > I_c$, then the beam width collapses to zero in a finite time. These results from nonlinear optics show that there is an authentic link between the EHFE and the NSE, which at least partly supports Conjecture 1.

Another piece of evidence for the conjecture comes from the work of Section 5.2. The Maxwellian approximation, although it is only a first-order approximation to a solution to the EHFE, it gives information on the coordinate velocities of effective geodesics up to second-order (see Theorem 8). When we look at the coordinate velocities of the outgoing geodesics to second-order, we find that they are trapped within a certain radius. (There is a black hole.)

Since Conjecture 1 concerns solutions of a nonlinear variational problem, we suspect that its proof will use tools from Morse theory (i.e., the calculus of variations in the large).

1.6 Organization

This thesis is organized as follows.

Chapter 2 is a pedestrian introduction to the required mathematical physics. Chapter 3 is a self-contained review of Novello's theory of effective geometry. In Chapter 4 (which can be omitted on a first reading), we study the effective geometry of plane waves, and calculate the index of refraction through a plane wave confirming earlier approximations done by others using different methods. In Chapter 5, we use well-known solutions from Maxwell's theory (for imploding cylindrically symmetric waves) and investigate the corresponding effective geometries which resemble black holes. At the end of Chapter 5, we prove Theorem 1 by

explicitly finding an exact solution to the EHFE with the required properties. Although this exact solution is static, it shares some similarities with an ingoing cylindrical wave solution because its Poynting vector points radially inward.

Chapter 2

Preliminaries

The present chapter is meant to be a self-contained pedestrian introduction to the relevant mathematical physics.

2.1 Nonlinearity of the vacuum

According to quantum electrodynamics, photons can scatter off of each other. This photon-photon scattering effect, also known as the nonlinearity of the vacuum, was calculated by Euler and Heisenberg[5] in the mid-1930s, but it is so subtle that no currently available experiment is yet sensitive enough to measure it.

Photon-photon scattering arises from processes that involve virtual electron-positron pairs (see Figure 2.1). In the classical limit, the effect of these virtual particles on real photons can be approximated by introducing nonlinear terms to the Maxwellian Lagrangian. In this so-called effective field theory, the photons do not necessarily follow null geodesics in the background metric. Instead, they follow null geodesics with respect to a so-called effective metric, as will be explained in Chapter 3.

2.2 The background spacetime

In a curved background, according to Drummond and Hathrell,[12] the physical Lagrangian for the effective field theory acquires a nontrivial dependence on the spacetime curvature.

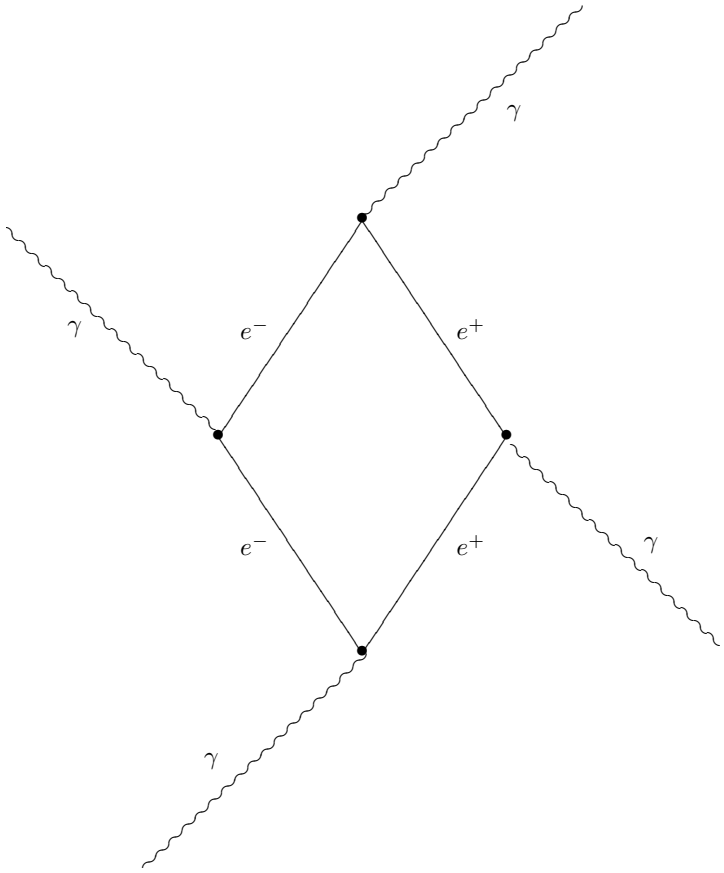

Figure 2.1: *Feynman diagram of photon-photon scattering.*

In the present thesis, we restrict ourselves to a Minkowskian background, so these curvature coupling effects can be ignored.

The background metric tensor is denoted by $g_{\mu\nu}$. Its inverse, the so-called *cometric,* is denoted $g^{\mu\nu}$ and one has that $g^{\mu\lambda}g_{\lambda\nu} = \delta^{\mu}{}_{\nu}$, where $\delta^{\mu}{}_{\nu}$ is the Kronecker delta (and the Einstein summation convention is followed as usual). The present work uses the $+---$ signature convention.

Recall that a given metric determines a unique torsion-free connection ∇ by requiring that the covariant derivative of the metric be zero (e.g. Hawking and Ellis[4] p. 40, or Spivak[13] pp. 236 - 237):

$$\nabla_{\lambda} g_{\mu\nu} = 0. \tag{2.1}$$

The connection coefficients $\Gamma^{\lambda}{}_{\mu\nu}$ (Christoffel symbols) thus determined are given by:

$$\Gamma^{\lambda}{}_{\mu\nu} = \frac{1}{2} g^{\lambda\alpha} \left(\partial_\mu g_{\alpha\nu} + \partial_\nu g_{\alpha\mu} - \partial_\alpha g_{\mu\nu} \right), \tag{2.2}$$

where the operator ∂_μ denotes partial differentiation with respect to the x^μ coordinate. I.e., $\partial_\mu := \partial / \partial x^\mu$.

2.3 Electromagnetic fields

The electromagnetic field $F_{\mu\nu}$ is a closed 2-form, and locally there exists an A-field A_μ such that:

$$F_{\mu\nu} \;\; = \;\; \partial_\mu A_\nu - \partial_\nu A_\mu \quad \left(= \nabla_\mu A_\nu - \nabla_\nu A_\mu \right). \tag{2.3}$$

Note the Bianchi identity:

$$0 = \partial_\lambda F_{\mu\nu} + \partial_\nu F_{\lambda\mu} + \partial_\mu F_{\nu\lambda} = \; (\nabla_\lambda F_{\mu\nu} + \nabla_\nu F_{\lambda\mu} + \nabla_\mu F_{\nu\lambda}). \tag{2.4}$$

The antisymmetrization of an indexed quantity is indicated by placing square brackets around indices. For example, given the tensor $T_{\alpha_1\alpha_2\cdots\alpha_n}$, we can write:

$$T_{[\alpha_1\alpha_2\cdots\alpha_n]} = \frac{1}{n!} \sum_\sigma \mathrm{sgn}(\sigma) T_{\sigma(\alpha_1)\sigma(\alpha_2)\cdots\sigma(\alpha_n)}, \tag{2.5}$$

where the sum is taken over all permutations σ of the indices $\alpha_1, \alpha_2, \cdots, \alpha_n$. The value of $\mathrm{sgn}(\sigma)$ is $+1$ if σ is an even permutation of the sequence $\alpha_1\alpha_2\cdots\alpha_n$ and is -1 if σ is an odd permutation.

Using antisymmetrization, Equation (2.4) can be written as:

$$0 = \partial_{[\lambda} F_{\mu\nu]} \; (= \nabla_{[\lambda} F_{\mu\nu]}). \tag{2.6}$$

The Levi-Civita tensor $\varepsilon_{\alpha\beta\mu\nu}$ is defined such that:

$$\varepsilon_{\alpha\beta\mu\nu} := 4! \sqrt{|g|} \delta^0{}_{[\alpha} \delta^1{}_\beta \delta^2{}_\mu \delta^3{}_{\nu]}, \tag{2.7}$$

where g denotes the determinant of the metric $g_{\mu\nu}$. Note that the value of $\varepsilon_{\alpha\beta\mu\nu}$ is 0 unless the indices α, β, μ, ν are all distinct. Furthermore, note that $\varepsilon_{\alpha\beta\mu\nu}$ is $+\sqrt{|g|}$ if the sequence $\alpha\beta\mu\nu$ is an even permutation of the sequence 0123 and is $-\sqrt{|g|}$ if $\alpha\beta\mu\nu$ is an odd permutation.

The Levi-Civita tensor allows us to express the Hodge dual of $F_{\mu\nu}$ by writing:

$$F^*_{\alpha\beta} := \frac{1}{2}\varepsilon_{\alpha\beta\mu\nu}F^{\mu\nu}. \tag{2.8}$$

Unless otherwise specified (e.g., in Section 3.3), indices are always raised or lowered with respect to the *background* metric. So, e.g., $F^{\mu\nu} = g^{\alpha\mu}g^{\beta\nu}F_{\alpha\beta}$.

Note that the Bianchi identity (2.4) can be expressed in terms of the dual tensor by writing (cf. Landau and Lifshitz[14] p. 67):

$$0 = \partial_\mu F^{*\mu\nu} \ (= \nabla_\mu F^{*\mu\nu}). \tag{2.9}$$

2.4 Effective Lagrangians

The physical behavior of the electromagnetic field is governed by a Lagrangian L which is a scalar function of the field A_μ, its covariant derivatives $\nabla_\mu A_\nu$, and the background metric. The field equations are obtained from the principle of least action:

$$\nabla_\mu \frac{\partial L}{\partial(\nabla_\mu A_\nu)} = \frac{\partial L}{\partial A_\nu}. \tag{2.10}$$

In the case of Maxwell's theory, the Lagrangian in the absence of charges and currents (a field in the vacuum) can be written out as:

$$L \ = \ -\frac{1}{4}g^{\alpha\mu}g^{\beta\nu}\left(\nabla_\mu A_\nu - \nabla_\nu A_\mu\right)\left(\nabla_\alpha A_\beta - \nabla_\beta A_\alpha\right). \tag{2.11}$$

If we define $F := F_{\mu\nu}F^{\mu\nu}$, then Equation (2.11) simplifies to $L = -F/4$. Using (2.10), one recovers the familiar form of Maxwell's equation for the vacuum:

$$\nabla_\mu F^{\mu\nu} = 0. \tag{2.12}$$

The quantity F introduced here is a scalar invariant of the electromagnetic field tensor. In fact, there are only two algebraically independent scalar invariants for $F_{\mu\nu}$. These are represented by the so-called *Poincaré invariants* $F := F_{\mu\nu}F^{\mu\nu}$ and $G := F^{\mu\nu}F^{*}_{\mu\nu}$ (Landau and Lifshitz[14] p. 64).

We define the class of $L(F,G)$-*theories* as electromagnetic theories in which the Lagrangian L can be expressed in terms of the Poincaré scalars F and G alone, i.e., $L = L(F,G)$. It is assumed that the partial derivatives of $L = L(F,G)$, with respect to F and G, exist at least up to second-order, and that they are continuous. We will use the notations $L_F := \partial L/\partial F$, $L_G := \partial L/\partial G$, $L_{FF} := \partial^2 L/\partial F^2$, $L_{GG} := \partial^2 L/\partial G^2$, $L_{FG} := \partial^2 L/(\partial G \partial F)$, etc. We observe that $L(F,G)$-theories are guaranteed to be Lorentz invariant since both F and G are Lorentz invariant quantities. A particularly important $L(F,G)$-theory is the Euler-Heisenberg theory (to be introduced in Section 2.5).

Chapter 3 is primarily concerned not with a particular theory but with general $L(F,G)$-theories. However, in subsequent chapters, attention is restricted to the Euler-Heisenberg theory.

Although effective field theories more elaborate than the $L(F,G)$-type can be constructed by writing Lagrangians that include terms involving the covariant derivatives of the field (e.g., terms like $\nabla_\lambda F^\lambda{}_\nu \nabla_\mu F^{\mu\nu}$),[10] we will not deal with such things in the present work.

2.5 Euler-Heisenberg theory

Euler-Heisenberg theory is an effective field theory which approximates the physical theory of quantum electrodynamics in Minkowski spacetime.

Up to second order in the fine-structure constant α, the *Euler-Heisenberg Lagrangian* is given by (cf. Euler and Heisenberg,[5] Schwinger,[6] Novello[7] p. 292, Boer and van Holten[8]):

$$L = -\frac{1}{4}F + \frac{\alpha^2}{90}\left(F^2 + \frac{7}{4}G^2\right). \tag{2.13}$$

Since we are presently working in natural units, the speed of light c, the reduced Planck constant $\hbar$, the mass of the electron m_e, and the permittivity of free space ϵ_0, are here set

equal to 1. Conventional Lorentz-Heaviside units can be restored by replacing α^2 with $\alpha^2\hbar^3 m_e^{-4} c^{-5}$. (Sometimes we use the letter α as a tensor or pseudotensor index, but no confusion between α as the fine-structure constant and α as an index should arise because the context will make the meaning of α clear.)

Equation (2.13) applies to fields having strength A and frequency ω such that:[5]

$$A \ll \frac{1}{\sqrt{4\pi\alpha}} \tag{2.14}$$

$$\omega \ll 1. \tag{2.15}$$

In other words, the field strength should be much weaker than the critical field $1/\sqrt{4\pi\alpha}$ and it should be approximately constant on scales much less than the Compton wavelength of the electron (which is unity, in our units). In the present work however, we will not worry about these physical restrictions (2.14) and (2.15).

2.6 Field equations

Theorem 2. *For a Lagrangian of type $L = L(F, G)$, the principle of least action (2.10) yields the field equations:*

$$\nabla_\mu \left(L_F F^{\mu\nu} + L_G F^{*\mu\nu} \right) = 0. \tag{2.16}$$

Proof. For a Lagrangian of type $L = L(F, G)$, we get that $\partial L / \partial A_\nu = 0$. So Equation (2.10) reduces to

$$\nabla_\mu \frac{\partial L}{\partial(\nabla_\mu A_\nu)} = 0. \tag{2.17}$$

We get that:

$$\frac{\partial L}{\partial(\nabla_\mu A_\nu)} = L_F \frac{\partial F}{\partial(\nabla_\mu A_\nu)} + L_G \frac{\partial G}{\partial(\nabla_\mu A_\nu)}. \tag{2.18}$$

because:

$$\frac{\partial F}{\partial(\nabla_\mu A_\nu)} = 4F^{\mu\nu}, \tag{2.19}$$

and:

$$\frac{\partial G}{\partial(\nabla_\mu A_\nu)} = 4F^{*\mu\nu}. \tag{2.20}$$

When an index μ is free and not to be summed over by the Einstein convention, we draw a bar over it:

$$\begin{aligned}
\frac{\partial F}{\partial(\nabla_{\bar\mu} A_{\bar\nu})} &= \frac{\partial}{\partial(\nabla_{\bar\mu} A_{\bar\nu})}\left(F_{\alpha\beta}F^{\alpha\beta}\right) \\
&= \frac{\partial}{\partial(\nabla_{\bar\mu} A_{\bar\nu})}\left(g^{\alpha\lambda}g^{\beta\rho}F_{\alpha\beta}F_{\lambda\rho}\right) \\
&= \frac{\partial}{\partial(\nabla_{\bar\mu} A_{\bar\nu})}\left(g^{\alpha\lambda}g^{\beta\rho}\left(\nabla_\alpha A_\beta - \nabla_\beta A_\alpha\right)\left(\nabla_\lambda A_\rho - \nabla_\rho A_\lambda\right)\right) \\
&= \frac{\partial}{\partial(\nabla_{\bar\mu} A_{\bar\nu})}\Big(g^{\bar\mu\lambda}g^{\bar\nu\rho}\left(\nabla_{\bar\mu} A_{\bar\nu} - \nabla_{\bar\nu} A_{\bar\mu}\right)\left(\nabla_\lambda A_\rho - \nabla_\rho A_\lambda\right) \\
&\qquad + g^{\bar\nu\lambda}g^{\bar\mu\rho}\left(\nabla_{\bar\nu} A_{\bar\mu} - \nabla_{\bar\mu} A_{\bar\nu}\right)\left(\nabla_\lambda A_\rho - \nabla_\rho A_\lambda\right) \\
&\qquad + g^{\alpha\bar\mu}g^{\beta\bar\nu}\left(\nabla_\alpha A_\beta - \nabla_\beta A_\alpha\right)\left(\nabla_{\bar\mu} A_{\bar\nu} - \nabla_{\bar\nu} A_{\bar\mu}\right) \\
&\qquad + g^{\alpha\bar\nu}g^{\beta\bar\mu}\left(\nabla_\alpha A_\beta - \nabla_\beta A_\alpha\right)\left(\nabla_{\bar\nu} A_{\bar\mu} - \nabla_{\bar\mu} A_{\bar\nu}\right)\Big) \\
&= g^{\bar\mu\lambda}g^{\bar\nu\rho}\left(\nabla_\lambda A_\rho - \nabla_\rho A_\lambda\right) \\
&\quad - g^{\bar\nu\lambda}g^{\bar\mu\rho}\left(\nabla_\lambda A_\rho - \nabla_\rho A_\lambda\right) \\
&\quad + g^{\alpha\bar\mu}g^{\beta\bar\nu}\left(\nabla_\alpha A_\beta - \nabla_\beta A_\alpha\right) \\
&\quad + g^{\alpha\bar\nu}g^{\beta\bar\mu}\left(\nabla_\alpha A_\beta - \nabla_\beta A_\alpha\right) \\
&= F^{\bar\mu\bar\nu} - F^{\bar\nu\bar\mu} + F^{\bar\mu\bar\nu} - F^{\bar\nu\bar\mu} \\
&= 4F^{\bar\mu\bar\nu}.
\end{aligned}$$

Equation (2.20) can be established similarly.

The result (2.16) follows from Equations (2.18) - (2.20). □

Specializing (2.16) to the Euler-Heisenberg Lagrangian (2.13), we get the Euler-Heisenberg field equations:

$$\nabla_\mu F^{\mu\nu} = \frac{\alpha^2}{45}\nabla_\mu\left(4FF^{\mu\nu} + 7GF^{*\mu\nu}\right). \tag{2.21}$$

For an arbitrary $L(F,G)$-theory, Equation (2.16) implies:

$$\begin{aligned} 0 &= \nabla_\mu \left(L_F F^{\mu\nu}\right) + \nabla_\mu \left(L_G F^{*\mu\nu}\right) \\ &= \left(L_{FF}\nabla_\mu F + L_{FG}\nabla_\mu G\right) F^{\mu\nu} + L_F \nabla_\mu F^{\mu\nu} \\ &\quad + \left(L_{FG}\nabla_\mu F + L_{GG}\nabla_\mu G\right) F^{*\mu\nu} + L_G \underbrace{\nabla_\mu F^{*\mu\nu}}_{zero}. \end{aligned} \tag{2.22}$$

The last term is zero by the Bianchi identity (2.9). By computation, one notes that $\nabla_\mu F = 2F^{\alpha\beta}\nabla_\mu F_{\alpha\beta}$ and $\nabla_\mu G = 2F^{*\alpha\beta}\nabla_\mu F_{\alpha\beta}$. Hence, if we define the tensor:[15]

$$Q^{\alpha\beta\mu\nu} := L_{FF}F^{\alpha\beta}F^{\mu\nu} + L_{FG}\left(F^{\alpha\beta}F^{*\mu\nu} + F^{*\alpha\beta}F^{\mu\nu}\right) + L_{GG}F^{*\alpha\beta}F^{*\mu\nu}, \tag{2.23}$$

then we can rewrite the field equations (2.16) as:

$$L_F \nabla_\mu F^{\mu\nu} + 2Q^{\alpha\beta\mu\nu}\nabla_\mu F_{\alpha\beta} = 0. \tag{2.24}$$

Assuming $L_F \neq 0$, Equation (2.24) can be rearranged:

$$\nabla_\mu F^{\mu\nu} = -\frac{2}{L_F} Q^{\alpha\beta\mu\nu}\nabla_\mu F_{\alpha\beta}. \tag{2.25}$$

(The case $L_F = 0$ is discarded since it is not physically interesting.)

2.7 Stress-energy tensor

Given a Lagrangian L, one can define a stress-energy tensor $T_{\mu\nu}$ through the equation:

$$T_{\mu\nu} := 2\frac{\partial L}{\partial g^{\mu\nu}} - L g_{\mu\nu}. \tag{2.26}$$

This expression for the stress-energy tensor is implicit in e.g. Novello[7] pp. 271, 275, Landau and Lifshitz[14] p. 77, Hawking and Ellis[4] p. 66, and Poisson[16] p. 125. Observe that different authors disagree on the overall sign on $T_{\mu\nu}$ due to differing signature conventions for the metric.

For a Lagrangian of the form $L = L(F,G)$, Equation (2.26) gives:

$$\begin{aligned} T_{\mu\nu} &= 2\left(L_F\frac{\partial F}{\partial g^{\mu\nu}} + L_G\frac{\partial G}{\partial g^{\mu\nu}}\right) - L g_{\mu\nu} \\ &= -4L_F F_\mu{}^\alpha F_{\alpha\nu} - 4L_G F_\mu{}^\alpha F^*_{\alpha\nu} - L g_{\mu\nu}. \end{aligned} \tag{2.27}$$

Using the well-known identity $4F_{\mu}{}^{\alpha}F^{*}_{\alpha\nu} = -Gg_{\mu\nu}$ (cf. Novello[7] p. 272), we get (in agreement with Novello[7] p. 275):

$$T_{\mu\nu} = -4L_F F_{\mu}{}^{\alpha} F_{\alpha\nu} - (L - GL_G)g_{\mu\nu}. \tag{2.28}$$

Chapter 3

Effective geometries

The purpose of this chapter is to give a quick self-contained review of Novello's theory of effective geometries in nonlinear electrodynamics.[7,15,17–19] Our exposition is informed by the existing literature, most notably the work of Novello.[7] However, we do not follow any specific work too closely.

3.1 Electromagnetic shock waves

The *wave front* of an electromagnetic shock wave is defined by a hypersurface Σ across which the field derivatives are discontinuous. Given a set of local coordinates x^μ for the (background) spacetime manifold, this hypersurface Σ can be described as the set of solutions to the equation:

$$z(x^\mu) = 0. \tag{3.1}$$

We will need to assume that the first-order partial derivatives of $z(x^\mu)$ exist and are continuous on Σ, and that the gradient $k_\mu := \partial_\mu z$ does not vanish on Σ. The hypersurface Σ, at least locally, splits the manifold into two regions $\mathfrak{M}^+ := \{x^\mu : \ z(x^\mu) > 0\}$ and $\mathfrak{M}^- := \{x^\mu : \ z(x^\mu) < 0\}$.

The jump of an arbitrary function J through Σ is denoted by the *Hadamard bracket* $[J]_\Sigma$. For each point p of Σ, we define:

$$[J]_\Sigma(p) := \lim_{p^+ \to p} J(p^+) - \lim_{p^- \to p} J(p^-), \tag{3.2}$$

where the points p^+ and p^-, which tend towards p, belong to the regions $\mathfrak{M}^+$ and $\mathfrak{M}^-$ respectively (Papapetrou[20] p. 170). Note that if J is continuous across Σ, then $[J]_\Sigma = 0$. The converse is not strictly true, since it is possible to have a function with a so-called *simple discontinuity* whereby $\lim_{p^+ \to p} J(p^+) = \lim_{p^- \to p} J(p^-) \neq J(p)$. On the other hand, the derivative of a function can be discontinuous but the discontinuity is never of the simple type (Rudin[21] p. 109). In light of this, a partial derivative $\partial_\mu J$ is discontinuous across Σ if and only if $[\partial_\mu J]_\Sigma \neq 0$.

Since Σ is the front of an electromagnetic shock wave, the electromagnetic field is continuous across Σ but some of its derivatives are discontinuous across Σ. We express this by writing:

$$[F_{\mu\nu}]_\Sigma = 0, \tag{3.3}$$

and:

$$[\nabla_\lambda F_{\mu\nu}]_\Sigma \neq 0 \text{ for some } \lambda, \mu, \nu. \tag{3.4}$$

Similar conditions hold for the dual tensor $F^*_{\mu\nu}$.

Note that since the field $F_{\mu\nu}$ and the Christoffel symbols $\Gamma^\lambda_{\mu\nu}$ are continuous, we have:

$$[\nabla_\lambda F_{\mu\nu}]_\Sigma \;=\; [\partial_\lambda F_{\mu\nu}]_\Sigma. \tag{3.5}$$

Now consider a second coordinate system $\{x^{\breve{\mu}}\}$ such that $x^{\breve{0}} = z(x^\mu)$ (cf. Papapetrou[20] p. 171). Then Σ can be described by the equation $x^{\breve{0}} = 0$. Moreover, since $z(x^\mu)$ has continuous first-order partial derivatives, we get that:

$$\begin{aligned}
[\partial_\lambda F_{\mu\nu}]_\Sigma &= \left[(\partial_{\breve{0}} F_{\mu\nu})\frac{\partial x^{\breve{0}}}{\partial x^\lambda}\right]_\Sigma \\
&= [(\partial_{\breve{0}} F_{\mu\nu})\partial_\lambda z]_\Sigma \\
&= [\partial_{\breve{0}} F_{\mu\nu}]_\Sigma \cdot \partial_\lambda z \\
&= f_{\mu\nu} k_\lambda,
\end{aligned} \tag{3.6}$$

where $f_{\mu\nu} := [\partial_{\breve{0}} F_{\mu\nu}]_\Sigma$ is the so-called *discontinuity* or *disturbance* in the field, and the 1-form $k_\lambda := \partial_\lambda z$ is called the *propagation vector*. It is required that k_λ be nonzero.

Theorem 3. *The quantity $f_{\mu\nu}$ is a tensor. Moreover, it is a 2-form.*

Proof. We verify that if we go to another coordinate system $\{x^{\mu'}\}$, then the quantity $f_{\mu\nu}$ transforms as a tensor should.

$$\begin{aligned}
f_{\mu'\nu'} &= [\partial_{\check{0}} F_{\mu'\nu'}]_\Sigma \\
&= \left[\partial_{\check{0}} \left(F_{\mu\nu} \frac{\partial x^\mu}{\partial x^{\mu'}} \frac{\partial x^\nu}{\partial x^{\nu'}} \right)\right]_\Sigma \\
&= \left[(\partial_{\check{0}} F_{\mu\nu}) \frac{\partial x^\mu}{\partial x^{\mu'}} \frac{\partial x^\nu}{\partial x^{\nu'}} + F_{\mu\nu} \partial_{\check{0}} \left(\frac{\partial x^\mu}{\partial x^{\mu'}} \frac{\partial x^\nu}{\partial x^{\nu'}} \right)\right]_\Sigma \\
&= \left[(\partial_{\check{0}} F_{\mu\nu}) \frac{\partial x^\mu}{\partial x^{\mu'}} \frac{\partial x^\nu}{\partial x^{\nu'}}\right]_\Sigma + \left[\underbrace{F_{\mu\nu} \partial_{\check{0}} \left(\frac{\partial x^\mu}{\partial x^{\mu'}} \frac{\partial x^\nu}{\partial x^{\nu'}} \right)}_{\text{continuous}}\right]_\Sigma \\
&= [(\partial_{\check{0}} F_{\mu\nu})]_\Sigma \left(\frac{\partial x^\mu}{\partial x^{\mu'}} \frac{\partial x^\nu}{\partial x^{\nu'}} \right) \\
&= f_{\mu\nu} \frac{\partial x^\mu}{\partial x^{\mu'}} \frac{\partial x^\nu}{\partial x^{\nu'}}.
\end{aligned} \tag{3.7}$$

Moreover, $f_{\mu\nu}$ is a 2-form since $f_{\mu\nu} = -f_{\nu\mu}$. (Note that the above underlined "continuous" term is continuous since the background spacetime, which is Minkowskian, is C^2.) □

Note that for the dual $F^*_{\mu\nu}$ we write, in analogy with Equation (3.6):

$$[\partial_\lambda F^*_{\mu\nu}]_\Sigma = f^*_{\mu\nu} k_\lambda, \tag{3.8}$$

where $f^*_{\mu\nu} := [\partial_{0'} F^*_{\mu\nu}]_\Sigma$ is the discontinuity of the dual field. Analogously to the relation $F^*_{\alpha\beta} = \frac{1}{2}\varepsilon_{\alpha\beta\mu\nu} F^{\mu\nu}$, one has:

$$f^*_{\alpha\beta} = \frac{1}{2}\varepsilon_{\alpha\beta\mu\nu} f^{\mu\nu}. \tag{3.9}$$

Moreover:

$$[\partial_\lambda F^{\mu\nu}]_\Sigma = f^{\mu\nu} k_\lambda, \tag{3.10}$$

and:

$$[\partial_\lambda F^{*\mu\nu}]_\Sigma = f^{*\mu\nu} k_\lambda. \tag{3.11}$$

3.2 Dispersion laws and polarization

In nonlinear field theory, field discontinuities (or *photons*, in a classical corpuscular sense) can exhibit birefringent behavior.[7,15,17] This means that the way a photon propagates through the field depends on its polarization state. Whether a theory predicts birefringence or not depends on the Lagrangrian used. For example, in Born-Infeld electrodynamics, there is no birefringence (see e.g. Novello[7] p. 276). In the Euler-Heisenberg theory however, there is.

The goal of the present section is to derive the dispersion laws for $L(F, G)$-theories. We begin with the following observation:

Theorem 4. *Locally, there exists a 1-form p_μ such that $f_{\mu\nu} = p_\mu k_\nu - p_\nu k_\mu$.*

Proof. Applying the Hadamard bracket to both sides of Equation (2.9) gives:

$$f^{*\mu\nu} k_\mu = 0, \tag{3.12}$$

which implies that $\det(f^{*\mu\nu}) = -|g|^{-1/2} \det(f_{\mu\nu}) = 0$. Since we are in four dimensions, it follows that $f_{\mu\nu}$ is simple (e.g., Penrose and Rindler[22] p. 166). That is, locally there exist 1-forms u_μ and v_μ such that:

$$f_{\mu\nu} = u_{[\mu} v_{\nu]} = \frac{1}{2}(u_\mu v_\nu - u_\nu v_\mu). \tag{3.13}$$

Taking the Hadamard bracket of the Bianchi identity (2.4) gives:

$$f_{[\mu\nu} k_{\lambda]} = 0. \tag{3.14}$$

Equations (3.13) and (3.14) imply that the triple wedge product of u_μ, v_ν and k_λ vanishes. Hence u_μ, v_ν and k_λ must be linearly dependent (e.g., Madsen and Tornehave[23] pp. 11 - 12) and so locally there exists a 1-form p_μ for which we have the decomposition:

$$f_{\mu\nu} = p_\mu k_\nu - p_\nu k_\mu. \tag{3.15}$$

□

Theorem 4/Equation (3.15) says that the field discontinuity $f_{\mu\nu}$ (or *photon*, as we are apt to call it) is the wedge product of the propagation vector k_μ together with p_μ. Without loss of generality we can assume that p_μ is orthogonal to k_μ and thereby interpret p_μ as being the (non-normalized) polarization vector (actually a 1-form) for the photon.

Let us take the Hadamard bracket of both sides of Equation (2.24). After a bit of rearranging, one gets that:

$$L_F g^{\lambda\nu} f_{\mu\nu} k_\lambda = -2Q_\mu{}^{\nu\alpha\beta} f_{\alpha\beta} k_\nu. \tag{3.16}$$

Substituting (3.15) into (3.16), and using the assumption that p_μ is orthogonal to k_μ, it follows that:

$$L_F k^2 p_\mu = -4Q_\mu{}^{\alpha\nu\beta} k_\alpha k_\beta p_\nu, \tag{3.17}$$

where $k^2 := g^{\mu\nu} k_\mu k_\nu$. Assuming $L_F \neq 0$, we can write:

$$k^2 p_\mu = -\frac{4}{L_F} Q_\mu{}^{\alpha\nu\beta} k_\alpha k_\beta p_\nu. \tag{3.18}$$

For convenience, define the tensor (cf. De Lorenci *et al.*[15]):

$$S^{\mu\nu} := k^2 g^{\mu\nu} + \frac{4}{L_F} Q^{\mu\alpha\nu\beta} k_\alpha k_\beta. \tag{3.19}$$

Then Equation (3.18) can be expressed as:

$$S^\mu{}_\nu p_\mu = 0. \tag{3.20}$$

If $k^2 \neq 0$, Equation (3.18) implies that p_μ can be expressed as a linear combination of $h_\mu := F_\mu{}^\lambda k_\lambda$ and $h^*_\mu := F^{*\lambda}_\mu k_\lambda$. (Note that both h_μ and h^*_μ are orthogonal to k_μ: since $F^{\mu\nu}$ and $F^{*\mu\nu}$ are skew-symmetric we get that $h^\mu k_\mu = F^{\mu\lambda} k_\lambda k_\mu = 0$ and $h^{*\mu} k_\mu = F^{*\mu\nu} k_\lambda k_\mu = 0$.)

Writing:

$$p_\mu = a h_\mu + b h^*_\mu. \tag{3.21}$$

We get that:

$$S^\mu{}_\nu h_\mu = \frac{4}{L_F} \left(\left(\frac{L_F k^2}{4} + L_{FF} h^2 + L_{FG} h^\alpha h^*_\alpha \right) h_\nu + \left(L_{GG} h^\alpha h^*_\alpha + L_{FG} h^2 \right) h^*_\nu \right), \tag{3.22}$$

and

$$S^{\mu}{}_{\nu}h^{*}_{\mu} = \frac{4}{L_F}\left(\left(L_{FF}h^{\alpha}h^{*}_{\alpha} + L_{FG}h^{*\alpha}h^{*}_{\alpha}\right)h_{\nu} + \left(\frac{L_F k^2}{4} + L_{GG}h^{*\alpha}h^{*}_{\alpha} + L_{FG}h^{\alpha}h^{*}_{\alpha}\right)h^{*}_{\nu}\right). \quad (3.23)$$

Equations (3.22) and (3.23) can be recast into a somewhat more useful form by exploiting the well-known identities (cf. Novello[7] p. 272):

$$F^{\nu}{}_{\lambda}F^{*\mu\lambda} = \frac{1}{4}G g^{\mu\nu}, \quad (3.24)$$

and:

$$F^{*\mu}{}_{\alpha}F^{*\alpha\nu} - F^{\mu}{}_{\alpha}F^{\alpha\nu} = \frac{1}{2}F g^{\mu\nu}. \quad (3.25)$$

For (3.24) and (3.25) respectively, contracting both sides with $k_\mu k_\nu$ gives:

$$h^{\alpha}h^{*}_{\alpha} = \frac{1}{4}G k^2, \quad (3.26)$$

and:

$$-h^{*\alpha}h^{*}_{\alpha} + h^2 = \frac{1}{2}F k^2. \quad (3.27)$$

Using (3.26) and (3.27), Equations (3.22) and (3.23) become:

$$S^{\mu}{}_{\nu}h_{\mu} = \frac{4}{L_F}\left(\left(\left(\frac{L_F}{4} + \frac{1}{4}GL_{FG}\right)k^2 + L_{FF}h^2\right)h_{\nu} + \left(\frac{1}{4}GL_{GG}k^2 + L_{FG}h^2\right)h^{*}_{\nu}\right), \quad (3.28)$$

and:

$$\begin{aligned} S^{\mu}{}_{\nu}h^{*}_{\mu} \;=\; & \frac{4}{L_F}\left(\left(\left(\frac{1}{4}GL_{FF} - \frac{1}{2}FL_{FG}\right)k^2 + L_{FG}h^2\right)h_{\nu}\right. \\ & \left. + \left(\left(\frac{L_F}{4} - \frac{1}{2}FL_{GG} + \frac{1}{4}GL_{FG}\right)k^2 + L_{GG}h^2\right)h^{*}_{\nu}\right). \end{aligned} \quad (3.29)$$

Equations (3.20), (3.21), (3.28), and (3.29) give:

$$\begin{aligned} 0 \;=\; & \left(a\left(\left(\frac{L_F}{4} + \frac{1}{4}GL_{FG}\right)k^2 + L_{FF}h^2\right) + b\left(\left(\frac{1}{4}GL_{FF} - \frac{1}{2}FL_{FG}\right)k^2 + L_{FG}h^2\right)\right)h_{\nu} \\ & + \left(a\left(\frac{1}{4}GL_{GG}k^2 + L_{FG}h^2\right) + b\left(\left(\frac{L_F}{4} - \frac{1}{2}FL_{GG} + \frac{1}{4}GL_{FG}\right)k^2 + L_{GG}h^2\right)\right)h^{*}_{\nu}. \end{aligned} \quad (3.30)$$

First we consider the case where h_ν and h^*_ν are linearly independent. In this case, we have the following linear system in the variables a and b:

$$\begin{cases} a\left(\left(\frac{L_F}{4}+\frac{1}{4}GL_{FG}\right)k^2+L_{FF}h^2\right)+b\left(\left(\frac{1}{4}GL_{FF}-\frac{1}{2}FL_{FG}\right)k^2+L_{FG}h^2\right)=0 \\ a\left(\frac{1}{4}GL_{GG}k^2+L_{FG}h^2\right)+b\left(\left(\frac{L_F}{4}-\frac{1}{2}FL_{GG}+\frac{1}{4}GL_{FG}\right)k^2+L_{GG}h^2\right)=0. \end{cases} \tag{3.31}$$

The determinant of this system has to be zero (there is a nontrivial solution for a and b because the polarization vector $p_\mu = ah_\mu + bh^*_\mu$ is nonzero). Thus:

$$\begin{aligned} &\left(\left(\frac{L_F}{4}+\frac{1}{4}GL_{FG}\right)k^2+L_{FF}h^2\right)\left(\left(\frac{L_F}{4}-\frac{1}{2}FL_{GG}+\frac{1}{4}GL_{FG}\right)k^2+L_{GG}h^2\right) \\ &\qquad=\left(\left(\frac{1}{4}GL_{FF}-\frac{1}{2}FL_{FG}\right)k^2+L_{FG}h^2\right)\left(\frac{1}{4}GL_{GG}k^2+L_{FG}h^2\right). \end{aligned} \tag{3.32}$$

In the case where h_μ and h^*_μ are linearly dependent, it follows that $S^\mu{}_\nu h_\mu = S^\mu{}_\nu h^*{}_\mu = 0$ since $p_\mu = ah_\mu + bh^*{}_\mu$ and $S^\mu{}_\nu p_\mu = 0$. We thereby obtain the system:

$$\begin{cases} \left(\left(\frac{L_F}{4}+\frac{1}{4}GL_{FG}\right)k^2+L_{FF}h^2\right)h_\nu+\left(\frac{1}{4}GL_{GG}k^2+L_{FG}h^2\right)h^*_\nu=0 \\ \left(\left(\frac{1}{4}GL_{FF}-\frac{1}{2}FL_{FG}\right)k^2+L_{FG}h^2\right)h_\nu+\left(\left(\frac{L_F}{4}-\frac{1}{2}FL_{GG}+\frac{1}{4}GL_{FG}\right)k^2+L_{GG}h^2\right)h^*_\nu=0. \end{cases} \tag{3.33}$$

Since we require at least one component of h_μ or h^*_μ to be nonzero ($p_\mu = ah_\mu + bh^*_\mu$ is nonzero), Equation (3.32) holds even if h_μ and h^*_μ are linearly dependent.

Expanding the products and combining like terms, Equation (3.32) can be put in the form:

$$\Lambda_1 k^4 + \Lambda_2 h^2 k^2 + \Lambda_3 h^4 = 0, \tag{3.34}$$

where we define:

$$\Lambda_1 := (L_F + GL_{FG})^2 - L_{GG}(2FL_F + G^2 L_{FF}), \tag{3.35}$$

$$\Lambda_2 := 4\left(L_F(L_{FF}+L_{GG}) + 2F(L^2_{FG} - L_{FF}L_{GG})\right), \tag{3.36}$$

$$\Lambda_3 := 16(L_{FF}L_{GG} - L^2_{FG}). \tag{3.37}$$

We now have the following result:

Theorem 5. *Assuming that* $L_F \neq 0$, $k^2 \neq 0$, $\Lambda_1 \neq 0$ *and* $\Lambda_2^2 - 4\Lambda_1\Lambda_3 \geq 0$ *(in order to ensure that Equation (3.34) gives real solutions for* k^2*), we have the dispersion law(s):*[24]

$$k^2 = \Lambda_\pm h^2, \tag{3.38}$$

where:

$$\Lambda_\pm := \frac{-\Lambda_2 \pm \sqrt{(\Lambda_2)^2 - 4\Lambda_1\Lambda_3}}{2\Lambda_1}. \tag{3.39}$$

Next, we will show that Equation (3.38) continues to hold even if $k^2 = 0$. More precisely:

Theorem 6. *If* $k^2 = 0$ *and* $L_{FF}L_{GG} - L_{FG}^2 \neq 0$, *then* $h^2 = 0$.
(Note that with the Euler-Heisenberg Lagrangian (2.13), we have $L_{FF}L_{GG} - L_{FG}^2 \neq 0$.)

Proof. For an indirect proof, suppose that $k^2 = 0$ and $h^2 \neq 0$. Note that when $k^2 = 0$, Equations (3.26) and (3.27) give $h^\alpha h^*_\alpha = 0$ and $h^{*\alpha}h^*_\alpha = h^2$. Note that h_μ cannot be timelike because otherwise h^*_μ would also be timelike and one cannot have two orthogonal timelike vectors in Minkowski spacetime. The only remaining possibility is that h_μ (and consequently h^*_μ) is spacelike. We show that this implies $L_{FF}L_{GG} - L_{FG}^2 = 0$.

To this end, note that with $k^2 = 0$, Equation (3.17) becomes:

$$\begin{aligned} 0 &= Q^{\mu\alpha\nu\beta}k_\alpha k_\beta p_\nu \\ &= L_{FF}h^\mu\left(h^\nu p_\nu\right) + L_{FG}\left(h^\mu\left(h^{*\nu}p_\nu\right) + h^{*\mu}\left(h^\nu p_\nu\right)\right) + L_{GG}h^{*\mu}\left(h^{*\nu}p_\nu\right). \end{aligned} \tag{3.40}$$

Contracting (3.40) with h_μ and $h^*{}_\mu$ respectively, and using the relations $h^{*\alpha}h^*_\alpha = h^2 \neq 0$ and $h^\alpha h^*_\alpha = 0$, it follows that:

$$\begin{cases} L_{FF}\left(h^\nu p_\nu\right) + L_{FG}\left(h^{*\nu}p_\nu\right) = 0 \\ L_{FG}\left(h^\nu p_\nu\right) + L_{GG}\left(h^{*\nu}p_\nu\right) = 0. \end{cases} \tag{3.41}$$

We claim that $h^\nu p_\nu$ and $h^{*\nu}p_\nu$ cannot simultaneously be zero. To establish this claim, note that since k_μ is null, and since p_μ is orthogonal (and not parallel) to k_μ, it must be that p_μ is spacelike. So if $h^\nu p_\nu$ and $h^{*\nu}p_\nu$ were both simultaneously zero, we would have an orthogonal

basis consisting of three spacelike 1-forms h_μ, h^*_μ, p_μ and a null 1-form k_μ, which is not possible.

Consequently, the system (3.41) has a nontrivial solution for $h^\nu p_\nu$ and $h^{*\nu} p_\nu$, and so it must have a vanishing determinant: $L_{FF}L_{GG} - L_{FG}^2 = 0$. □

Now, according to Theorem 5, there can be two possible values of k^2. This has to do with the fact that a given photon (field disturbance) is in one of two polarization states. To understand why this is true, note that (as explained in e.g., De Lorenci *et al.*[15]) for each possible value of k^2 there corresponds a certain solution space for the unknowns a and b in the system (3.31), and $p_\mu = ah_\mu + bh^*_\mu$. (Here we identify the solution space of a and b with the "polarization state.")

By defining:

$$\Omega_\pm := -\frac{4L_{FF} + (L_F + GL_{FG})\Lambda_\pm}{4L_{FG} + GL_{GG}\Lambda_\pm}, \tag{3.42}$$

Equation (3.38) becomes:

$$k^2 = -4\left(\frac{L_{FF} + L_{FG}\Omega_\pm}{L_F + (L_{FG} + L_{GG}\Omega_\pm)G}\right)h^2, \tag{3.43}$$

which matches Equation (24) in De Lorenci *et al.*[15]

We note that with the Euler-Heisenberg Lagrangian (2.13), Equation (3.39) reads:

$$\Lambda_\pm = \frac{224\alpha^2}{495 + 12F\alpha^2 \mp \sqrt{18225 - 18360F\alpha^2 + 4624F^2\alpha^4 + 3136G^2\alpha^4}}. \tag{3.44}$$

3.3 Effective null geodesics

The dispersion laws in nonlinear electrodynamics have an appealing geometric interpretation, where they are thought of as light cone conditions in a so-called *effective geometry*. Using the fact that $h^2 = -F^\mu{}_\alpha F^{\alpha\nu} k_\mu k_\nu$, we can write Equation (3.38) in the form:

$$\left(g^{\mu\nu} + \Lambda_\pm F^\mu{}_\alpha F^{\alpha\nu}\right) k_\mu k_\nu = 0. \tag{3.45}$$

Provided that the symmetric tensor $\widetilde{g}^{\mu\nu}$ defined by:

$$\widetilde{g}^{\mu\nu} := g^{\mu\nu} + \Lambda_{\pm} F^{\mu}{}_{\alpha} F^{\alpha\nu}, \tag{3.46}$$

is nonsingular, an *effective metric* $\widetilde{g}_{\mu\nu}$ can be defined such that $\widetilde{g}^{\mu\lambda}\widetilde{g}_{\lambda\nu} = \delta^{\mu}{}_{\nu}$. We get the *effective geometry* by treating $\widetilde{g}_{\mu\nu}$ as if it were the metric for spacetime.

We can think of k_{μ} as being null with respect to the effective metric since:

$$\widetilde{g}^{\mu\nu} k_{\mu} k_{\nu} = 0. \tag{3.47}$$

Moreover, the integral curves of k_{μ} (i.e., *photon worldlines*) turn out to be geodesics with respect to the effective metric:

Theorem 7. *The integral curves of k_{μ} are null geodesics with respect to the effective metric.*

Proof. The proof is given in Novello[7] pp. 273 - 274. We repeat it in order to be self-contained. The first step is to take the partial derivative of Equation (3.47) to get:

$$2(\partial_{\lambda} k_{\mu}) k_{\nu} \widetilde{g}^{\mu\nu} + k_{\mu} k_{\nu} \partial_{\lambda} \widetilde{g}^{\mu\nu} = 0. \tag{3.48}$$

Next, exploit the fact that the effective metric $\widetilde{g}^{\mu\nu}$, provided it is nonsingular, determines a set of torsion-free connection coefficients $\widetilde{\Gamma}^{\lambda}{}_{\mu\nu}$ (through the usual Christoffel formulae, i.e., Equation (2.2)) and thereby determines a covariant differential operator $\widetilde{\nabla}_{\lambda}$ such that:

$$\widetilde{\nabla}_{\lambda} \widetilde{g}^{\mu\nu} = \partial_{\lambda} \widetilde{g}^{\mu\nu} + \widetilde{\Gamma}^{\mu}{}_{\alpha\lambda} \widetilde{g}^{\alpha\nu} + \widetilde{\Gamma}^{\nu}{}_{\alpha\lambda} \widetilde{g}^{\alpha\mu} = 0. \tag{3.49}$$

Contracting Equation (3.49) with $k_{\mu} k_{\nu}$ one gets:

$$k_{\mu} k_{\nu} \partial_{\lambda} \widetilde{g}^{\mu\nu} = -2 k_{\mu} k_{\nu} \widetilde{\Gamma}^{\mu}{}_{\alpha\lambda} \widetilde{g}^{\alpha\nu}. \tag{3.50}$$

By substituting (3.50) into Equation (3.48), it follows that:

$$\begin{aligned} \widetilde{g}^{\mu\nu} \left(\widetilde{\nabla}_{\lambda} k_{\mu} \right) k_{\nu} &:= \widetilde{g}^{\mu\nu} \left(\partial_{\lambda} k_{\mu} - \widetilde{\Gamma}^{\alpha}{}_{\mu\lambda} k_{\alpha} \right) k_{\nu} \\ &= 0. \end{aligned} \tag{3.51}$$

Since $k_\mu := \partial_\mu z$, and since partial derivatives commute, one gets that:

$$\widetilde{\nabla}_\lambda k_\mu = \widetilde{\nabla}_\mu k_\lambda. \tag{3.52}$$

Defining $k^\mu := \widetilde{g}^{\mu\nu} k_\nu$, and using (3.52), Equation (3.51) can be rewritten as:

$$(\widetilde{\nabla}_\lambda k_\mu) k^\lambda = 0, \tag{3.53}$$

which implies that we have a geodesic (e.g., Poisson[16] p. 61). □

Note that a given effective metric is only defined up to conformal equivalence because all that we have are *null* geodesics. More precisely, an effective geometry is an equivalence class of conformally equivalent Lorentzian metrics. However, we will only work with one representative at a time, choosing whichever conformal factor suits our fancy.

In the case of Euler-Heisenberg theory, the effective cometric (3.46) becomes:

$$\widetilde{g}^{\mu\nu} = g^{\mu\nu} + \frac{224\alpha^2 F^\mu{}_\lambda F^{\lambda\nu}}{495 + 12F\alpha^2 \mp \sqrt{18225 - 18360F\alpha^2 + 4624F^2\alpha^4 + 3136G^2\alpha^4}}. \tag{3.54}$$

3.4 The relationship between the effective metric and the stress-energy tensor

For an electromagnetic field governed by a Lagrangian of the type $L = L(F, G)$, we found that the stress-energy tensor is (2.28):

$$T_{\mu\nu} = -4L_F F_\mu{}^\alpha F_{\alpha\nu} - (L - GL_G) g_{\mu\nu}. \tag{3.55}$$

Raising the indices of Equation (3.55), and rearranging, we get that the *substress* tensor $F^\mu{}_\alpha F^{\alpha\nu}$ is (assuming $L_F \neq 0$):

$$F^\mu{}_\alpha F^{\alpha\nu} = -\frac{1}{4L_F}\left(T^{\mu\nu} + (L - GL_G) g^{\mu\nu}\right). \tag{3.56}$$

Using Equation (3.56), we can rewrite Equation (3.46) as:

$$\widetilde{g}^{\mu\nu} = \left(1 + \frac{\Lambda_\pm (GL_G - L)}{4L_F}\right) g^{\mu\nu} - \frac{\Lambda_\pm}{4L_F} T^{\mu\nu} \tag{3.57}$$

Equation (3.57) is analogous to Einstein's field equation from general relativity in that it relates the effective geometry with the stress-energy tensor.

We note that since the effective metric has this direct dependence on the stress-energy tensor, de Oliveira and Perez Bergliaffa[25] have suggested that the Segrè classification of the stress-energy tensor yields a simple classification scheme for effective geometries in nonlinear electrodynamics.

Chapter 4

Plane waves

The main purpose of this chapter is to investigate the effective geometry of a circularly polarized plane wave. Our findings independently confirm those of a 2002 paper by Denisov and Denisova.[26] The effective geometry of a plane wave is conformally equivalent to Minkowski spacetime but it is distinguishable from the Minkowski background because the effective null geodesics are not necessarily null in the background.

Moreover, we show that, as viewed from the background coordinates, shock disturbances in a circularly polarized monochromatic plane wave field propagate with a directionally dependent index of refraction which can be easily computed. Our result for the index of refraction confirms, to lowest order, the calculations performed by Affleck[27] in 1988. Lorentz invariance is manifestly preserved throughout in our approach. This is in contrast to Affleck's non-invariant approximation.

We close the chapter with a discussion anticipating the possibility of optical black holes in vacuum.

4.1 Effective geometry of null fields

Recall that a null field is one such that $F^2 + G^2 \equiv 0$. In the case of a null field, the nonlinear field equations (2.16) reduce exactly to Maxwell's equations in the absence of charges and currents, provided that $L_G = 0$ when $F^2 + G^2 = 0$. Note that the Euler-Heisenberg Lagrangian (2.13) indeed satisfies this latter condition. Consequently, a null

field is an exact solution to the Euler-Heisenberg equations if and only if it is an exact solution to Maxwell's equations.

Let us consider the effective geometry corresponding to a general null field.

In Section 3.2, we found that field disturbances (shock waves) disperse according to:

$$\left(\left(1+\frac{\Lambda_{\pm}(GL_G-L)}{4L_F}\right)g^{\mu\nu}-\frac{\Lambda_{\pm}}{4L_F}T^{\mu\nu}\right)k_\mu k_\nu=0, \tag{4.1}$$

where $\Lambda_{\pm}$ is given by Equation (3.39). The choice of $\pm$ depends on the polarization of the disturbance. Accordingly, we will refer to the polarization modes as being either $+$ or $-$ modes.

Specializing to null fields, Equation (4.1) leads to an effective cometric given by:

$$\widetilde{g}^{\mu\nu}=g^{\mu\nu}+P_{\pm}T^{\mu\nu}, \tag{4.2}$$

where:

$$P_{\pm}=-\frac{\Lambda_{\pm}}{4L_F+\Lambda_{\pm}(GL_G-L)}\Big|_{F^2+G^2=0}. \tag{4.3}$$

For the Euler-Heisenberg Lagrangian, we get that $P_{\pm}=(22\pm 6)\alpha^2/45$ (cf. De Lorenci *et al.*[15]).

Locally, the stress-energy tensor for a null electromagnetic field satisfying the dominant energy condition (see e.g., Hawking and Ellis[4] p. 91) can be expressed as:[28]

$$T^{\mu\nu}=l^\mu l^\nu, \tag{4.4}$$

where l^μ is a null vector. Thus effective cometrics corresponding to null fields can be expressed by equations of the form:

$$\widetilde{g}^{\mu\nu}=g^{\mu\nu}+P_{\pm}l^\mu l^\nu. \tag{4.5}$$

4.2 Effective geometry of plane waves

Taking the usual t, x, y, z coordinates for Minkowski spacetime. The field tensor:

$$\begin{aligned} F_{\mu\nu} &= \begin{pmatrix} F_{tt} & F_{tx} & F_{ty} & F_{tz} \\ F_{xt} & F_{xx} & F_{xy} & F_{xz} \\ F_{yt} & F_{yx} & F_{yy} & F_{yz} \\ F_{zt} & F_{zx} & F_{zy} & F_{zz} \end{pmatrix} \\ &= \begin{pmatrix} 0 & A\cos(\omega(t-z)) & B\sin(\omega(t-z)) & 0 \\ -A\cos(\omega(t-z)) & 0 & 0 & A\cos(\omega(t-z)) \\ -B\sin(\omega(t-z)) & 0 & 0 & B\sin(\omega(t-z)) \\ 0 & -A\cos(\omega(t-z)) & -B\sin(\omega(t-z)) & 0 \end{pmatrix} \end{aligned} \tag{4.6}$$

describes a monochromatic plane wave propagating along the $+z$ direction, having frequency ω, and elliptical polarization with fixed amplitudes A and B. The stress-energy tensor corresponding to this field is:

$$\begin{aligned} T^{\mu\nu} &= \begin{pmatrix} T^{tt} & T^{tx} & T^{ty} & T^{tz} \\ T^{xt} & T^{xx} & T^{xy} & T^{xz} \\ T^{yt} & T^{yx} & T^{yy} & T^{yz} \\ T^{zt} & T^{zx} & T^{zy} & T^{zz} \end{pmatrix} \\ &= \begin{pmatrix} A^2\cos^2(\omega(t-z)) + B^2\sin^2(\omega(t-z)) & 0 & 0 & A^2\cos^2(\omega(t-z)) + B^2\sin^2(\omega(t-z)) \\ 0 & 0 & 0 & 0 \\ 0 & 0 & 0 & 0 \\ A^2\cos^2(\omega(t-z)) + B^2\sin^2(\omega(t-z)) & 0 & 0 & A^2\cos^2(\omega(t-z)) + B^2\sin^2(\omega(t-z)) \end{pmatrix} \\ &= l^\mu l^\nu, \end{aligned} \tag{4.7}$$

where:

$$\begin{aligned} l^\mu &= \begin{pmatrix} l^t \\ l^x \\ l^y \\ l^z \end{pmatrix} \\ &= \begin{pmatrix} \sqrt{A^2\cos^2(\omega(t-z)) + B^2\sin^2(\omega(t-z))} \\ 0 \\ 0 \\ \sqrt{A^2\cos^2(\omega(t-z)) + B^2\sin^2(\omega(t-z))} \end{pmatrix}. \end{aligned} \tag{4.8}$$

Note that in the case of circular polarization ($A = B$), the stress-energy tensor takes on a particularly simple form; it becomes constant:

$$T^{\mu\nu} = \begin{pmatrix} A^2 & 0 & 0 & A^2 \\ 0 & 0 & 0 & 0 \\ 0 & 0 & 0 & 0 \\ A^2 & 0 & 0 & A^2 \end{pmatrix}. \tag{4.9}$$

Since the stress-energy tensor (4.9) is constant, the corresponding effective geometry (4.2) must be flat. In the case of an arbitrary elliptically polarized plane wave, the stress-energy tensor is no longer constant but one can nevertheless calculate that the Riemann curvature of the effective geometry still vanishes identically. This confirms results first published by Denisov and Denisova in 2002, who found that the effective geometries corresponding to monochromatic plane waves are flat using the Euler-Heisenberg Lagrangian (2.13).[26] More generally, we note that if we have a Lagrangian of the form $L = L(F, G)$ and if $L_G = 0$ when $F^2 + G^2 = 0$, then the resulting field theory will have plane waves as exact solutions and these will yield flat effective geometries.

Although the effective geometry of the plane wave is flat, the effective null geodesics are not necessarily null with respect to the flat background metric (the precise manner in which the effective light cones embed in the background is studied in Section 4.4). Thus we see that effective geometries which are flat can nevertheless be distinguishable from the flat background spacetime. This phenomenon is not limited to plane waves or even to null fields. Just to give a concrete example, a constant uniform electric field (e.g., in a rest frame, $(A_t, A_x, A_y, A_z) = (0, 0, 0, Et)$ with E constant), satisfies the Euler-Heisenberg equations (2.21) and its effective geometry is a copy of Minkowksi spacetime. Indeed if the stress energy tensor of a field is constant then its effective geometry must be flat. Considering the symmetry of such a situation, this should be expected.

4.3 Refraction in a circularly polarized plane wave

The purpose of this section is to calculate the index of refraction for field disturbances (low-intensity external "photons") propagating in a circularly polarized plane wave field.

Note that the stress-energy tensor of a null field given by two constant perpendicularly crossed electric and magnetic fields is the same as that of the circularly polarized plane wave (4.9). Thus, the effective geometry of crossed null fields is the same as that of the circularly polarized plane wave.

Using the stress-energy tensor (4.9), together with Equation (4.2), we calculate that the effective metrics corresponding to a circularly polarized plane wave (propagating in the $+z$ direction, with amplitude A) are:

$$ds^2 \;=\; (1 - P_{\pm}A^2)dt^2 + 2P_{\pm}A^2 dt dz - dx^2 - dy^2 - (1 + P_{\pm}A^2)dz^2. \tag{4.10}$$

Since the Christoffel symbols for the effective metric (4.10) vanish identically, the null geodesics in the effective geometry are simply rectilinear curves in the coordinates t, x, y, z.

Consider an effective null geodesic that passes through the origin of the coordinates t, x, y, z. The corresponding projection (i.e., light ray) for this geodesic in the three-dimensional x, y, z space issues from the origin and intersects the unit sphere at spherical coordinates θ by φ (see Figure 4.1). The angle φ measures the angle that the ray makes with respect to the $+z$ axis, as measured in the x, y, z system.

Using the standard conversion formulae between rectilinear and spherical coordinates ($x = r\sin\varphi\cos\theta,\ y = r\sin\varphi\sin\theta,\ z = r\cos\varphi$), Equation (4.10) implies that, along an effective null geodesic through the origin:

$$\left(1 + P_{\pm}A^2\cos^2\varphi\right)\left(\frac{dz}{dt}\right)^2 - 2P_{\pm}A^2\cos^2\varphi\left(\frac{dz}{dt}\right) - (1 - P_{\pm}A^2)\cos^2\varphi = 0. \tag{4.11}$$

Thus:

$$\frac{dz}{dt} = \frac{P_{\pm}A^2\cos^2\varphi + \cos\varphi\sqrt{1 - P_{\pm}A^2\sin^2\varphi}}{1 + P_{\pm}A^2\cos^2\varphi}. \tag{4.12}$$

Consequently, as measured in the t, x, y, z coordinates with respect to the background metric, discontinuities in the plane wave field propagate with a φ-dependent velocity:

$$\begin{aligned} v(\varphi) \;&=\; \sqrt{\frac{dx^2 + dy^2 + dz^2}{dt^2}} \\ &=\; \frac{P_{\pm}A^2\cos\varphi + \sqrt{1 - P_{\pm}A^2\sin^2\varphi}}{1 + P_{\pm}A^2\cos^2\varphi}. \end{aligned} \tag{4.13}$$

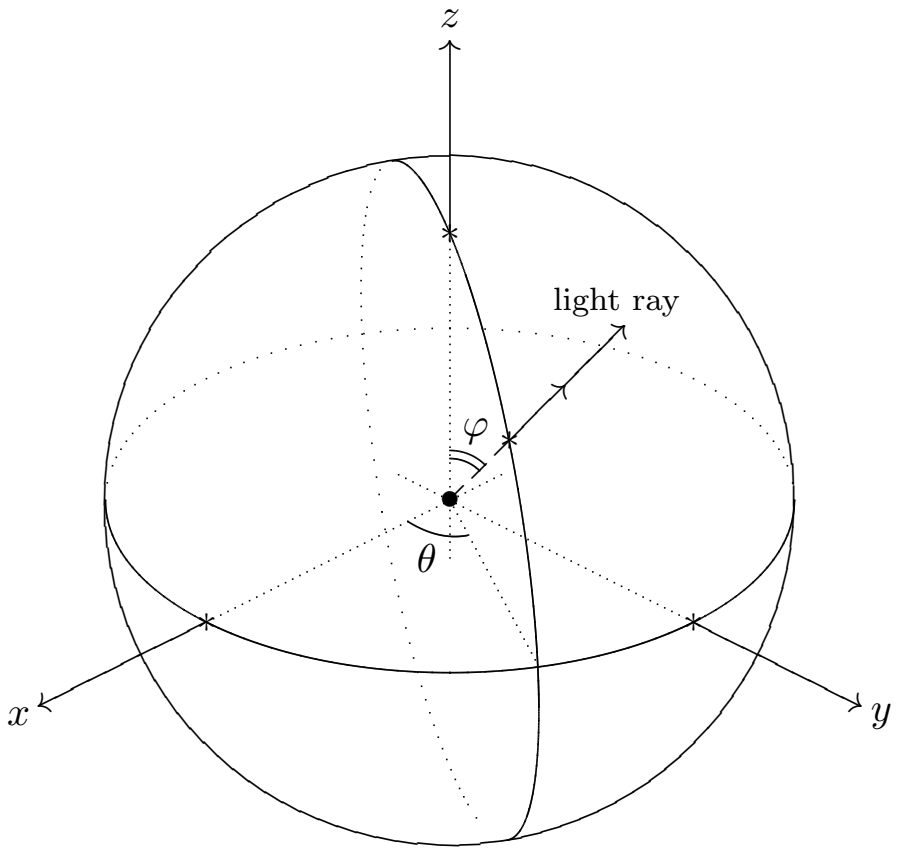

Figure 4.1: *A light ray issuing from the origin intersects the unit sphere at θ by φ.*

So the plane wave has an index of refraction, $n(\varphi) = 1/v(\varphi)$:

$$n(\varphi) \;=\; \frac{1 + P_{\pm}A^2\cos^2\varphi}{P_{\pm}A^2\cos\varphi + \sqrt{1 - P_{\pm}A^2\sin^2\varphi}}. \tag{4.14}$$

Expressing Equation (4.14) as a power series in A, one gets:

$$n(\varphi) \;=\; 1 + 2P_{\pm}A^2\sin^4\left(\frac{\varphi}{2}\right) + P_{\pm}^2 O(A^4). \tag{4.15}$$

Affleck[27] approximated a formula for $n(\varphi)$ using methods different from ours. The formula which he obtained (correcting for typos) is nothing but the first two nonzero terms in the expansion (4.15). (Note that Affleck's formula for $n(\varphi)$ was apparently published with a small typo: in his Equation (14), the factor (eE_0/m^2) should be $(eE_0/m^2)^2$.)

4.4 Visualizing effective light cones

The purpose of this section is to describe how the light cone structure of the effective geometry given by Equation (4.10) embeds in the background spacetime.

From Equation (4.13) we get that, as seen in the background, the plane wave induces a drag effect for field disturbances. Low-intensity photons that probe the field along the direction of the plane wave (the direction given by the so-called Poynting vector) will continue to travel at the usual speed of light: $v(0) = 1$. Along any other direction, the field disturbances are made to travel at less than the speed of light. This drag effect is most pronounced for $\varphi = \pi$, the direction exactly opposite to the Poynting vector.

According to Equation (4.13), when $P_{\pm}A^2 \geq 1$, field disturbances are confined to propagate only in directions such that $\csc^2 \varphi \leq P_{\pm}A^2$.

If a shock wave issues from the origin, then we can calculate the location of the wavefront in x, y, z space after a unit t-time by plotting Equation (4.13) in the xz-plane using (v, φ)-polar coordinates (i.e., $z = v\cos\varphi$ and $x = v\sin\varphi$). One can then rotate this graph about the z-axis ($\varphi = 0$) in order to visualize the wavefront as a surface of revolution (in fact, the surfaces in this case are ellipsoids). Plots of (4.13), representing the range of qualitative behaviors, are given in Figure 4.2. Note that disturbances propagating against the direction of the field experience a kind of drag effect. The case $A = 0$ (solid red in the figure) is a limiting case in which the plane wave has vanishing intensity. The standard propagation law for field discontinuities (propagation at the speed of light) is recovered in this limiting case.

It is straightforward to verify that the polar plots of Equation (4.13) are genuine ellipses with eccentricity:

$$\epsilon = \sqrt{\frac{P_{\pm}A^2}{1 + P_{\pm}A^2}}. \tag{4.16}$$

Similar observations were made by Boillat, who was however interested in the Born-Infeld rather than the Euler-Heisenberg Lagrangian. Note Equation (2.39) in his 1970 paper.[29]

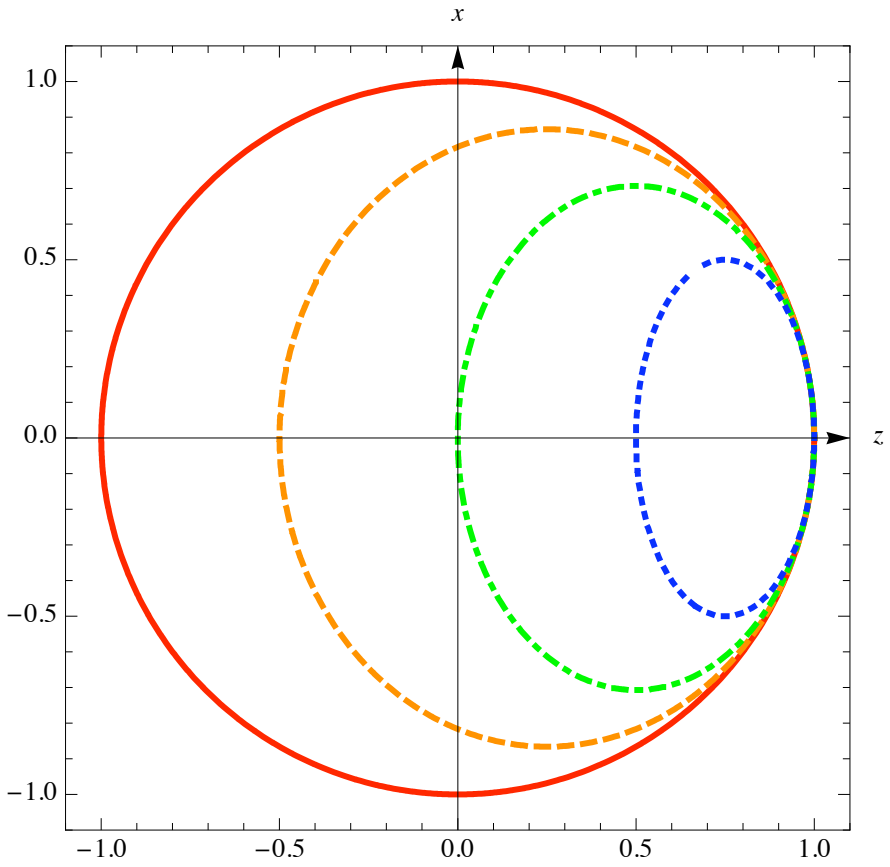

Figure 4.2: *Shock wave fronts in circularly polarized plane wave fields. Four separate cases are shown simultaneously for comparison purposes. In a monochromatic circularly polarized plane wave of amplitude A propagating in the $+z$ direction, a shock wave initiated at the origin is allowed to propagate for a unit t-time. The resulting shock fronts are plotted according to Equation (4.13) for four representative cases: (1) $P_{\pm}A = 0$ (solid red), (2) $0 < P_{\pm}A < 1$ (dashed orange, plotted using $P_{\pm}A = 1/3$), (3) $P_{\pm}A = 1$ (dot-dashed green), and (4) $P_{\pm}A > 1$ (dotted blue, plotted using $P_{\pm}A = 3$).*

Figure 4.3 visualizes how the effective light cones of (4.10) embed in the background geometry. The y-dimension is suppressed. Again, four representative cases (the same cases used in Figure 4.2) are presented simultaneously for comparison purposes. We note that de Oliveira Costa and Perez Bergliaffa[25] have classified effective light cones according to the Segré type of the stress-energy tensor for the field.

Due to birefringence, there are actually two different effective light cones for a given field configuration. We did not try to depict both of them in the cases shown in Figures 4.2 and

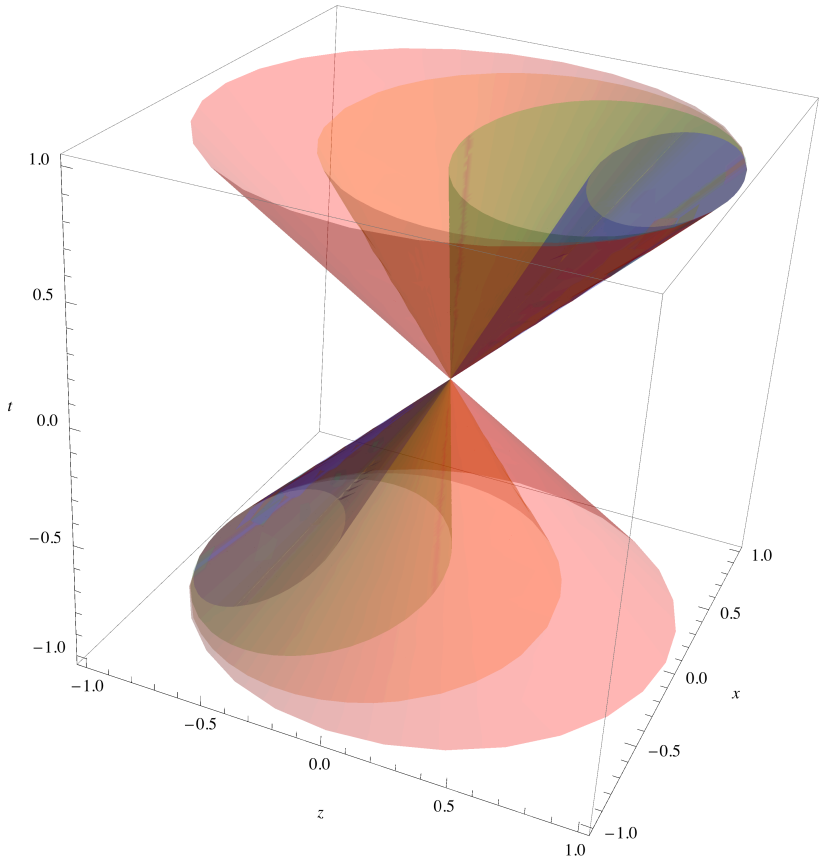

Figure 4.3: *Effective light cones in circularly polarized plane wave fields. The transparent red, orange, green, and blue cones (outermost to innermost) correspond to the cases plotted in Figure 4.2. In fact, Figure 4.2 is just the cross section through the plane $t = 1$. The transparent red cone (outermost) corresponds to a standard light cone in the background Minkowksi spacetime. The transparent orange, green, and blue cones show how the effective light cones embed in the background for plane waves of increasingly intense amplitude.*

4.3 in order to avoid unnecessary clutter. Note however that the difference between the light cones of the two polarization states becomes more pronounced at higher intensities.

As we see from these calculations, the effective light cones are tilted in the direction given by the Poynting vector of the field. Based on this observation, we make the following conjecture:

Conjecture 2. *For any given carrier field, the corresponding effective light cones tilt into the direction of the Poynting vector of the field. Moreover, the higher the field intensity, the more pronounced the tilt.*

This conjecture suggests that an optical black hole can form if one contrives to create a field, with an inwardly-directed Poynting vector, intense enough to tilt the effective light cones all the way to form a trapped surface.

4.5 Distortion of clock readings

Consider an observer at rest at the origin in t, x, y, z coordinates. Surround the observer with clocks, so that in the coordinates these clocks form a sphere S of unit radius. Let these clocks be set in such a way that if light travels along null geodesics in the background geometry, then the clocks appear to the observer as if precisely synchronized.

Now assume that the observer is immersed in a plane wave of amplitude A such that the effective geometries given by Equation (4.10) pertain. We stipulate that the observer sees objects only by way of small disturbances in the plane wave field; the "photons" seen by the observer follow null geodesics in the effective geometries (4.10). The readings on the stationary clocks at S will no longer appear to be synchronized since the effective null geodesics propagate anisotropically with respect to the t, x, y, z coordinates. Moreover, due to birefringence, two clock readings may be seen at once. An additional consequence of such birefringence effects would be that moving bodies could appear to have double images.

Since the field disturbances that travel in the direction $\varphi = 0$ travel at the usual speed of light, the apparent reading of a clock on S as viewed in the direction $\varphi = \pi$ will not be affected by the effective geometry. By contrast, the other clock readings will be affected. One can show that the difference in readings $\Delta\tau$ between a clock viewed at angle φ, and the unaffected clock at $\varphi = \pi$, is given by the formula:

$$\begin{aligned} \Delta\tau &= 1 - n(\pi - \varphi) \\ &= 1 + \frac{1 + P_{\pm} A^2 \cos^2 \varphi}{P_{\pm} A^2 \cos\varphi - \sqrt{1 - P_{\pm} A^2 \sin^2 \varphi}}. \end{aligned} \tag{4.17}$$

Since there are actually two distinct values of $P_{\pm}$ corresponding to birefringence, there are double images. If one sees both polarization states, then two clock readings can be seen.

In the critical case $P_{\pm}A^2 = 1$, the clock reading viewed through $\varphi = 0$ is infinitely delayed (and not visible). If $P_{\pm}A^2 \geq 1$, then the only visible clocks are at angles φ such that $\csc^2 \varphi > P_{\pm}A^2$. In a special range of cases where $P_{-}A^2 < 1 \leq P_{+}A^2$, the + polarization modes cannot be seen at all when viewed through φ-angles such that $\csc^2 \varphi \leq P_{\pm}A^2$.

Since the wave fronts of field disturbances are ellipsoidal in the t, x, y, z coordinates, one might consider reconfiguring S into an ellipsoidal arrangement so that the clocks will appear to be synchronized to the observer (provided that the field intensity is kept small enough that all points on S are visible to the observer). However, due to birefringence, one would only be able to manage the appearance of the clocks as viewed through one polarization mode at a time.

4.6 Hints of an optical black hole?

In the present chapter, we have found that effective light cones in plane wave fields are tilted towards the direction of the Poynting vector of the plane wave (Figure 4.3). Field disturbances propagating in the direction of the Poynting travel at the usual speed of light, but in other directions there is a drag effect. This drag effect is most pronounced for disturbances that propagate in the direction exactly opposite to the Poynting vector. The speed of these field disturbances, as measured with respect to the background coordinates, is:

$$v(\pi) = \frac{1 - P_{\pm}A^2}{1 + P_{\pm}A^2}, \tag{4.18}$$

where A is the intensity of the plane wave.

Comparing effective light cones for plane wave fields of higher and higher intensities as in Figure 4.3, one finds that the light cones become progressively more tilted. A similar phenomenon occurs in the geometry of gravitational black holes, where light cones become progressively more and more tilted as one approaches the event horizon. At the event horizon, the light cones are so tilted that information cannot flow from the event horizon

to the outside world. We suggest the notion that an optical black hole would form if one could increase the intensity of an electromagnetic wave by a sufficiently large amount in a localized region of space.

Though such a field will no longer correspond to a true plane wave, we propose the following Gedankenexperiment. Consider an electromagnetic wave that is focusing to a point. Let us consider a spherical point-like implosion in which the intensity of the wave is assumed to follow the inverse square law. Assuming that the wave front is locally like a plane wave, field disturbances that propagate radially outwards would travel at a coordinate speed:

$$v = \frac{dr}{dt} = \frac{r^4 - P_{\pm}A^2}{r^4 + P_{\pm}A^2}. \tag{4.19}$$

Here, spherical coordinates (t, r, θ, φ) are implied. Equation (4.19) is calculated by replacing A with A/r^2 in Equation (4.18) - in order to take the inverse square law into account.

Equation (4.19) suggests that a spherical event horizon will form at a critical radius $P_{\pm}^{1/4}A^{1/2}$. That is, within the critical radius, "outgoing" disturbances are not able to escape to infinity.

However, it is not possible to have a nontrivial spherically symmetric electromagnetic wave. The fundamental reason for this is that the polarization vectors due to such a field configuration would introduce a continuous nowhere-vanishing vector field tangent to the 2-sphere, thereby contradicting the well-known fact that the 2-sphere is not parallelizable.

For this reason, we turn our attention to other configurations. Since the cylinder $S^1 \times \mathbb{R}$ is parallelizable, the case of cylindrical collapse can be considered. The next chapter will look into this.

As a tentative calculation for the cylindrical case, replacing A with A/r into Equation (4.18) - in order to take the inverse distance law for cylindrical radiation into account - we have:

$$v = \frac{dr}{dt} = \frac{r^2 - P_{\pm}A^2}{r^2 + P_{\pm}A^2}, \tag{4.20}$$

with cylindrical coordinates (t, r, θ, z) implied. Equation (4.20) suggests an effective event horizon at $r = P_{\pm}^{1/2} A$. Slightly more refined approximations, done in Chapter 5, yield an effective horizon at a radius that is proportional to the square of the intensity A and inversely proportional to the frequency.

Using Equation (4.20) as an estimate for the coordinate velocity of radial null effective geodesics which are "outgoing" in a cylindrically imploding wave field, and assuming that the ingoing null geodesics propagate at the speed of light, we can use *Mathematica* to draw a graph of the coordinate velocities (see Figure 4.4). More detailed calculations, done in Chapter 5, will confirm that this guess is qualitatively on the right track. In Figure 4.4, we are guessing ingoing rays will propagate at the usual speed of light. This guess is motivated by our experience with plane waves; we have seen that field disturbances that propagate along with the flow of a plane wave simply propagate at the usual speed of light.

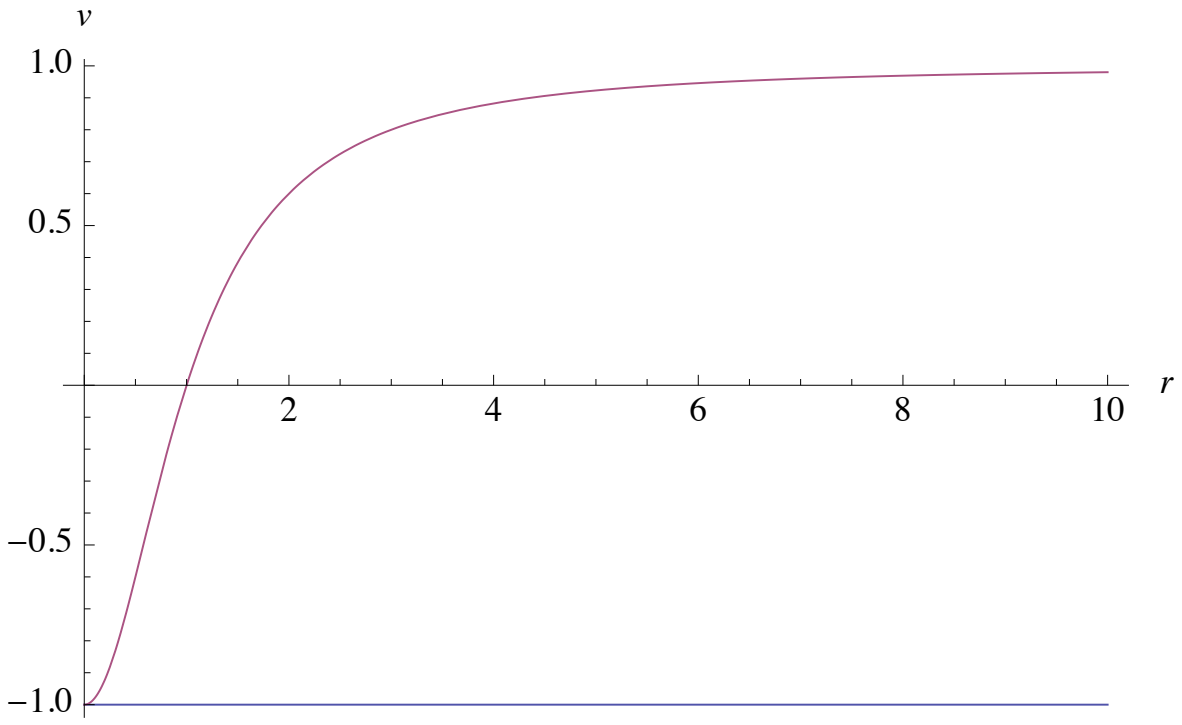

Figure 4.4: *Thought experiment. In this graph, we have plotted (in red) our tentative guess on how the coordinate velocity v of a radially outgoing light ray will vary with distance r in a cylindrically symmetric imploding field. This plot of Equation (4.20) uses $P_{\pm}A^2 = 1$. The horizontal blue line (at $v = -1$) corresponds to our tentative guess that the ingoing ray propagate at the usual speed of light.*

Chapter 5

Cylindrical fields

In Section 4.6 we suggested, by means of a crude Gedankenexperiment, that optical black holes might arise in the effective geometry of an imploding electromagnetic wave. As we have noted, a spherically symmetric implosion is not possible because the 2-sphere S^2 is not parallelizable. On the other hand, the cylinder $S^1 \times \mathbb{R}$ by contrast is parallelizable. For this reason, in the present chapter we move our focus to cylindrically symmetric fields. The main formulas derived in Sections 5.1 and 5.2 have been checked with *Mathematica*, as we detail in Appendix A.

Naturally then, we will be working with cylindrical coordinates (t, r, θ, z) in which the background (Minkowskian) metric $g_{\mu\nu}$ is given by:

$$ds^2 = dt^2 - dr^2 - r^2 d\theta^2 - dz^2. \tag{5.1}$$

The nonvanishing Christoffel symbols are:

$$\Gamma^r_{\theta\theta} = -r, \tag{5.2}$$

$$\Gamma^\theta_{r\theta} = \frac{1}{r} = \Gamma^\theta_{\theta r}. \tag{5.3}$$

We will define a *cylindrically symmetric electromagnetic field* as being an A-field whose

components are functions of the coordinates t and r only:

$$A_t = A_t(t,r), \tag{5.4}$$

$$A_r = A_r(t,r), \tag{5.5}$$

$$A_\theta = A_\theta(t,r), \tag{5.6}$$

$$A_z = A_z(t,r). \tag{5.7}$$

Although this is not a necessary condition for making the physical field $F_{\mu\nu} = \partial_\mu A_\nu - \partial_\nu A_\mu$ cylindrically symmetric, it is a sufficient one.

The Euler-Heisenberg field equation (2.21), is:

$$\nabla_\mu F^{\mu\nu} = \frac{\alpha^2}{45}\left(4\nabla_\mu(FF^{\mu\nu}) + 7\nabla_\mu(GF^{*\mu\nu})\right). \tag{5.8}$$

This amounts to a system of nonlinear PDEs (as shown explicitly in Section 5.1 below). There are no known general methods for finding exact solutions to such systems. We note however, that to first order in α, Equation (5.8) reproduces the Maxwell vacuum equations: $\nabla_\mu F^{\mu\nu} = 0$. This means that the familiar exact solutions from Maxwell's theory (whether they are cylindrically symmetric or not) are approximations of solutions to Equation (5.8), up to first-order in α.

In Section 5.2 we will treat ingoing cylindrical wave solutions from Maxwell's theory as approximate first-order solutions to the nonlinear theory. We will plug the Maxwellian field into the equations for the effective geometry from Chapter 3 and we will study the resulting geometry to second-order in α. As expected, we find that the effective geometry is analogous to a black hole. This is evidence for our main conjecture on the existence of black hole soliton solutions as we explained in the Introduction.

Since the Maxwellian solution is only valid up to first-order, one might worry about whether it is meaningful to do second-order calculations with it. However, as we show in Section 5.2, the geometric quantities that we calculate to second-order only depend on the first-order (Maxwellian) part of the exact solution, so the approximation is justified.

In Section 5.3, we will derive an exact static solution to Equation (5.8). This solution corresponds to a constant electric field running in the z-direction together with a magnetic field circulating around the z-axis. In the linear case, such a field configuration corresponds to that of a constant current through an infinitely long straight wire together with a constant electric field. With the fields arranged so as to give an inwardly-directed Poynting vector, the resulting effective geometry is analogous to that of a black hole.

5.1 Cylindrical fields of a particular type

Here we present formulas for the effective metrics and field equations for cylindrically symmetric fields of a particular type. These will be needed in later sections.

5.1.1 Field tensors

The particular type of cylindrical field considered here is one in which the t and r-components of the A-field vanish. This would be the case, for example, with an elliptically polarized imploding cylindrical radiation field in the radiation gauge.

Let us write:

$$A_t \equiv 0, \tag{5.9}$$

$$A_r \equiv 0, \tag{5.10}$$

$$A_\theta = u(t,r), \tag{5.11}$$

$$A_z = v(t,r). \tag{5.12}$$

The corresponding electromagnetic field tensor $F_{\mu\nu} = \partial_\mu A_\nu - \partial_\nu A_\mu$ is:

$$\begin{aligned} F_{\mu\nu} &= \begin{pmatrix} F_{tt} & F_{tr} & F_{t\theta} & F_{tz} \\ F_{rt} & F_{rr} & F_{r\theta} & F_{rz} \\ F_{\theta t} & F_{\theta r} & F_{\theta\theta} & F_{\theta z} \\ F_{zt} & F_{zr} & F_{z\theta} & F_{zz} \end{pmatrix} \\ &= \begin{pmatrix} 0 & 0 & \partial_t u & \partial_t v \\ 0 & 0 & \partial_r u & \partial_r v \\ -\partial_t u & -\partial_r u & 0 & 0 \\ -\partial_t v & -\partial_r v & 0 & 0 \end{pmatrix}. \end{aligned} \tag{5.13}$$

Raising the first index, one gets that $F^{\mu}{}_{\nu} = g^{\lambda\mu}F_{\lambda_\nu}$ is:

$$F^{\mu}{}_{\nu} = \begin{pmatrix} 0 & 0 & \partial_t u & \partial_t v \\ 0 & 0 & -\partial_r u & -\partial_r v \\ \frac{1}{r^2}\partial_t u & \frac{1}{r^2}\partial_r u & 0 & 0 \\ \partial_t v & \partial_r v & 0 & 0 \end{pmatrix}. \tag{5.14}$$

Raising the second index, one gets that $F^{\mu\nu} = g^{\lambda\nu}F^{\mu}{}_{\lambda}$ is:

$$F^{\mu\nu} = \begin{pmatrix} 0 & 0 & -\frac{1}{r^2}\partial_t u & -\partial_t v \\ 0 & 0 & \frac{1}{r^2}\partial_r u & \partial_r v \\ \frac{1}{r^2}\partial_t u & -\frac{1}{r^2}\partial_r u & 0 & 0 \\ \partial_t v & -\partial_r v & 0 & 0 \end{pmatrix}. \tag{5.15}$$

Using (5.13) and (5.15), one gets that the invariant $F = F_{\mu\nu}F^{\mu\nu}$ is:

$$F = \frac{2}{r^2}\left[(\partial_r u)^2 - (\partial_t u)^2 + r^2(\partial_r v)^2 - r^2(\partial_t v)^2\right]. \tag{5.16}$$

The dual tensor $F^*_{\mu\nu} = \frac{1}{2}\varepsilon_{\alpha\beta\mu\nu}F^{\alpha\beta}$ is:

$$F^*_{\mu\nu} = \begin{pmatrix} 0 & 0 & -r\partial_r v & \frac{1}{r}\partial_r u \\ 0 & 0 & -r\partial_t v & \frac{1}{r}\partial_t u \\ r\partial_r v & r\partial_t v & 0 & 0 \\ -\frac{1}{r}\partial_r u & -\frac{1}{r}\partial_t u & 0 & 0 \end{pmatrix}. \tag{5.17}$$

Using (5.15) and (5.17), one gets that $G = F^*_{\mu\nu}F^{\mu\nu}$ is:

$$G = \frac{4}{r}\left[(\partial_t u)(\partial_r v) - (\partial_r u)(\partial_t v)\right]. \tag{5.18}$$

Raising the indices of the dual, one gets that $F^{*\mu\nu} = g^{\alpha\mu}g^{\beta\nu}F^*_{\alpha\beta}$ is:

$$F^{*\mu\nu} = \begin{pmatrix} 0 & 0 & \frac{1}{r}\partial_r v & -\frac{1}{r}\partial_r u \\ 0 & 0 & -\frac{1}{r}\partial_t v & \frac{1}{r}\partial_t u \\ -\frac{1}{r}\partial_r v & \frac{1}{r}\partial_t v & 0 & 0 \\ \frac{1}{r}\partial_r u & -\frac{1}{r}\partial_t u & 0 & 0 \end{pmatrix}. \tag{5.19}$$

5.1.2 Effective metric

As we saw in Section 3.3, for the Euler-Heisenberg theory, the effective metric $\widetilde{g}_{\mu\nu}$ is given by the inverse of:

$$\widetilde{g}^{\mu\nu} = g^{\mu\nu} + \Lambda_{\pm}F^{\mu}{}_{\lambda}F^{\lambda\nu}, \tag{5.20}$$

where:

$$\Lambda_{\pm} = \frac{224\alpha^2}{495 + 12F\alpha^2 \mp \sqrt{18225 - 18360F\alpha^2 + 4624F^2\alpha^4 + 3136G^2\alpha^4}}. \tag{5.21}$$

Henceforth let us write $\Lambda := \Lambda_{\pm}$, keeping in mind that there is a choice of $\pm$ involved in the calculation of Λ (this Λ has nothing to do with the cosmological constant). As we explained in Section 3.2, this choice of $\pm$ depends on the polarization state of the field disturbance.

Using Equations (5.14) and (5.15), we get that the only nonvanishing components of the substress tensor $F^{\mu}{}_{\lambda}F^{\lambda\nu}$ are:

$$F^{t}{}_{\lambda}F^{\lambda t} = \frac{1}{r^2}\left[(\partial_t u)^2 + r^2(\partial_t v)^2\right] \tag{5.22}$$

$$F^{t}{}_{\lambda}F^{\lambda r} = F^{r}{}_{\lambda}F^{\lambda t} = -\frac{1}{r^2}\left[(\partial_t u)(\partial_r u) + r^2(\partial_t v)(\partial_r v)\right] \tag{5.23}$$

$$F^{r}{}_{\lambda}F^{\lambda r} = \frac{1}{r^2}\left[(\partial_r u)^2 + r^2(\partial_r v)^2\right] \tag{5.24}$$

$$F^{\theta}{}_{\lambda}F^{\lambda\theta} = \frac{1}{r^4}\left[(\partial_r u)^2 - (\partial_t u)^2\right] \tag{5.25}$$

$$F^{\theta}{}_{\lambda}F^{\lambda z} = F^{z}{}_{\lambda}F^{\lambda\theta} = \frac{1}{r^2}\left[(\partial_r u)(\partial_r v) - (\partial_t u)(\partial_t v)\right] \tag{5.26}$$

$$F^{z}{}_{\lambda}F^{\lambda z} = (\partial_r v)^2 - (\partial_t v)^2 \tag{5.27}$$

Plugging our result for the substress tensor into Equation (5.20), we get the effective cometric $\widetilde{g}^{\mu\nu}$. Taking the inverse of $\widetilde{g}^{\mu\nu}$, we find that the only nonvanishing components of the effective metric are (up to a conformal factor κ):

$$\kappa\widetilde{g}_{tt} = 1 - \frac{\Lambda(\partial_r u)^2}{r^2} - \Lambda(\partial_r v)^2 \tag{5.28}$$

$$\kappa\widetilde{g}_{tr} = \kappa\widetilde{g}_{rt} = -\frac{\Lambda(\partial_t u)(\partial_r u)}{r^2} - \Lambda(\partial_t v)(\partial_r v) \tag{5.29}$$

$$\kappa\widetilde{g}_{rr} = -1 - \frac{\Lambda(\partial_t u)^2}{r^2} - \Lambda(\partial_t v)^2 \tag{5.30}$$

$$\kappa\widetilde{g}_{\theta\theta} = -r^2 + \Lambda r^2(\partial_r v)^2 - \Lambda r^2(\partial_t v)^2 \tag{5.31}$$

$$\kappa\widetilde{g}_{\theta z} = \kappa\widetilde{g}_{\theta z} = \Lambda(\partial_t u)(\partial_t v) - \Lambda(\partial_r u)(\partial_r v) \tag{5.32}$$

$$\kappa\widetilde{g}_{zz} = -1 + \frac{\Lambda(\partial_r u)^2}{r^2} - \frac{\Lambda(\partial_t u)^2}{r^2}, \tag{5.33}$$

Since only the null geodesics are important, we can drop the conformal factor κ. Note that the effective metric becomes conformally equivalent to the background metric in the limit where $\Lambda \to 0$.

5.1.3 Radial null geodesics

Since the components of the metric tensor only depend on the coordinates t and r, it follows that radial null curves (that is, null curves with constant θ and z coordinates), are automatically geodesics. For such a curve we can write:

$$0 \;=\; \widetilde{g}_{tt} + 2\widetilde{g}_{tr}\frac{dr}{dt} + \widetilde{g}_{rr}\left(\frac{dr}{dt}\right)^2. \tag{5.34}$$

Solving (5.34) for dr/dt gives:

$$\begin{aligned}\frac{dr}{dt} &= \frac{-\widetilde{g}_{tr} \pm \sqrt{\widetilde{g}_{tr}^{\,2} - \widetilde{g}_{tt}\widetilde{g}_{rr}}}{\widetilde{g}_{rr}} \\ &= -\frac{(\partial_t u)(\partial_r u) + r^2(\partial_t v)(\partial_r v)}{(\partial_t u)^2 + r^2(\partial_t v)^2 + \frac{r^2}{\Lambda}} \\ &\quad \mp \frac{\sqrt{\left[(\partial_t u)(\partial_r u) + r^2(\partial_t v)(\partial_r v)\right]^2 + \left(\frac{r^2}{\Lambda} + r^2(\partial_t v)^2 + (\partial_t u)^2\right)\left(\frac{r^2}{\Lambda} - r^2(\partial_r v)^2 - (\partial_r u)^2\right)}}{(\partial_t u)^2 + r^2(\partial_t v)^2 + \frac{r^2}{\Lambda}}.\end{aligned} \tag{5.35}$$

We define *outgoing* geodesics as corresponding to choosing $+$ in (the second line of) Equation (5.35) and *ingoing* geodesics as corresponding to choosing $-$.

For radial geodesics of the ingoing type, one gets that to second-order in α:

$$\left.\frac{dr}{dt}\right|_{\text{in}} \;=\; -1 + \frac{(11 \pm 3)\alpha^2}{45r^2}\left((\partial_t u - \partial_r u)^2 \;+\; r^2(\partial_t v - \partial_r v)^2\right) + O(\alpha^4). \tag{5.36}$$

For the outgoing type:

$$\left.\frac{dr}{dt}\right|_{\text{out}} \;=\; 1 - \frac{(11 \pm 3)\alpha^2}{45r^2}\left((\partial_t u + \partial_r u)^2 \;+\; r^2(\partial_t v + \partial_r v)^2\right) + O(\alpha^4). \tag{5.37}$$

In Equations (5.36) and (5.37), the choice of $\pm$ has to do with the polarization state of the disturbance (there is birefringence). With the birefringence averaged out, we have:

$$\left.\left\langle\frac{dr}{dt}\right\rangle\right|_{\text{in}} \;=\; -1 + \frac{11\alpha^2}{45r^2}\left((\partial_t u - \partial_r u)^2 \;+\; r^2(\partial_t v - \partial_r v)^2\right) + O(\alpha^4), \tag{5.38}$$

and:

$$\left\langle \frac{dr}{dt} \right\rangle \Big|_{\text{out}} \;=\; 1 - \frac{11\alpha^2}{45r^2}\left((\partial_t u + \partial_r u)^2 \;+\; r^2(\partial_t v + \partial_r v)^2\right) + O(\alpha^4). \tag{5.39}$$

5.1.4 Field equations

Our next task is to express the field equations as a system of nonlinear PDEs. To this end, using (5.15), and introducing $\hat{u}(t,r) := u(t,r)/r$, we get that the left-hand side of the field equation (5.8) is:

$$\nabla_\mu F^{\mu\nu} \;=\; \begin{cases} 0 & \text{for } \nu = t \\ 0 & \text{for } \nu = r \\ \frac{1}{r^2}\partial_r(r\partial_r\hat{u}) - \frac{1}{r}\partial_t^2\hat{u} - \frac{\hat{u}}{r^3} & \text{for } \nu = \theta \\ \frac{1}{r}\partial_r(r\partial_r v) - \partial_t^2 v & \text{for } \nu = z. \end{cases} \tag{5.40}$$

Using (5.15), (5.16), (5.19) and (5.18), we get that the right-hand side of the field equation (5.8) is:

$$\frac{\alpha^2}{45}\left(4\nabla_\mu(FF^{\mu\nu}) + 7\nabla_\mu(GF^{*\mu\nu})\right) \;=\; \begin{cases} 0 & \text{for } \nu = t \\ 0 & \text{for } \nu = r \\ \frac{4\alpha^2}{45r^5}\mathcal{U} & \text{for } \nu = \theta \\ \frac{4\alpha^2}{45r^3}\mathcal{V} & \text{for } \nu = z. \end{cases} \tag{5.41}$$

Here,

$$\begin{aligned} \mathcal{U} \;=\;& 2r\hat{u}^2\left(3r\partial_r^2\hat{u} - 3\partial_r\hat{u} - r\partial_t^2\hat{u}\right) - 6\hat{u}^3 + \\ & r^2\hat{u}\left[6(\partial_r\hat{u})^2 - 2(\partial_r v)^2 - 5(\partial_t v)^2 - 2(\partial_t\hat{u})\left(\partial_t\hat{u} + 4r\partial_t\partial_r\hat{u}\right) + \right. \\ & \left. 3r(\partial_t v)(\partial_t\partial_r v) + 4r(\partial_r\hat{u})\left(3\partial_r^2\hat{u} - \partial_t^2\hat{u}\right) + r(\partial_r v)\left(4\partial_r^2 v - 7\partial_t^2 v\right)\right] + \\ & r^3\left\{6(\partial_r\hat{u})^3 - (\partial_r v)\left[7(\partial_t v)\left(\partial_t\hat{u} + 2r\partial_t\partial_r\hat{u}\right) - 3r(\partial_t\hat{u})(\partial_t\partial_r v)\right] + \right. \\ & r(\partial_r v)^2\left(2\partial_r^2\hat{u} + 5\partial_t^2\hat{u}\right) + (\partial_r\hat{u})^2\left(6r\partial_r^2\hat{u} - 2r\partial_t^2\hat{u}\right) + \\ & (\partial_r\hat{u})\left[2(\partial_r v)^2 - 6(\partial_t\hat{u})^2 - 8r(\partial_t\hat{u})(\partial_t\partial_r\hat{u}) + \right. \\ & \left. (\partial_t v)(5\partial_t v + 3r\partial_t\partial_r v) + r(\partial_r v)\left(4\partial_r^2 v - 7\partial_t^2 v\right)\right] + \\ & r\left[(\partial_r^2\hat{u})\left(5(\partial_t v)^2 - 2(\partial_t\hat{u})^2\right) - 7(\partial_r^2 v)(\partial_t\hat{u})(\partial_t v) + \right. \\ & \left.\left. 2(\partial_t^2\hat{u})\left(3(\partial_t\hat{u})^2 + (\partial_t v)^2\right) + 4(\partial_t\hat{u})(\partial_t v)(\partial_t^2 v)\right]\right\}, \end{aligned} \tag{5.42}$$

and:

$$\begin{aligned}
\mathcal{V} \;=\;& \hat{u}^2\left(2r\partial_r^2 v - 2\partial_r v + 5r\partial_t^2 v\right) + \\
& r\hat{u}\left[(\partial_t v)\left(10\partial_t\hat{u} + 3r\partial_t\partial_r\hat{u}\right) - 14r(\partial_t\hat{u})(\partial_t\partial_r v) + \right. \\
& \left. r(\partial_r v)\left(4\partial_r^2\hat{u} - 7\partial_t^2\hat{u}\right) + 2(\partial_r\hat{u})\left(2\partial_r v + 2r\partial_r^2 v + 5r\partial_t^2 v\right)\right] + \\
& r^2\left\{2(\partial_r v)^3 - (\partial_r v)\left[2(\partial_t\hat{u})^2 - 3r(\partial_t\hat{u})(\partial_t\partial_r\hat{u}) + 2(\partial_t v)\left(\partial_t v + 4r\partial_t\partial_r v\right)\right] + \right. \\
& (\partial_r\hat{u})\left[3r(\partial_t v)(\partial_t\partial_r\hat{u}) - 2(\partial_t\hat{u})\left(2\partial_t v + 7r\partial_t\partial_r v\right) + \right. \\
& \left. r(\partial_r v)\left(4\partial_r^2\hat{u} - 7\partial_t^2\hat{u}\right)\right] + (\partial_r v)^2\left(6r\partial_r^2 v - 2r\partial_t^2 v\right) + \\
& (\partial_r\hat{u})^2\left(6\partial_r v + 2r\partial_r^2 v + 5r\partial_t^2 v\right) + r\left[(\partial_r^2 v)\left(5(\partial_t\hat{u})^2 - 2(\partial_t v)^2\right) + \right. \\
& \left.\left. (\partial_t\hat{u})(\partial_t v)\left(4\partial_t^2\hat{u} - 7\partial_r^2\hat{u}\right) + 2(\partial_t^2 v)\left((\partial_t\hat{u})^2 + 3(\partial_t v)^2\right)\right]\right\}. \qquad (5.43)
\end{aligned}$$

The field equations for a field of the kind specified by Equations (5.9) - (5.12) can thus be expressed as a nonlinear system of PDEs:

$$\begin{cases} \frac{1}{r}\partial_r(r\partial_r\hat{u}) - \partial_t^2\hat{u} - \frac{\hat{u}}{r^2} = \frac{4\alpha^2}{45r^4}\mathcal{U} \\ \frac{1}{r}\partial_r(r\partial_r v) - \partial_t^2 v = \frac{4\alpha^2}{45r^3}\mathcal{V} \end{cases} \qquad (5.44)$$

5.2 Maxwellian approximation

To first-order in α, in which Maxwell's theory is recovered, the field equations (5.44) become:

$$\begin{cases} \frac{1}{r}\partial_r(r\partial_r\hat{u}) - \partial_t^2\hat{u} - \frac{\hat{u}}{r^2} = 0 \\ \frac{1}{r}\partial_r(r\partial_r v) - \partial_t^2 v = 0. \end{cases} \qquad (5.45)$$

Seeking solutions to (5.45) for a monochromatic field of constant frequency $\omega > 0$, we express the components of the A-field (5.9) - (5.12) in the form:

$$A_\mu = \mathrm{Re}\left[S_\mu \exp(i\omega t)\right], \qquad (5.46)$$

where S_μ is a function of r only. Note that the ansatz (5.46) implies that $\partial_t^2 A_\mu = -\omega^2 A_\mu$, and so (5.45) becomes:

$$\begin{cases} \frac{1}{r}\partial_r(r\partial_r\hat{u}) + \left(\omega^2 - \frac{1}{r^2}\right)\hat{u} = 0 \\ \frac{1}{r}\partial_r(r\partial_r v) + \omega^2 v = 0. \end{cases} \qquad (5.47)$$

These equations are of the form:

$$\frac{1}{r}\partial_r\left(r\partial_r\psi\right)+\left(\omega^2-\frac{n}{r^2}\right)\psi=0, \tag{5.48}$$

where n is either 0 or 1. Equation (5.48) is a Bessel-type differential equation, having solutions of the form (see e.g., Bowman[30] p. 116):

$$\psi=c_1J_n(\omega r)+c_2Y_n(\omega r), \tag{5.49}$$

where c_1 and c_2 are complex constants, and J_n and Y_n denote the nth order Bessel functions of the first and second kinds respectively. Monochromatic solutions to (5.45) are therefore given by:

$$\hat{u} = \mathrm{Re}\left[\left(c_{\hat{u}1}J_1(\omega r)+c_{\hat{u}2}Y_1(\omega r)\right)\exp(i\omega t)\right] \tag{5.50}$$

$$v = \mathrm{Re}\left[\left(c_{v1}J_0(\omega r)+c_{v2}Y_0(\omega r)\right)\exp(i\omega t)\right], \tag{5.51}$$

where the c_{ij} are complex constants.

In order to choose the constants c_{ij} so that one gets radially propagating solutions, consider the fact that the graphs of J_n and Y_n look like dampened sine and cosine graphs. In this sense, combinations such as $J_n(\omega r)\pm iY_n(\omega r)$ are like dampened versions of $\exp(i\omega r)$. So, after taking the real part, the functions $\left(J_n(\omega r)\pm iY_n(\omega r)\right)\exp(i\omega t)$ describe radially propagating waves (which can be either ingoing or outgoing depending on the choice of $\pm$).

Accordingly, for an elliptically polarized ingoing cylindrical wave, we write:

$$\begin{aligned} u(t,r) &= r\cdot\mathrm{Re}\left[\frac{U}{\omega}\left(J_1(\omega r)+iY_1(\omega r)\right)\exp(i\omega t)\right] \\ &= \frac{Ur}{\omega}\Big(J_1(\omega r)\cos(\omega t) \;-\; Y_1(\omega r)\sin(\omega t)\Big), \end{aligned} \tag{5.52}$$

and:

$$\begin{aligned} v(t,r) &= \mathrm{Re}\left[\frac{V}{\omega}\left(J_0(\omega r)+iY_0(\omega r)\right)\exp(i\omega t)\right] \\ &= \frac{V}{\omega}\Big(J_0(\omega r)\cos(\omega t) \;-\; Y_0(\omega r)\sin(\omega t)\Big), \end{aligned} \tag{5.53}$$

where U and V are real-valued constants (not to be confused with the functions $\mathcal{U}$ and $\mathcal{V}$ as defined by (5.42) and (5.43)).

Our task is to study the effective metric corresponding to this wave field. More specifically, we want to have a look at the effective radial null geodesics using (5.38) and (5.39) to calculate dr/dt to second-order in α, where we use the Maxwellian solution to evaluate the field variables. We claim that, up to second-order in α, the calculation of dr/dt only depends on the first-order (Maxwellian) part of the exact solution to (5.44). In other words:

Theorem 8. *Maxwellian approximations for dr/dt (along radial null geodesics in the effective geometry) are accurate up to second-order.*

Proof. Suppose that we have an exact solution $(\hat{u}, v) = (s_\theta/r, s_z)$ for the nonlinear system (5.44). In the limit $\alpha^2 \to 0$, this solution becomes a solution to (5.45). So expanding the exact solution as a power series in α would yield $s_\theta = m_\theta + O(\alpha^2)$ and $s_z = m_z + O(\alpha^2)$, where $(\hat{u}, v) = (m_\theta/r, m_z)$ is an exact solution to (5.45). (Note: *a priori* the series may only be asymptotic.) Using Equation (5.39):

$$\begin{aligned}
\left\langle \frac{dr}{dt} \right\rangle\Big|_{\text{out}} &= 1 - \frac{11\alpha^2}{45r^2}\left((\partial_t s_\theta + \partial_r s_\theta)^2 \ + \ r^2(\partial_t s_z + \partial_r s_z)^2\right) + O(\alpha^4) \\
&= 1 - \frac{11\alpha^2}{45r^2}\left((\partial_t m_\theta + \partial_r m_\theta + O(\alpha^2))^2 \ + \ r^2(\partial_t m_z + \partial_r m_z + O(\alpha^2))^2\right) + O(\alpha^4) \\
&= 1 - \frac{11\alpha^2}{45r^2}\left((\partial_t m_\theta + \partial_r m_\theta)^2 \ + \ r^2(\partial_t m_z + \partial_r m_z))^2\right) + O(\alpha^4). \qquad (5.54)
\end{aligned}$$

Similar calculations can be done using Equations (5.36) - (5.38). □

Proceeding now, by specializing Equations (5.38) and (5.39) to the Maxwellian solution (5.52) and (5.53), we find that the radial null geodesics are described by:

$$\begin{aligned}
\left\langle \frac{dr}{dt} \right\rangle\Big|_{\text{in}} \ = \ -1 + \frac{11\alpha^2}{45}\Big\{ & U^2\left[(J_0(\omega r) + Y_1(\omega r))\cos(\omega t) \ + \ (J_1(\omega r) - Y_0(\omega r))\sin(\omega t)\right]^2 + \\
& V^2\left[(Y_0(\omega r) - J_1(\omega r))\cos(\omega t) \ + \ (Y_1(\omega r) + J_0(\omega r))\sin(\omega t)\right]^2\Big\} + O(\alpha^4), \qquad (5.55)
\end{aligned}$$

and:

$$\left\langle \frac{dr}{dt} \right\rangle\Big|_{\text{out}} = 1 - \frac{11\alpha^2}{45}\left\{U^2\left[(Y_1(\omega r) - J_0(\omega r))\cos(\omega t) + (J_1(\omega r) + Y_0(\omega r))\sin(\omega t)\right]^2 + V^2\left[(J_1(\omega r) + Y_0(\omega r))\cos(\omega t) + (J_0(\omega r) - Y_1(\omega r))\sin(\omega t)\right]^2\right\} + O(\alpha^4), \tag{5.56}$$

We note that the oscillatory terms involving trigonometric functions of t disappear in the case of circular polarization (where $U = V$). One might have expected this out of consideration of the fact that, as we saw in Chapter 4, a similar simplification occurs in the effective geometry of circularly polarized plane waves. In fact, the stress-energy tensor (at least, as computed using the Maxwellian Lagrangian $L = -F/4$) for the field given by Equations (5.52) and (5.53) does not have any oscillatory terms in the case where $U = V$.

Henceforth, let us assume that the wave is circularly polarized, with $U = V =: A$. In this case, we get that the effective radial geodesics are described by:

$$\left\langle \frac{dr}{dt} \right\rangle\Big|_{\text{in}} = -1 + \frac{11\alpha^2 A^2}{45}\left(-\frac{4}{\pi\omega r} + J_0(\omega r)^2 + J_1(\omega r)^2 + Y_0(\omega r)^2 + Y_1(\omega r)^2\right) + O(\alpha^4), \tag{5.57}$$

and:

$$\left\langle \frac{dr}{dt} \right\rangle\Big|_{\text{out}} = 1 - \frac{11\alpha^2 A^2}{45}\left(\frac{4}{\pi\omega r} + J_0(\omega r)^2 + J_1(\omega r)^2 + Y_0(\omega r)^2 + Y_1(\omega r)^2\right) + O(\alpha^4). \tag{5.58}$$

For simplicity, we are using the formulas in which the birefringence is averaged out. To recover the birefringence, replace the factor $11\alpha^2$ with $(11 \pm 3)\alpha^2$.

We note that, for large x, one has the approximations (Arfken and Weber[31] p. 718):

$$J_n(x) \approx \sqrt{\frac{2}{\pi x}}\cos\left[x - \left(n + \frac{1}{2}\right)\left(\frac{\pi}{2}\right)\right], \tag{5.59}$$

and:

$$Y_n(x) \approx \sqrt{\frac{2}{\pi x}}\sin\left[x - \left(n + \frac{1}{2}\right)\left(\frac{\pi}{2}\right)\right]. \tag{5.60}$$

Consequently, for large x:

$$\begin{aligned} J_0(x)^2 + J_1(x)^2 + Y_0(x)^2 + Y_1(x)^2 &\approx \frac{2}{\pi x}\cos^2\left[x - \left(\frac{1}{2}\right)\left(\frac{\pi}{2}\right)\right] \\ &\quad + \frac{2}{\pi x}\cos^2\left[x - \left(1+\frac{1}{2}\right)\left(\frac{\pi}{2}\right)\right] \\ &\quad + \frac{2}{\pi x}\sin^2\left[x - \left(\frac{1}{2}\right)\left(\frac{\pi}{2}\right)\right] \\ &\quad + \frac{2}{\pi x}\sin^2\left[x - \left(1+\frac{1}{2}\right)\left(\frac{\pi}{2}\right)\right] \\ &= \frac{4}{\pi x}. \end{aligned} \tag{5.61}$$

In fact, one could have guessed at Equation (5.61) using the following idea. Far from the origin, the cylindrical wave should look like a plane wave and we know that field disturbances in a plane wave, when they travel along the same direction as the plane wave (the Poynting vector), travel at the usual speed of light. Hence one should have $\left\langle \frac{dr}{dt} \right\rangle\Big|_{\text{in}} \approx -1$ in the limit where ωr is large, and this implies (5.61).

So in the limit where the quantity ωr is large, we have, to second-order in α:

$$\left\langle \frac{dr}{dt} \right\rangle\Big|_{\text{in}} \approx -1, \tag{5.62}$$

and:

$$\left\langle \frac{dr}{dt} \right\rangle\Big|_{\text{out}} \approx 1 - \frac{88\alpha^2 A^2}{45\pi\omega r}. \tag{5.63}$$

Equation (5.63) suggests that within radii $r \leq r_c$, where:

$$r_c \approx \frac{88\alpha^2 A^2}{45\pi\omega}, \tag{5.64}$$

even the "outward" geodesics are compelled to fall inward. Hence the critical radius r_c is the event horizon of a black hole. (Note: we have only checked this for outward geodesics in the radial direction.)

Since (5.64) was derived assuming that ωr is large, we only expect this approximation to hold in the limit of very large A^2. (We could also mention that, due to birefringence, there

are actually two event horizons. If we had taken this into account in the above, then we would have estimated the critical radii as occurring at $r_c \approx (88 \pm 24)\alpha^2 A^2/(45\pi\omega)$, where the $\pm$ depends on the polarization of the disturbance.)

Plotting Equations (5.62) and (5.63) on the same graph (Figure 5.1), we can compare to our earlier naïve guess of (4.20). We note that there are substantial quantitative differences between our initial guess and our slightly more refined calculation, but the qualitative picture is basically the same.

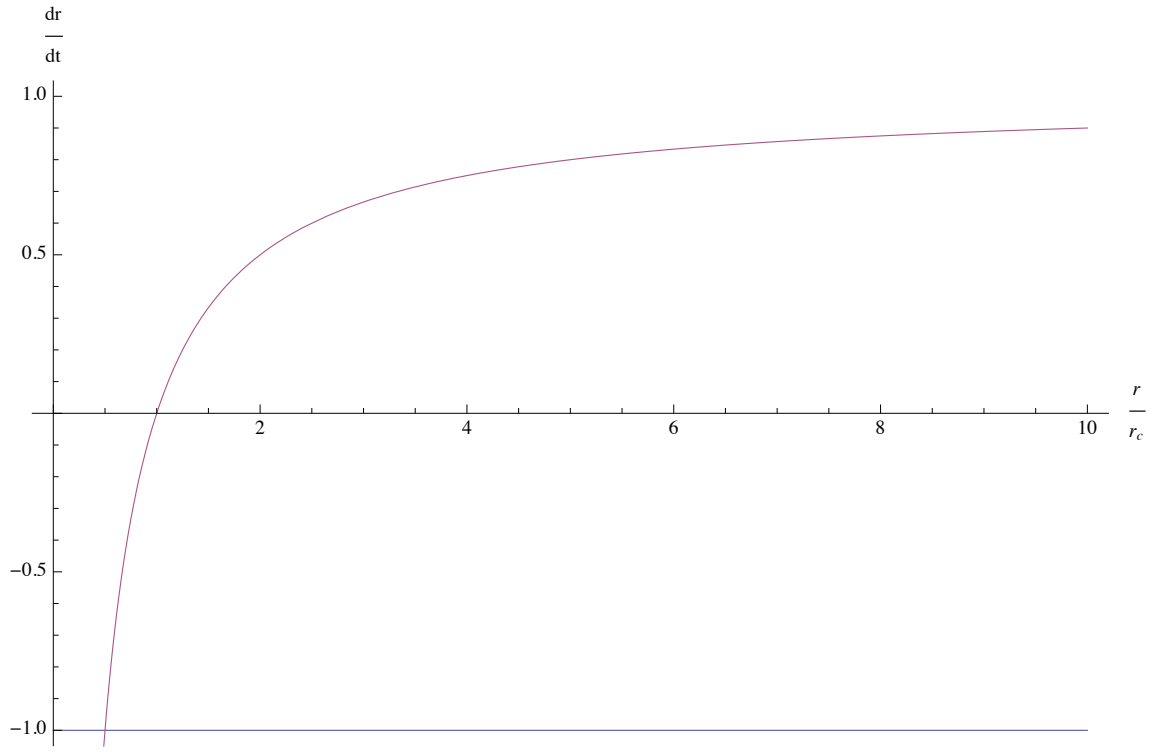

Figure 5.1: *In this graph, the coordinate velocities of effective null geodesics are plotted using the asymptotic approximations (5.62) and (5.63), which assume that the quantity ωr is large. The horizontal blue line at $dr/dt = -1$ corresponds to the ingoing geodesics, and the red curve corresponds to the "outgoing" radial geodesics. Compare to Figure 4.4.*

Treating the asymptotic approximations (5.62) and (5.63) as ordinary differential equations, and solving them by integration, we obtain approximate equations for the radial null

geodesics. Specifically:

$$t \;=\; -r + r_0, \tag{5.65}$$

for the ingoing geodesics (r_0 := the radial coordinate of the geodesic when $t = 0$), and:

$$t \;=\; \begin{cases} r + r_c \ln(r - r_c) - r_0 - r_c \ln(r_0 - r_c) & \text{if } r_0 > r_c \\ r + r_c \ln(r_c - r) - r_0 - r_c \ln(r_c - r_0) & \text{if } r_0 < r_c, \end{cases} \tag{5.66}$$

for the "outgoing" geodesics. An outgoing radial null geodesic that initiates from $r = r_c$ would just remain there. Using *Mathematica*, we have plotted Equations (5.65) and (5.66) for a few values of r_0. The resulting plot is shown in Figure 5.2. Note that the effective light cones are tilted in towards the origin, just like in the situation of gravitational black holes.

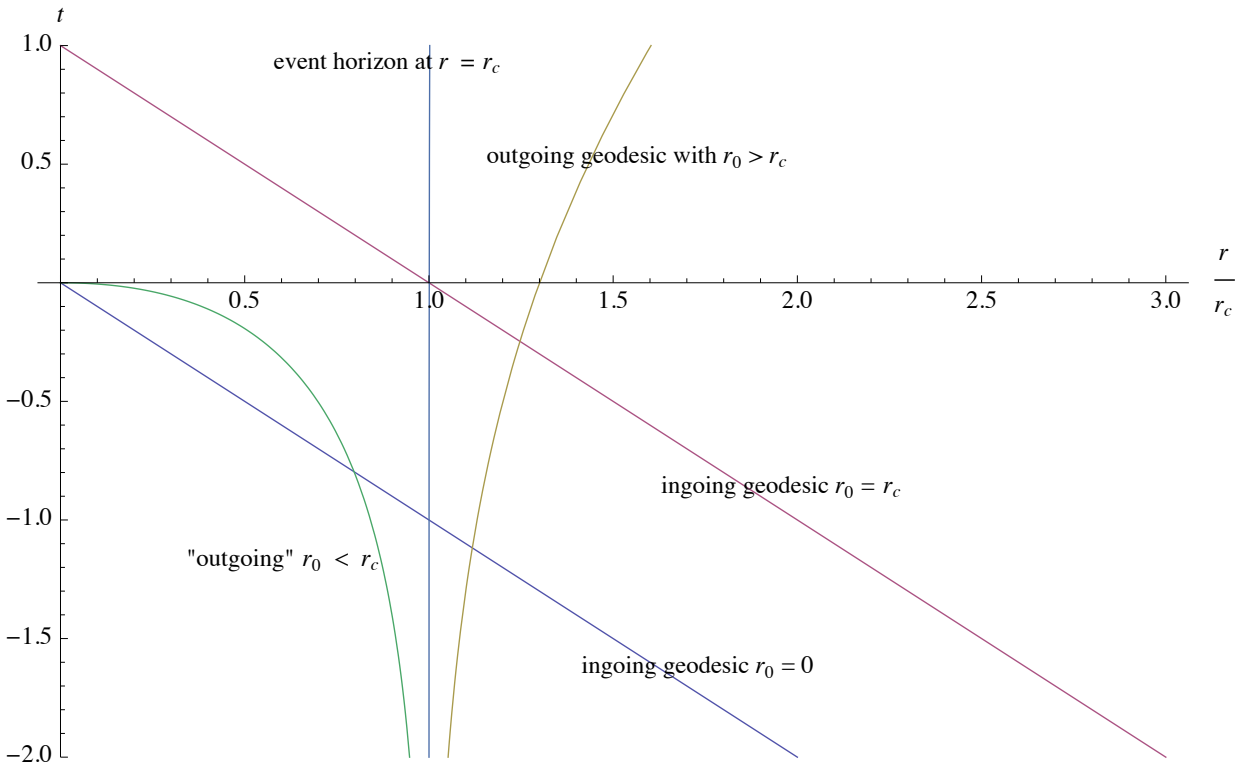

Figure 5.2: *In this graph, effective null geodesics are plotted using Equations (5.65) and (5.66). Equations (5.65) and (5.66) are themselves based on the asymptotic approximations (5.62) and (5.63), which assumes that the quantity ωr is large.*

In fact, using the numerical integration capabilities of *Mathematica*, we can make space-time diagrams for the effective null geodesics, as described by Equations (5.57) and (5.58) to second-order in α, without recourse to the asymptotic approximations (5.62) and (5.63). These diagrams, shown in Figures 5.3 - 5.5, are similar to Figures 5.1 - 5.2. Again we find that the effective geometry contains a black hole. That is, the effective light cones are tilted towards the origin, and there is an effective event horizon. In making the plots for Figures 5.3 - 5.5, we have set $\omega = 1$ and we have chosen A^2 such that $88\alpha^2 A^2/(45\pi\omega) = 1$.

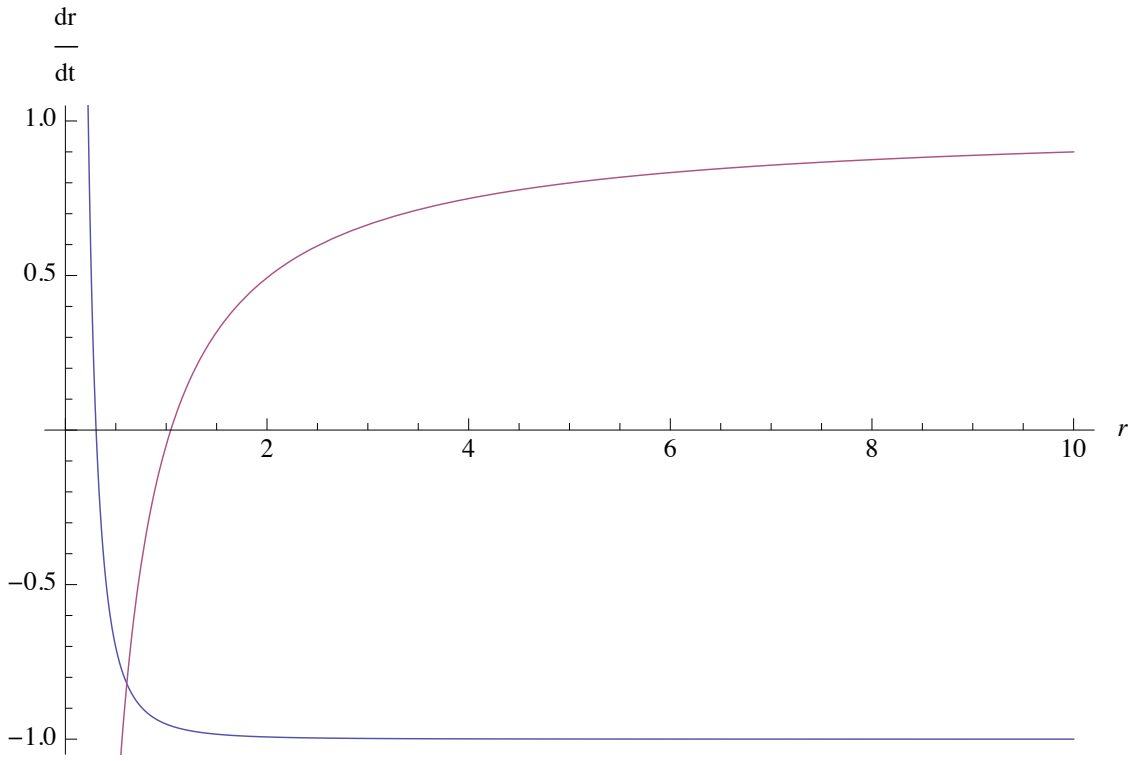

Figure 5.3: *In this graph, the coordinate velocities of effective null geodesics are plotted using Equations (5.57) and (5.58) up to to second-order in α. In plotting this graph, we have set $\omega = 1$ and we have chosen A^2 so that the quantity $88\alpha^2 A^2/(45\pi\omega)$ (our crude estimate for the effective horizon radius) is unity. The blue curve corresponds to the ingoing geodesics, and the red curve corresponds to the "outgoing" radial geodesics. Compare to Figure 5.1.*

As we see from these plots, the radially outgoing rays are significantly slowed down near the critical radius. This means that if we slowly move a clock radially inwards, then an

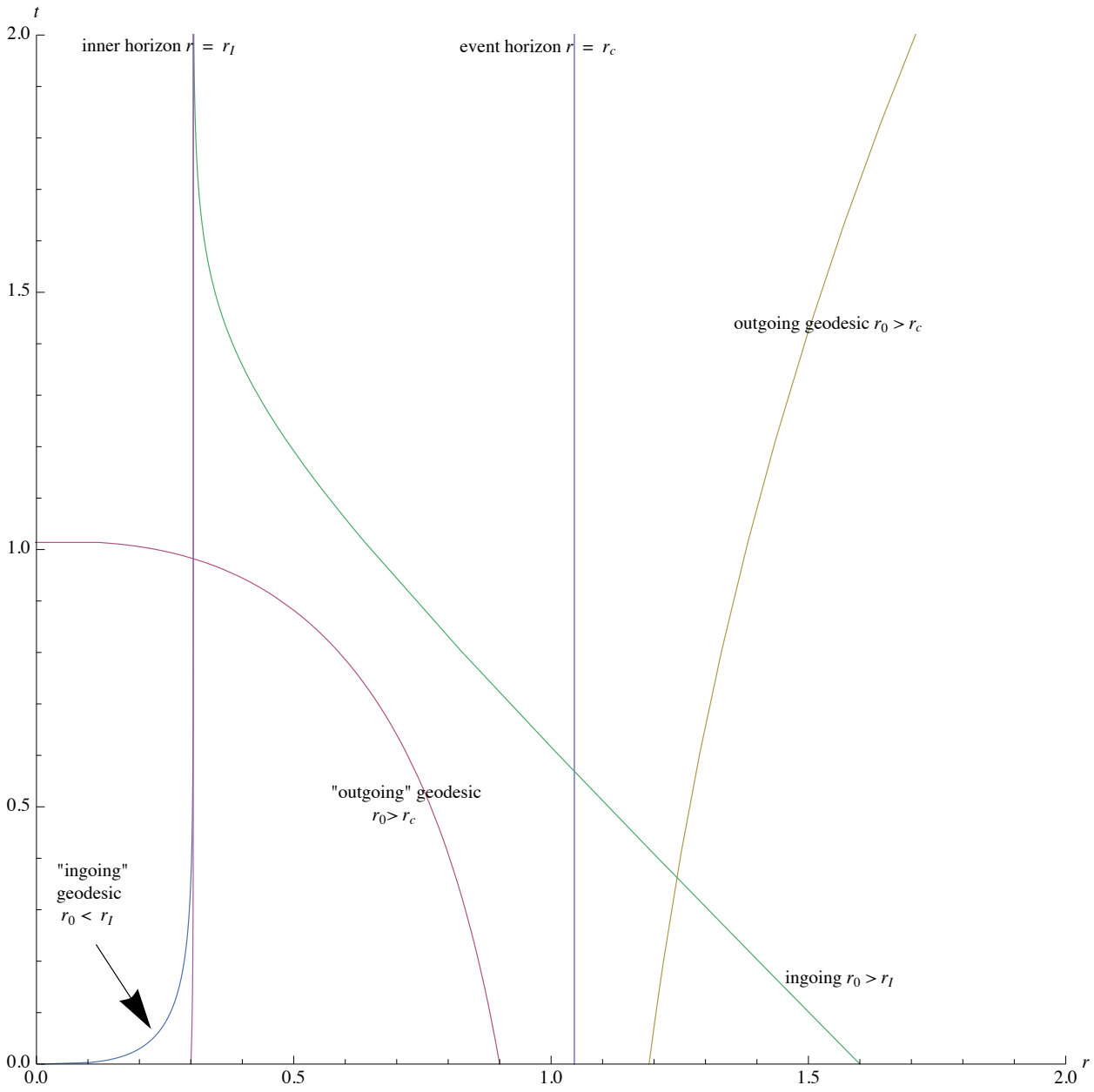

Figure 5.4: *In this graph, effective null geodesics are plotted by numerically integrating Equations (5.57) and (5.58). We have set* $\omega = 1$ *and we have chosen* A^2 *so that the quantity* $88\alpha^2 A^2/(45\pi\omega)$ *is unity. Compare to Figure 5.2.*

observer at infinity would see it ticking at a progressively slower rate. Actually, due to birefringence, the situation is even more complicated since there will also be double images, but we are ignoring birefringent effects for now. When the clock reaches the critical radius, its light rays will not travel beyond the critical radius, and the clock will no longer be visible from the outside.

We note that, according to the second-order approximations (5.57) and (5.58), there is a small radius within the event horizon where the ingoing geodesics are brought to zero coordinate velocity. Thereby the ingoing geodesics coming in from infinity do not penetrate all the way to the origin, but instead are blocked by an "inner horizon" at $r = r_I$ (see Figure (5.4)). Also, we note that null geodesics exceed the usual speed of light, as viewed in the background coordinates. Some of the phenomena shown in Figure 5.4, especially at the smaller radii, may be mere artifacts of the approximation. We note however that the superluminal photons, if such exist, will not violate causality if the effective spacetime which they propagate is a causal spacetime.

Note also that there is a radius between the inner and outer horizons where the "ingoing" and "outgoing" geodesics cannot be locally distinguished. At this special radius, the ingoing and outgoing radial geodesics travel in the same direction at the same velocity, so the effective light cone is degenerate at this radius.

We remark that if one were to take ω as negative, which amounts to turning our ingoing wave into an *outgoing* cylindrical wave, then one would obtain an effective spacetime which contains an optical white hole rather than a black hole.

5.3 A static exact solution

In the case of a field with z-polarization, $u \equiv 0$, the field equations (5.44) reduce to a single nonlinear PDE:

$$\begin{aligned} \partial_r^2 v - \partial_t^2 v + \frac{\partial_r v}{r} &= \frac{8\alpha^2}{45r}\left[(\partial_r v)^3 - (\partial_t v)(\partial_r v)(\partial_t v + 4r\partial_t\partial_r v)\right. \\ &\quad \left. + r(\partial_t v)^2(3\partial_t^2 v - \partial_r^2 v) + r(\partial_r v)^2(3\partial_r^2 v - \partial_t^2 v)\right]. \end{aligned} \tag{5.67}$$

A particularly interesting case in which Equation (5.67) can be solved exactly is that of a field where $\partial_t v \equiv E =$ constant. In this case (5.67) reads:

$$\frac{d^2v}{dr^2} + \frac{1}{r}\frac{dv}{dr} = \frac{8\alpha^2}{45r}\left[\left(\frac{dv}{dr}\right)^3 - E^2\left(\frac{dv}{dr}\right) - rE^2\left(\frac{d^2v}{dr^2}\right) + 3r\left(\frac{dv}{dr}\right)^2\left(\frac{d^2v}{dr^2}\right)\right]. \tag{5.68}$$

Introducing the function $B(r) := dv/dr$, Equation (5.68) becomes:

$$\frac{dB}{dr} + \frac{1}{r}B = \frac{8\alpha^2}{45r}\left[B^3 - E^2B - rE^2\left(\frac{dB}{dr}\right) + 3rB^2\left(\frac{dB}{dr}\right)\right]. \tag{5.69}$$

This can be rearranged into:

$$\frac{dB}{dr} = -\left(\frac{8\alpha^2B^3 - 8\alpha^2E^2B - 45B}{r(24\alpha^2B^2 - 8\alpha^2E^2 - 45)}\right). \tag{5.70}$$

Equation (5.70) is solvable by integration. The general solution is given through the relation:

$$B + \frac{8\alpha^2}{45}\left(E^2B - B^3\right) = \frac{k}{r}, \tag{5.71}$$

where k is an arbitrary constant. A sketch of the graph of Equation (5.71) is shown in Figure 5.5. There are three asymptotic values of B as $r \to \infty$, namely: $B = 0$, and $B = \pm\sqrt{E^2 + 45/(8\alpha^2)}$.

Note that dB/dr has a singularity when $r = 0$ and when $B = \pm\sqrt{E^2/3 + 15/(8\alpha^2)}$. Let us define $B_s := \sqrt{E^2/3 + 15/(8\alpha^2)}$, and let r_s denote the radius where $B^2 = B_s^2$.

We remark that (5.71) corresponds physically to a constant electric field E directed along the $\pm z$-direction ($\pm$ depending on where E is positive or negative, respectively), together with a magnetic field B, which in the Maxwellian limit $\alpha^2 \to 0$, would be produced by a constant current $2\pi k$ running along the $\pm z$-direction ($\pm$ depending on whether k is positive or negative, respectively). The magnetic field circulates around counterclockwise around the the z-axis if B is positive, clockwise if negative. In other words, Equation (5.71) refines the familiar undergraduate physics formula $B = k/r$.

Using Equations (5.16) and (5.18), we get that the F and G invariants are:

$$F = 2\left(B^2 - E^2\right), \tag{5.72}$$

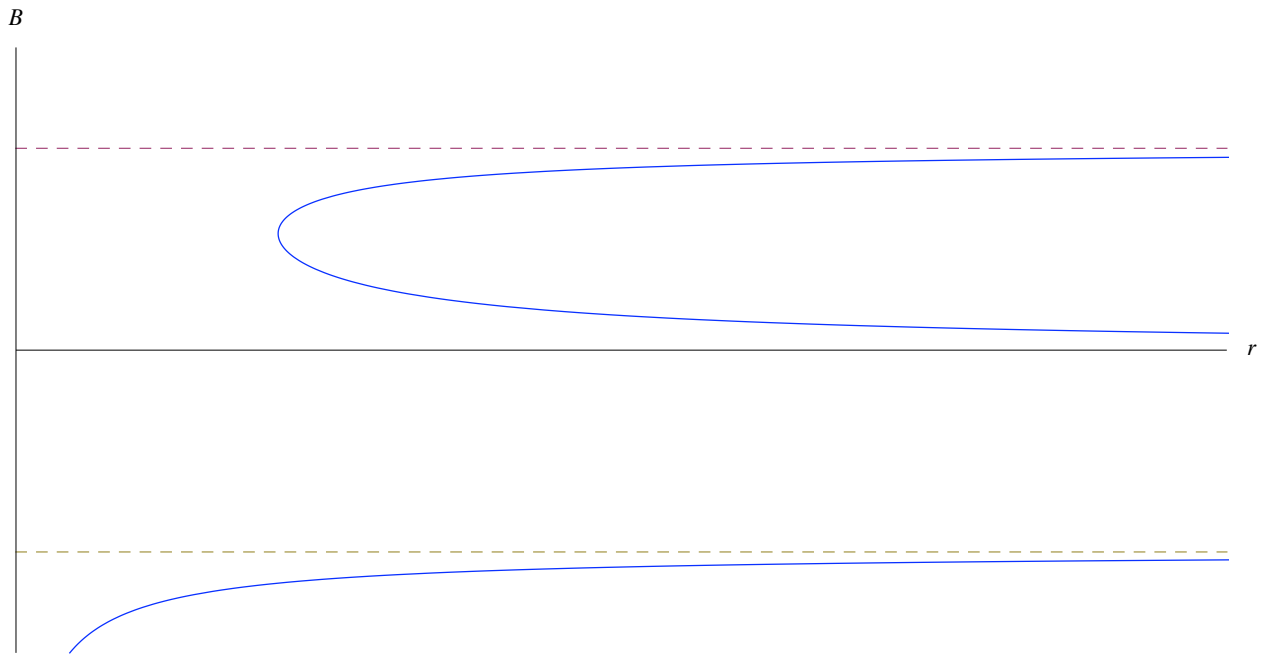

Figure 5.5: *A sketch of the graph of Equation (5.71) for* $k > 0$.

and:

$$G \;=\; 0. \tag{5.73}$$

So Equation (3.44) gives:

$$\frac{1}{\Lambda} \;=\; \frac{495 + 24\alpha^2(B^2 - E^2) \mp \left|135 - 136\alpha^2(B^2 - E^2)\right|}{224\alpha^2}, \tag{5.74}$$

where the choice of $\pm$ depends on the polarization state of the field disturbance. We shall call the polarization corresponding to choosing $+$ in Equation (5.74) the "(+) polarization state," and we call the other state the "(−) polarization state." (Note that our naming schemes for the polarization states are always *ad hoc* and the naming scheme in the preset section is not meant to be consistent with e.g., Section 4.1 or Appendix A.)

Using Equations (5.28) - (5.33), we get that the only nonzero components of the effective

metric are, up to a conformal factor:

$$\widetilde{g}_{tt} = 1 - \Lambda B^2 \tag{5.75}$$

$$\widetilde{g}_{tr} = \widetilde{g}_{rt} = -\Lambda E B \tag{5.76}$$

$$\widetilde{g}_{rr} = -1 - \Lambda E^2 \tag{5.77}$$

$$\widetilde{g}_{\theta\theta} = -r^2 + \Lambda r^2 \left(B^2 - E^2\right) \tag{5.78}$$

$$\widetilde{g}_{zz} = -1. \tag{5.79}$$

Using Equation (5.35), we get that the radial null geodesics are given by:

$$\frac{dr}{dt} = \frac{-EB \mp \sqrt{\frac{1}{\Lambda^2} - \frac{1}{\Lambda}\left(B^2 - E^2\right)}}{E^2 + \frac{1}{\Lambda}}. \tag{5.80}$$

The outgoing radial geodesics correspond to choosing $+$ in Equation (5.80), and the ingoing geodesics correspond to choosing $-$.

5.3.1 Proof of the main theorem

Since Equation (5.71) gives a cubic equation in B, there are three branches giving B as a real function of r (see the Table below).

branch	range of B^2
I	0 to B_s^2
II	B_s^2 to $3B_s^2$
III	B_s^2 to ∞

Table 5.1: *The three branches of B classified according to their ranges.*

Let us consider the case where the field is prescribed by branch I, with $k > 0$. This field is defined only for $r \geq r_s$. Note that Equation (5.70) can be rewritten as:

$$\frac{dB}{dr} = \frac{B\left(3B_s^2 - B^2\right)}{3r\left(B^2 - B_s^2\right)}. \tag{5.81}$$

Thus we have that B is a strictly decreasing function of r. As shown below, both effective geometries for this field contain black holes, if $\sqrt{\frac{45}{34\alpha^2}} < E < \sqrt{\frac{9}{4\alpha^2}}$. This section constitutes proof of Theorem 1 from Chapter 1.

Theorem 9. *For $E^2 \geq \frac{45}{34\alpha^2}$, the effective geometry corresponding to the (+) polarization state contains a black hole (if $E > 0$), or a white hole (if $E < 0$), with the event horizon at $r = r_s$.*

Proof. For the (+) polarization state, with $E^2 \geq 45/(34\alpha^2)$, Equation (5.74) gives:

$$\frac{1}{\Lambda} = \frac{45}{16\alpha^2} - \frac{1}{2}\left(B^2 - E^2\right). \tag{5.82}$$

At $r = r_s$:

$$\frac{1}{\Lambda}\Big|_{r=r_s} = B_s^2. \tag{5.83}$$

In fact, since $1/\Lambda \geq 1/\Lambda|_{r=r_s}$, we have that $\Lambda > 0$ for all $r \geq r_s$.

Equation (5.80) yields:

$$\begin{aligned}\frac{dr}{dt}\Big|_{\text{out, } r\geq r_s} &= \frac{-EB + \sqrt{\frac{1}{\Lambda^2} - \frac{1}{\Lambda}\left(B^2 - E^2\right)}}{E^2 + \frac{1}{\Lambda}} \\ &= \frac{-EB + \sqrt{\left(\frac{45}{16\alpha^2} - \frac{1}{2}\left(B^2 - E^2\right)\right)^2 - \left(\frac{45}{16\alpha^2} - \frac{1}{2}\left(B^2 - E^2\right)\right)\left(B^2 - E^2\right)}}{E^2 + \frac{45}{16\alpha^2} - \frac{1}{2}\left(B^2 - E^2\right)}.\end{aligned} \tag{5.84}$$

For $r > r_s$, the numerator in Equation (5.84) is positive by virtue of the fact that $B^2 < B_s^2$ in the region $r > r_s$. Since $\Lambda > 0$, the denominator is also positive. So $dr/dt|_{\text{out, } r>r_s}$ is positive in the region $r > r_s$.

For ingoing radial null geodesics, we have:

$$\frac{dr}{dt}\Big|_{\text{in, } r\geq r_s} = \frac{-EB - \sqrt{\left(\frac{45}{16\alpha^2} - \frac{1}{2}\left(B^2 - E^2\right)\right)^2 - \left(\frac{45}{16\alpha^2} - \frac{1}{2}\left(B^2 - E^2\right)\right)\left(B^2 - E^2\right)}}{E^2 + \frac{45}{16\alpha^2} - \frac{1}{2}\left(B^2 - E^2\right)}, \tag{5.85}$$

and $dr/dt|_{\text{in, } r>r_s}$ is negative since $B^2 < B_s^2$ in the region $r > r_s$.

At $r = r_s$, we get:

$$\frac{dr}{dt}\Big|_{\text{out, } r\,=\,r_s} = \frac{B_s\left(|E| - E\right)}{E^2 + B_s^2}, \tag{5.86}$$

and:

$$\left.\frac{dr}{dt}\right|_{\text{in, } r=r_s} = -\frac{B_s\left(|E|+E\right)}{E^2+B_s^2}. \tag{5.87}$$

If E is positive, then $\left.dr/dt\right|_{\text{out, } r=r_s} = 0$; radial outgoing null geodesics at $r = r_s$ are trapped. On the other hand, if E is negative, then $\left.dr/dt\right|_{\text{in, } r=r_s} = 0$; radial ingoing geodesics cannot reach $r = r_s$ from $r > r_s$ (the outside).

It remains to be shown that the nonradial curves are trapped at $r = r_s$. To this end, suppose that we have an arbitrary null curve in the effective spacetime. We write:

$$0 = \widetilde{g}_{tt} + 2\widetilde{g}_{tr}\frac{dr}{dt} + \widetilde{g}_{rr}\left(\frac{dr}{dt}\right)^2 + \widetilde{g}_{\theta\theta}\left(\frac{d\theta}{dt}\right)^2 + \widetilde{g}_{zz}\left(\frac{dz}{dt}\right)^2, \tag{5.88}$$

with $\widetilde{g}_{\mu\nu}$ given by Equations (5.75) - (5.79). Then:

$$\frac{dr}{dt} = \frac{-\widetilde{g}_{tr} \pm \sqrt{\widetilde{g}_{tr}^{\,2} - \widetilde{g}_{tt}\widetilde{g}_{rr} - \widetilde{g}_{rr}\left(\widetilde{g}_{\theta\theta}\left(\frac{d\theta}{dt}\right)^2 + \widetilde{g}_{zz}\left(\frac{dz}{dt}\right)^2\right)}}{\widetilde{g}_{rr}} \tag{5.89}$$

We claim that:

$$\frac{-\widetilde{g}_{tr} + \sqrt{\widetilde{g}_{tr}^{\,2} - \widetilde{g}_{tt}\widetilde{g}_{rr}}}{\widetilde{g}_{rr}} \leq \frac{dr}{dt} \leq \frac{-\widetilde{g}_{tr} - \sqrt{\widetilde{g}_{tr}^{\,2} - \widetilde{g}_{tt}\widetilde{g}_{rr}}}{\widetilde{g}_{rr}}. \tag{5.90}$$

That is, an arbitrary null curve cannot climb up to larger radii faster than a radially outward geodesic, and cannot fall down to smaller radii faster than a radially inward geodesic. In other words, nonradial null curves are trapped if the radial null geodesics are trapped.

Note that in order to prove the claim, it suffices to show that $\widetilde{g}_{rr} < 0$ and $\widetilde{g}_{\theta\theta} < 0$.

We get that $\widetilde{g}_{rr}$ $(= -1 - \Lambda E^2)$ is negative since $\Lambda > 0$.

To get $\widetilde{g}_{\theta\theta} = -r^2 + \Lambda r^2(B^2 - E^2) < 0$, it suffices to show that $B^2 - E^2 < 1/\Lambda$. To this end, note that:

$$\begin{aligned} B^2 - E^2 &\leq B_s^2 - E^2 \\ &< \frac{15}{8\alpha^2}. \end{aligned} \tag{5.91}$$

Muliplying both sides of (5.91) by 3/2, we get:

$$\frac{3}{2}\left(B^2-E^2\right)<\frac{45}{16\alpha^2}, \tag{5.92}$$

so:

$$\begin{aligned} B^2-E^2 &< \frac{45}{16\alpha^2}-\frac{1}{2}\left(B^2-E^2\right) \\ &= \frac{1}{\Lambda}. \end{aligned} \tag{5.93}$$

□

Theorem 10. *For* $\frac{45}{34\alpha^2} < E^2 < \frac{9}{4\alpha^2}$*, the effective geometry for the* $(-)$ *polarization state contains a black hole (if* $E>0$*), or a white-hole (if* $E<0$*), with an effective event horizon at* $r=r_c$ *such that* $r>r_s$*. In fact,* $r_c = 9k\sqrt{5}/\left(7\alpha E^2\sqrt{18-8\alpha^2E^2}\right)$*.*

Proof. For the $(-)$ polarization state, with $E^2>45/(34\alpha^2)$, Equation (5.74) gives:

$$\frac{1}{\Lambda} = \frac{45}{28\alpha^2}+\frac{5}{7}\left(B^2-E^2\right). \tag{5.94}$$

Since $E^2<9/(4\alpha^2)$, we have that $\Lambda>0$.

At $r=r_s$:

$$\frac{1}{\Lambda}\Big|_{r=r_s} = \frac{495-80\alpha^2E^2}{168\alpha^2}. \tag{5.95}$$

Moreover, for outgoing radial null geodesics, Equation (5.80) gives:

$$\frac{dr}{dt}\Big|_{\text{out, } r=r_s} = \left(\frac{-168\alpha^2E+4\alpha\sqrt{30(99-16\alpha^2E^2)}}{495+88\alpha^2E^2}\right)B_s, \tag{5.96}$$

which is negative if $E>+\sqrt{45/(34\alpha^2)}$. This means that the outgoing radial geodesics, initiated from $r=r_s$, are compelled to fall down to smaller radii. At the other extreme ($r=\infty$), note that:

$$\frac{dr}{dt}\Big|_{\text{out, } r=\infty} = \frac{1}{\sqrt{1+\Lambda E^2}}>0. \tag{5.97}$$

Hence, by the intermediate-value-theorem, there is a radius r_c, which is greater than r_s and less than ∞, where $dr/dt\Big|_{\text{out},\ r=r_c} = 0$ (black hole event horizon at r_c, if $E > \sqrt{45/(34\alpha^2)}$).

In fact, the critical radius r_c is unique and we can calculate it. If we set the left hand side of Equation (5.80) equal to 0, and solve for B, then we find that there is only one real-valued positive solution, namely:

$$B_c = \sqrt{\frac{45 - 20\alpha^2 E^2}{8\alpha^2}}. \tag{5.98}$$

Thereby, using (5.71), we get:

$$\begin{aligned} r_c &= \frac{k}{B_c + \frac{8\alpha^2}{45}\left(E^2 B_c - B_c^3\right)} \\ &= \frac{9k\sqrt{5}}{7\alpha E^2\sqrt{18 - 8\alpha^2 E^2}}. \end{aligned} \tag{5.99}$$

Note that $dr/dt|_{\text{out}}$ changes sign at $r = r_c$ since $dr/dt|_{\text{out},r=r_s}$ is negative and $dr/dt|_{\text{out},r=\infty}$ is positive. That is, any outgoing geodesic in the region $r < r_c$ is compelled to fall inward to smaller r; any outgoing geodesic in the region $r > r_c$ will escape to larger r.

Next we consider the ingoing null geodesics. For these, Equation (5.80) gives:

$$\frac{dr}{dt}\Big|_{\text{in},\ r\,=\,r_s} = \left(\frac{-168\alpha^2 E - 4\alpha\sqrt{30(99 - 16\alpha^2 E^2)}}{495 + 88\alpha^2 E^2}\right) B_s, \tag{5.100}$$

This is positive if $E < -\sqrt{45/(34\alpha^2)}$. At $r = \infty$, we have:

$$\frac{dr}{dt}\Big|_{\text{in},\ r=\infty} = -\frac{1}{\sqrt{1 + \Lambda E^2}} < 0. \tag{5.101}$$

Thus, if E is negative, there is a radius r_c, between r_s and ∞, where $dr/dt\Big|_{\text{in},\ r=r_c} = 0$ (white hole event horizon at r_c). The quantity $dr/dt\Big|_{\text{in}}$ changes sign at r_c in such a way that ingoing geodesics issuing from the region $r < r_c$ will be compelled to escape outward to larger r, and ingoing geodesics issuing from $r > r_c$ will fall inward to smaller r.

As in the proof of the previous theorem, we get that the nonradial geodesics are trapped by the event horizon by showing that $\widetilde{g}_{\theta\theta} < 0$ and $\widetilde{g}_{rr} < 0$. The fact that $\Lambda > 0$ gives $\widetilde{g}_{rr} < 0$.

As before, to get $\widetilde{g}_{\theta\theta} < 0$, it suffices to show that $B^2 - E^2 < 1/\Lambda$. To this end, note that:

$$\begin{aligned} B^2 - E^2 &\leq B_s^2 - E^2 \\ &< \frac{45}{8\alpha^2}. \end{aligned} \tag{5.102}$$

Multiplying both sides of (5.102) by $2/7$, we get:

$$\frac{2}{7}\left(B^2 - E^2\right) < \frac{45}{28\alpha^2}, \tag{5.103}$$

so:

$$\begin{aligned} B^2 - E^2 &< \frac{45}{28\alpha^2} + \frac{5}{7}\left(B^2 - E^2\right) \\ &= \frac{1}{\Lambda}. \end{aligned} \tag{5.104}$$

□

Bibliography

[1] Gibbons. "Solitons and black holes in 4, 5 dimensions". *Lecture Notes in Physics*, 246, 1986.

[2] Sulem and Sulem. *The Nonlinear Schrödinger Equation: Self-Focusing and Wave Collapse*. New York: Spinger-Verlag, 1999.

[3] Drazin and Johnson. *Solitons: an Introduction*. Cambridge: Cambridge University Press, 1989.

[4] Hawking and Ellis. *The Large Scale Structure of Space-time*. Cambridge: Cambridge University Press, 1973.

[5] Heisenberg and Euler. "Folgerungen aus der Diracschen theorie des positrons". *Zeitschrift für Physik*, 98, 1936. An English translation by Korolevski and Kleinert is available at arXiv:physics/0605038.

[6] Schwinger. "On gauge invariance and vacuum polarization". *Physical Review*, 82, 1951.

[7] Novello. *Artificial Black Holes*, chapter 11, pages 267 – 306. New Jersey: World Scientific, 2002.

[8] Boer and van Holten. "Exploring the QED vacuum with laser interferemeters". arXiv:hep-ph/0204207.

[9] Delphenich. "Nonlinear optical analogies in quantum electrodynamics". arXiv:hep-th/0610088.

[10] Soljačić and Segev. "Self-trapping of electromagnetic beams in vacuum supported by QED nonlinear effects". *Physical Review A*, 62, 2000.

[11] Brodin, Stenflo, Anderson, Lisak, Marklund, and Johannisson. "Light bullets and optical collapse in vacuum". *Physics Letters A*, 306, 2003. arXiv:physics/0204013.

[12] Drummond and Hathrell. "QED vacuum polarization in a background gravitational field and its effect on the velocity of photons". *Physical Review D*, 22(2), 1980.

[13] Spivak. *A Comprehensive Introduction to Differential Geometry*, volume 2. Houston: Publish or Perish, Inc., 3rd edition, 1999.

[14] Landau and Lifshitz. *The Classical Theory of Fields*. Oxford: Pergamon Press, 4th edition, 1975. English translation by Hamermesh.

[15] De Lorenci, Klippert, Novello, and Salim. "Light propagation in non-linear electrodynamics". *Physics Letters B*, 482, 2000. arXiv:gr-qc/005049.

[16] Poisson. *A Relativist's Toolkit: The Mathematics of Black-Hole Mechanics*. Cambridge: Cambridge University Press, 2004.

[17] Novello, De Lorenci, Salim, and Klippert. "Geometrical aspects of light propagation in nonlinear electrodynamics". *Physical Review D*, 61, 2000. arXiv:gr-qc/9911085.

[18] Novello and Salim. "Effective electromagnetic geometry". *Physical Review D*, 63, 2001.

[19] Novello and Perez Bergliaffa. "Effective geometry". *AIP Conf. Proc.*, 668, 2003. arXiv:gr-qc/0302052.

[20] Papapetrou. *Lectures on General Relativity*. Dordrecht-Holland; Boston: D. Reidel Publishing Co., 1974.

[21] Rudin. *Principles of Mathematical Analysis*. Auckland: McGraw-Hill International, 3rd edition, 1976.

[22] Penrose and Rindler. *Spinors and Space-time: Two-spinor calculus and relativistic fields*, volume 1. Cambridge: Cambridge University Press, 1984.

[23] Madsen and Tornehave. *From Calculus to Cohomology: de Rham cohomology and characteristic classes*. Cambridge: Cambridge University Press, 1997.

[24] Bialynicka-Birula and Bialynicki-Birula. "Nonlinear effects in quantum electrodynamics. photon propagation and photon splitting in an external field". *Physical Review D*, 2, 1970.

[25] de Oliveira Costa and Perez Bergliaffa. "A classification of the effective metric in nonlinear electrodynamics". *Class. Quantum Grav.*, 26, 2009. arXiv:gr-qc/0905.3673.

[26] Denisov and Denisova. "On the effective metric for an electromagnetic wave propagating in the field of an intense laser radiation". *Russian Physics Journal*, 45, 2002. English translation by Tsiolkovsky, from *Izvestiya Vysshykh Uchebnykh Zavedenii, Fizika*, No. 1, pp. 11 - 13, January 2002. Original article submitted May 11, 2000.

[27] Affleck. "Photon propagation in a plane-wave field". *J. Phys. A: Math. Gen.*, 21, 1988.

[28] Hall and Negm. "Physical structure of the energy-momentum tensor in general relativity". *International Journal of Theoretical Physics*, 25, 1986.

[29] Boillat. "Nonlinear electrodynamics: Lagrangians and equations of motion". *Journal of Mathematical Physics*, 11, 1970.

[30] Bowman. *Introduction to Bessel Functions*. New York: Dover Publications Inc., 1958.

[31] Arfken and Weber. *Mathematical Methods for Physicists*. San Diego: Harcourt Academic Press, 5th edition, 2001.

[32] Müller and Grave. "Catalogue of spacetimes". arXiv:gr-qc/0904.4184.

[33] Parker. `http://wps.aw.com/aw_hartle_gravity_1/7/2001/512494.cw/index.html`. *Mathematica* notebooks. Supplementary material for the textbook *Gravity* by Hartle.

Appendix A

Mathematica notebook

The purpose of this appendix is to show how *Mathematica* (version 8) can be used to check or carry out the calculations in 5.1 and 5.2. Our implementation of tensor calculus in *Mathematica* is modeled on applications found elsewhere, such Müller and Grave[32] and the downloadable notebooks of Parker.[33]

Let us begin by clearing out the variables that will be used:

Clear[coord, $t, r, \theta, z, i, j, k, l, u, v$, metric,cometric, affine, Afield, faraday, faraday1, faraday2, Fspecialcase, maxwell, Gspecialcase,maxwell1, maxwell2, substress, ecometric, Λ, emetric, simplifiedemetric, α, lambdaplus, lambdaminus, radA1, radA2, radB1, radB2, CDfaraday2, s, o, Ffaraday2, CDFfaraday2, Gmaxwell2, CDGmaxwell2, righthandside, U, V, ω, A]

Next, we specify the coordinate system (cylindrical coordinates) and the background metric (Minkowski spacetime):

coord:=coord = $\{t, r, \theta, z\}$

metric:=metric = $\{\{1,0,0,0\},\{0,-1,0,0\},\{0,0,-r^2,0\},\{0,0,0,-1\}\}$

The background cometric is computed by entering:

cometric:=cometric = Inverse[metric]

The Christoffel symbols (for the background metric) are calculated by entering:

affine:=affine = FullSimplify[

Table[$\frac{1}{2}$Sum[(cometric[[k, l]])$*$ (D[metric[[i, l]], coord[[j]]]+

D[metric[[j, l]], coord[[i]]] − D[metric[[i, j]], coord[[l]]]),

{l, 1, 4}], {k, 1, 4}, {i, 1, 4}, {j, 1, 4}]]

A.1 The field tensors

Our first task is to check the results given in Section 5.1.1. To this end, we input the A-field that we wish to study (coinciding with Equations (5.9) - (5.12)):

Afield:=Afield = {0, 0, u[t, r], v[t, r]}

Next we computer the field tensor $F_{\mu\nu}$, called "faraday:"

faraday:= faraday =

Table[D[Afield[[j]], coord[[i]]] − D[Afield[[i]], coord[[j]]], {i, 1, 4}, {j, 1, 4}]

The components of $F_{\mu\nu}$ are displayed by entering:

faraday//MatrixForm

$$\begin{pmatrix} 0 & 0 & u^{(1,0)}[t,r] & v^{(1,0)}[t,r] \\ 0 & 0 & u^{(0,1)}[t,r] & v^{(0,1)}[t,r] \\ -u^{(1,0)}[t,r] & -u^{(0,1)}[t,r] & 0 & 0 \\ -v^{(1,0)}[t,r] & -v^{(0,1)}[t,r] & 0 & 0 \end{pmatrix} \tag{A.1}$$

In *Mathematica*, $u^{(1,0)}[t,r]$ denotes $\partial_t u$, and $u^{(0,1)}[t,r]$ denotes $\partial_r u$, etc. This output agrees with Equation (5.13).

Raising the first index, we get $F^{\mu}{}_{\nu}$. Call this "faraday1:"

faraday1:= faraday1 = FullSimplify[

Table[Sum[cometric[[i, k]]faraday[[k, j]],{k, 1, 4}], {i, 1, 4}, {j, 1, 4}]]

Displaying the components of $F^{\mu}{}_{\nu}$ in matrix form, as in Equation (5.14):

faraday1//MatrixForm

$$\begin{pmatrix} 0 & 0 & u^{(1,0)}[t,r] & v^{(1,0)}[t,r] \\ 0 & 0 & -u^{(0,1)}[t,r] & -v^{(0,1)}[t,r] \\ \frac{u^{(1,0)}[t,r]}{r^2} & \frac{u^{(0,1)}[t,r]}{r^2} & 0 & 0 \\ v^{(1,0)}[t,r] & v^{(0,1)}[t,r] & 0 & 0 \end{pmatrix} \tag{A.2}$$

Raising the second index, we get $F^{\mu\nu}$ ("faraday2"):

faraday2:= faraday2 = FullSimplify[

Table[Sum[cometric[[k, j]]faraday1[[i, k]],{k, 1, 4}], {i, 1, 4}, {j, 1, 4}]]

As in Equation (5.15), we have:

faraday2//MatrixForm

$$\begin{pmatrix} 0 & 0 & -\frac{u^{(1,0)}[t,r]}{r^2} & -v^{(1,0)}[t,r] \\ 0 & 0 & \frac{u^{(0,1)}[t,r]}{r^2} & v^{(0,1)}[t,r] \\ \frac{u^{(1,0)}[t,r]}{r^2} & -\frac{u^{(0,1)}[t,r]}{r^2} & 0 & 0 \\ v^{(1,0)}[t,r] & -v^{(0,1)}[t,r] & 0 & 0 \end{pmatrix} \tag{A.3}$$

We get that the F-invariant is, in agreement with (5.16):

Fspecialcase = Simplify[Sum[faraday[[i, j]]faraday2[[i, j]],{i, 1, 4}, {j, 1, 4}]]

$$2\left(\frac{u^{(0,1)}[t,r]^2}{r^2} + v^{(0,1)}[t,r]^2 - \frac{u^{(1,0)}[t,r]^2}{r^2} - v^{(1,0)}[t,r]^2\right) \tag{A.4}$$

For the dual tensor ${F^*}_{\mu\nu}$ ("maxwell":)

maxwell:=maxwell = FullSimplify[Table [$\frac{1}{2}$Sqrt[−Det[metric]]

Sum[Signature[{i, j, k, l}]faraday2[[i, j]],{i, 1, 4}, {j, 1, 4}], {k, 1, 4}, {l, 1, 4}], r ≥ 0]

Displaying ${F^*}_{\mu\nu}$ as a matrix, as in Equation (5.17):

maxwell//MatrixForm

$$\begin{pmatrix} 0 & 0 & -rv^{(0,1)}[t,r] & \frac{u^{(0,1)}[t,r]}{r} \\ 0 & 0 & -rv^{(1,0)}[t,r] & \frac{u^{(1,0)}[t,r]}{r} \\ rv^{(0,1)}[t,r] & rv^{(1,0)}[t,r] & 0 & 0 \\ -\frac{u^{(0,1)}[t,r]}{r} & -\frac{u^{(1,0)}[t,r]}{r} & 0 & 0 \end{pmatrix} \tag{A.5}$$

The G-invariant is, in agreement with Equation (5.18):

Gspecialcase = Sum[maxwell[[i, j]]faraday2[[i, j]],{i, 1, 4}, {j, 1, 4}]

$$\frac{4v^{(0,1)}[t,r]u^{(1,0)}[t,r]}{r} - \frac{4u^{(0,1)}[t,r]v^{(1,0)}[t,r]}{r} \tag{A.6}$$

To get $F^{*\mu}{}_{\nu}$, enter:

```
maxwell1:= maxwell1 = FullSimplify[
Table[Sum[cometric[[i, k]]maxwell[[k, j]],{k, 1, 4}], {i, 1, 4}, {j, 1, 4}]]
```

For $F^{*\mu\nu}$, enter:

```
maxwell2:= maxwell2 = FullSimplify[
Table[Sum[cometric[[k, j]]maxwell1[[i, k]],{k, 1, 4}], {i, 1, 4}, {j, 1, 4}]]
```

The components of $F^{*\mu\nu}$, as in (5.19), are:

```
maxwell2//MatrixForm
```

$$\begin{pmatrix} 0 & 0 & \frac{v^{(0,1)}[t,r]}{r} & -\frac{u^{(0,1)}[t,r]}{r} \\ 0 & 0 & -\frac{v^{(1,0)}[t,r]}{r} & \frac{u^{(1,0)}[t,r]}{r} \\ -\frac{v^{(0,1)}[t,r]}{r} & \frac{v^{(1,0)}[t,r]}{r} & 0 & 0 \\ \frac{u^{(0,1)}[t,r]}{r} & -\frac{u^{(1,0)}[t,r]}{r} & 0 & 0 \end{pmatrix} \tag{A.7}$$

A.2 The effective metric coefficients

Now let us check Section 5.1.2. To this end, we calculate the substress tensor $F^{\mu}{}_{\lambda}F^{\lambda\nu}$:

```
substress:= substress = FullSimplify[
Table[Sum[faraday1[[i, k]]faraday2[[k, j]],{k, 1, 4}], {i, 1, 4}, {j, 1, 4}]]
```

The nonzero components of the substress are displayed upon entering the lines:

```
Do[If[UnsameQ[substress[[i, j]], 0],
CellPrint[
DisplayForm[
RowBox[
{SubscriptBox[SuperscriptBox["F", coord[[i]]],
"λ"], SuperscriptBox["F",
RowBox[{"λ", coord[[j]]}]], "=",
substress[[i, j]]}]]
] ], {i, 1, 4}, {j, 1, 4}]
```

$F^t{}_\lambda F^{\lambda t} = \frac{u^{(1,0)}[t,r]^2}{r^2} + v^{(1,0)}[t,r]^2$

$F^t{}_\lambda F^{\lambda r} = -\frac{u^{(0,1)}[t,r]u^{(1,0)}[t,r]}{r^2} - v^{(0,1)}[t,r]v^{(1,0)}[t,r]$

$F^r{}_\lambda F^{\lambda t} = -\frac{u^{(0,1)}[t,r]u^{(1,0)}[t,r]}{r^2} - v^{(0,1)}[t,r]v^{(1,0)}[t,r]$

$F^r{}_\lambda F^{\lambda r} = \frac{u^{(0,1)}[t,r]^2}{r^2} + v^{(0,1)}[t,r]^2$

$F^\theta{}_\lambda F^{\lambda \theta} = \frac{u^{(0,1)}[t,r]^2 - u^{(1,0)}[t,r]^2}{r^4}$

$F^\theta{}_\lambda F^{\lambda z} = \frac{u^{(0,1)}[t,r]v^{(0,1)}[t,r] - u^{(1,0)}[t,r]v^{(1,0)}[t,r]}{r^2}$

$F^z{}_\lambda F^{\lambda \theta} = \frac{u^{(0,1)}[t,r]v^{(0,1)}[t,r] - u^{(1,0)}[t,r]v^{(1,0)}[t,r]}{r^2}$

$F^z{}_\lambda F^{\lambda z} = v^{(0,1)}[t,r]^2 - v^{(1,0)}[t,r]^2$

The output above agrees with Equations (5.22) - (5.27).

To calculate the effective cometric, enter:

ecometric:=ecometric = cometric + Λ substress

Here, Λ stands for $\Lambda_\pm$ in Equation (3.44). The effective metric is calculated by entering:

emetric:=emetric = Inverse[ecometric]

Let us multiply the effective metric by a certain conformal factor; this choice of conformal factor considerably simplifies the effective metric coefficients:

simplifiedemetric:= simplifiedemetric =

FullSimplify[− (((−1 + Λ $v^{(0,1)}[t,r]^2$) (r^2 + Λ $u^{(1,0)}[t,r]^2$) −

2Λ^2 $u^{(0,1)}[t,r]v^{(0,1)}[t,r]u^{(1,0)}[t,r]$ $v^{(1,0)}[t,r]$−

r^2Λ $v^{(1,0)}[t,r]^2$ + Λ $u^{(0,1)}[t,r]^2$ (1 + Λ $v^{(1,0)}[t,r]^2$)) /r^2)emetric]

The nonzero components of the conformally rescaled effective metric are displayed upon entering the lines:

Do[If[UnsameQ[simplifiedemetric[[i, j]], 0],

CellPrint[DisplayForm[

RowBox[{coord[[i]], coord[[j]], "-comp",

"=", simplifiedemetric[[i, j]]}]]

]], {i, 1, 4}, {j, 1, 4}]

$$tt - \text{comp} = 1 - \frac{\Lambda u^{(0,1)}[t,r]^2}{r^2} - \Lambda v^{(0,1)}[t,r]^2$$

$$tr - \text{comp} = -\frac{\Lambda u^{(0,1)}[t,r] u^{(1,0)}[t,r]}{r^2} - \Lambda v^{(0,1)}[t,r] v^{(1,0)}[t,r]$$

$$rt - \text{comp} = -\frac{\Lambda u^{(0,1)}[t,r] u^{(1,0)}[t,r]}{r^2} - \Lambda v^{(0,1)}[t,r] v^{(1,0)}[t,r]$$

$$rr - \text{comp} = -1 - \frac{\Lambda u^{(1,0)}[t,r]^2}{r^2} - \Lambda v^{(1,0)}[t,r]^2$$

$$\theta\theta - \text{comp} = r^2 \left(-1 + \Lambda v^{(0,1)}[t,r]^2 - \Lambda v^{(1,0)}[t,r]^2\right)$$

$$\theta z - \text{comp} = -\Lambda u^{(0,1)}[t,r] v^{(0,1)}[t,r] + \Lambda u^{(1,0)}[t,r] v^{(1,0)}[t,r]$$

$$z\theta - \text{comp} = -\Lambda u^{(0,1)}[t,r] v^{(0,1)}[t,r] + \Lambda u^{(1,0)}[t,r] v^{(1,0)}[t,r]$$

$$zz - \text{comp} = -\frac{r^2 - \Lambda u^{(0,1)}[t,r]^2 + \Lambda u^{(1,0)}[t,r]^2}{r^2}$$

This output agrees with Equations (5.28) - (5.33).

A.3 The radial null geodesics

Now we check Equations (5.36) and (5.37) from Section 5.1.3, which concerns radial null geodesics in the effective geometry. To this end, we will need to let *Mathematica* compute the values $\Lambda_\pm$ from Equation (3.44). The value Λ_+ is designated "lambdaplus," and Λ_- is designated "lambdaminus:"

lambdaplus:= lambdaplus = (224α²)/(495 + 12Fspecialcase α²−
Sqrt [18225 − 18360Fspecialcase α²+ 4624Fspecialcase² α⁴ + 3136Gspecialcase² α⁴])

lambdaminus:= lambdaminus = (224α²)/(495 + 12Fspecialcase α²+
Sqrt [18225 − 18360Fspecialcase α²+ 4624Fspecialcase² α⁴ + 3136Gspecialcase² α⁴])

The choice of $\pm$ in the calculation of $\Lambda_\pm$ depends on the polarization state of the photon. We call these the $+$ and $-$ polarization states (corresponding to Λ_+ and Λ_-, respectively).

Using Equation (5.35), we get that for outgoing geodesics in the $+$ polarization state, dr/dt expanded as a series in α is:

radA1 = FullSimplify[Series[
(−D[u[t, r], t]D[u[t, r], r]− r²D[v[t, r], t]D[v[t, r], r]+

```
Sqrt[ (D[u[t, r], t] D[u[t, r], r] + r^2 D[v[t, r], t] D[v[t, r], r])^2 +
 (r^2/lambdaplus - D[u[t, r], r]^2 - r^2 D[v[t, r], r]^2)
  (r^2/lambdaplus + D[u[t, r], t]^2 + r^2 D[v[t, r], t]^2)]) /
 (r^2/lambdaplus + D[u[t, r], t]^2 + r^2 D[v[t, r], t]^2),
 {α, 0, 3}], r^2 ≥ 0]
```

$$1 - \frac{1}{45r^2} 14 \left(\left(u^{(0,1)}[t,r] + u^{(1,0)}[t,r] \right)^2 + r^2 \left(v^{(0,1)}[t,r] + v^{(1,0)}[t,r] \right)^2 \right) \alpha^2 + O[\alpha]^4 \qquad \text{(A.8)}$$

For outgoing geodesics in the − polarization state:

```
radA2 = FullSimplify[Series[
(-D[u[t, r], t] D[u[t, r], r] - r^2 D[v[t, r], t] D[v[t, r], r] +
 Sqrt[ (D[u[t, r], t] D[u[t, r], r] + r^2 D[v[t, r], t] D[v[t, r], r])^2 +
  (r^2/lambdaminus - D[u[t, r], r]^2 - r^2 D[v[t, r], r]^2)
   (r^2/lambdaminus + D[u[t, r], t]^2 + r^2 D[v[t, r], t]^2)]) /
 (r^2/lambdaminus + D[u[t, r], t]^2 + r^2 D[v[t, r], t]^2),
 {α, 0, 3}], r^2 ≥ 0]
```

$$1 - \frac{1}{45r^2} 8 \left(\left(u^{(0,1)}[t,r] + u^{(1,0)}[t,r] \right)^2 + r^2 \left(v^{(0,1)}[t,r] + v^{(1,0)}[t,r] \right)^2 \right) \alpha^2 + O[\alpha]^4 \qquad \text{(A.9)}$$

Outputs (A.8) and (A.9) imply Equation (5.37).

For the ingoing geodesics with + polarization:

```
radB1 = FullSimplify[Series[
(-D[u[t, r], t] D[u[t, r], r] - r^2 D[v[t, r], t] D[v[t, r], r] -
 Sqrt[ (D[u[t, r], t] D[u[t, r], r] + r^2 D[v[t, r], t] D[v[t, r], r])^2 +
  (r^2/lambdaplus - D[u[t, r], r]^2 - r^2 D[v[t, r], r]^2)
   (r^2/lambdaplus + D[u[t, r], t]^2 + r^2 D[v[t, r], t]^2)]) /
```

```
(r^2/lambdaplus + D[u[t,r],t]^2 + r^2 D[v[t,r],t]^2),
{α,0,3}],r^2 ≥ 0]
```

$$-1+\frac{1}{45r^2}14\left(\left(u^{(0,1)}[t,r]-u^{(1,0)}[t,r]\right)^2+r^2\left(v^{(0,1)}[t,r]-v^{(1,0)}[t,r]\right)^2\right)\alpha^2+O[\alpha]^4 \tag{A.10}$$

For the ingoing geodesics with $-$ polarization:

```
radB2 = FullSimplify[Series[
(-D[u[t,r],t]D[u[t,r],r]- r^2 D[v[t,r],t]D[v[t,r],r]-
Sqrt[ (D[u[t,r],t]D[u[t,r],r]+ r^2 D[v[t,r],t]D[v[t,r],r])^2 +
(r^2/lambdaminus - D[u[t,r],r]^2 - r^2 D[v[t,r],r]^2)
(r^2/lambdaminus + D[u[t,r],t]^2 + r^2 D[v[t,r],t]^2)]]/
(r^2/lambdaminus + D[u[t,r],t]^2 + r^2 D[v[t,r],t]^2),
{α,0,3}],r^2 ≥ 0]
```

$$-1+\frac{1}{45r^2}8\left(\left(u^{(0,1)}[t,r]-u^{(1,0)}[t,r]\right)^2+r^2\left(v^{(0,1)}[t,r]-v^{(1,0)}[t,r]\right)^2\right)\alpha^2+O[\alpha]^4 \tag{A.11}$$

Outputs (A.10) and (A.11) imply Equation (5.36).

A.4 The field equations

Our next task is to derive the nonlinear PDEs (5.44) which arise from the Euler-Heisenberg field equation (2.21) together with the cylindrical field ansatz presently under consideration. Since we wish to express these PDEs in terms of the functions v and $\hat{u} = u/r$, we will go back and re-enter the field tensor, so that *in the present section,* $u[t,r]$ *should be read as* "$\hat{u}[t,r]$". To this end, we will clear out and recompute the relevant variables:

```
Clear[Afield, faraday, faraday1, faraday2, Fspecialcase,
maxwell, Gspecialcase, maxwell1,maxwell2]
```

We re-enter the A-field as:

$$\textbf{Afield:=Afield} = \{0, 0, r\ u[t, r], v[t, r]\}$$

Recalculating $F_{\mu\nu}$:

$$\textbf{faraday:= faraday} = \textbf{Table}[D[\textbf{Afield}[[j]], \textbf{coord}[[i]]] -$$

$$D[\textbf{Afield}[[i]], \textbf{coord}[[j]]], \{i, 1, 4\}, \{j, 1, 4\}]$$

$F^{\mu}{}_{\nu}$:

$$\textbf{faraday1:= faraday1} = \textbf{FullSimplify}[\textbf{Table}[\textbf{Sum}[\textbf{cometric}[[i, k]]\textbf{faraday}[[k, j]],$$

$$\{k, 1, 4\}], \{i, 1, 4\}, \{j, 1, 4\}]]$$

$F^{\mu\nu}$:

$$\textbf{faraday2:= faraday2} = \textbf{FullSimplify}[\textbf{Table}[\textbf{Sum}[\textbf{cometric}[[k, j]]\textbf{faraday1}[[i, k]],$$

$$\{k, 1, 4\}], \{i, 1, 4\}, \{j, 1, 4\}]]$$

F:

$$\textbf{Fspecialcase:= Fspecialcase} = \textbf{Simplify}[\textbf{Sum}[\textbf{faraday}[[i, j]]\textbf{faraday2}[[i, j]],$$

$$\{i, 1, 4\}, \{j, 1, 4\}]]$$

$F^{*}_{\mu\nu}$:

$$\textbf{maxwell:=maxwell} = \textbf{FullSimplify}[\textbf{Table}\left[\tfrac{1}{2}\textbf{Sqrt}[-\textbf{Det}[\textbf{metric}]]\right.$$

$$\textbf{Sum}[\textbf{Signature}[\{i, j, k, l\}]\textbf{faraday2}[[i, j]],\{i, 1, 4\}, \{j, 1, 4\}], \{k, 1, 4\}, \{l, 1, 4\}], r \geq 0]$$

G:

$$\textbf{Gspecialcase:=Gspecialcase} = \textbf{Sum}[\textbf{maxwell}[[i, j]]\textbf{faraday2}[[i, j]],$$

$$\{i, 1, 4\}, \{j, 1, 4\}]$$

$F^{*\mu}{}_{\nu}$:

$$\textbf{maxwell1:= maxwell1} = \textbf{FullSimplify}[$$

$$\textbf{Table}[\textbf{Sum}[\textbf{cometric}[[i, k]]\textbf{maxwell}[[k, j]],\{k, 1, 4\}], \{i, 1, 4\}, \{j, 1, 4\}]]$$

$F^{*\mu\nu}$:

$$\textbf{maxwell2:= maxwell2} = \textbf{FullSimplify}[$$

$$\textbf{Table}[\textbf{Sum}[\textbf{cometric}[[k, j]]\textbf{maxwell1}[[i, k]],\{k, 1, 4\}], \{i, 1, 4\}, \{j, 1, 4\}]]$$

Next, we calculate and display the covariant derivative $\nabla_{\mu} F^{\mu\nu}$ by entering:

CDfaraday2:= CDfaraday2 = FullSimplify[

Table[Sum[D[faraday2[[s, o]], coord[[s]]], {s, 1, 4}]+ Sum[affine[[i, i, j]]faraday2[[j, o]],

{i, 1, 4}, {j, 1, 4}]+ Sum[affine[[o, k, l]]faraday2[[k, l]], {k, 1, 4}, {l, 1, 4}], {o, 1, 4}]]

MatrixForm[CDfaraday2]

$$\begin{pmatrix} 0 \\ 0 \\ \frac{-u[t,r]+r\left(u^{(0,1)}[t,r]+r\left(u^{(0,2)}[t,r]-u^{(2,0)}[t,r]\right)\right)}{r^3} \\ \frac{v^{(0,1)}[t,r]}{r}+v^{(0,2)}[t,r]-v^{(2,0)}[t,r] \end{pmatrix} \tag{A.12}$$

This matches Equation (5.40).

Now we must calculate $\frac{\alpha^2}{45}\left(4\nabla_\mu\left(FF^{\mu\nu}\right)+7\nabla_\mu\left(GF^{*\mu\nu}\right)\right)$, which we shall call "righthand-side." To this end, we define $FF^{\mu\nu}$ and $GF^{*\mu\nu}$ as variables "Ffaraday2" and "Gmaxwell2" respectively, then we take their covariant derivatives "CDFfaraday2" and "CDGmaxwell2." Finally, we combine these so as to calculate "righthandside."

We define $FF^{\mu\nu}$ by entering:

Ffaraday2:=Ffaraday2 = Fspecialcase faraday2

Taking the covariant derivative $\nabla_\mu(FF^{\mu\nu})$:

CDFfaraday2:= CDFfaraday2 = FullSimplify[

Table[Sum[D[Ffaraday2[[s, o]], coord[[s]]], {s, 1, 4}]+ Sum[affine[[i, i, j]]Ffaraday2[[j, o]],

{i, 1, 4}, {j, 1, 4}]+ Sum[affine[[o, k, l]]Ffaraday2[[k, l]], {k, 1, 4}, {l, 1, 4}], {o, 1, 4}]]

Defining $GF^{*\mu\nu}$:

Gmaxwell2:=Gmaxwell2 = Gspecialcase maxwell2

Taking the covariant derivative $\nabla_\mu\left(GF^{*\mu\nu}\right)$:

CDGmaxwell2:= CDGmaxwell2 = FullSimplify[

Table[Sum[D[Gmaxwell2[[s, o]], coord[[s]]], {s, 1, 4}]+ Sum[affine[[i, i, j]]Gmaxwell2[[j, o]],

{i, 1, 4}, {j, 1, 4}]+ Sum[affine[[o, k, l]]Gmaxwell2[[k, l]], {k, 1, 4}, {l, 1, 4}], {o, 1, 4}]]

We compute $\frac{\alpha^2}{45}\left(4\nabla_\mu\left(FF^{\mu\nu}\right)+7\nabla_\mu\left(GF^{*\mu\nu}\right)\right)$ by entering:

righthandside:= righthandside = FullSimplify $\left[\frac{4\alpha^2}{45}$CDFfaraday2 + $\frac{7\alpha^2}{45}$CDGmaxwell2$\right]$

We note that Equation (5.41) checks out since:

righthandside[[1]]

0

and:

righthandside[[2]]

0

moreover $\mathcal{U}$ is given by:

righthandside[[3]] * $(45r^5/(4\alpha^2))$

$$
\begin{aligned}
&-6u[t,r]^3+2ru[t,r]^2\left(-3u^{(0,1)}[t,r]+3ru^{(0,2)}[t,r]-ru^{(2,0)}[t,r]\right)+\\
&r^2u[t,r]\left(6u^{(0,1)}[t,r]^2-2v^{(0,1)}[t,r]^2-5v^{(1,0)}[t,r]^2-\right.\\
&\left.2u^{(1,0)}[t,r]\left(u^{(1,0)}[t,r]+4ru^{(1,1)}[t,r]\right)+\right.\\
&\left.3rv^{(1,0)}[t,r]v^{(1,1)}[t,r]+4ru^{(0,1)}[t,r]\left(3u^{(0,2)}[t,r]-u^{(2,0)}[t,r]\right)+\right.\\
&\left.rv^{(0,1)}[t,r]\left(4v^{(0,2)}[t,r]-7v^{(2,0)}[t,r]\right)\right)+\\
&r^3\left(6u^{(0,1)}[t,r]^3+v^{(0,1)}[t,r]\left(-7v^{(1,0)}[t,r]\left(u^{(1,0)}[t,r]+2ru^{(1,1)}[t,r]\right)+\right.\right.\\
&\left.\left.3ru^{(1,0)}[t,r]v^{(1,1)}[t,r]\right)+rv^{(0,1)}[t,r]^2\left(2u^{(0,2)}[t,r]+5u^{(2,0)}[t,r]\right)+\right.\\
&\left.u^{(0,1)}[t,r]^2\left(6ru^{(0,2)}[t,r]-2ru^{(2,0)}[t,r]\right)+\right.\\
&\left.u^{(0,1)}[t,r]\left(2v^{(0,1)}[t,r]^2-6u^{(1,0)}[t,r]^2-\right.\right.\\
&\left.\left.8ru^{(1,0)}[t,r]u^{(1,1)}[t,r]+v^{(1,0)}[t,r]\left(5v^{(1,0)}[t,r]+3rv^{(1,1)}[t,r]\right)+\right.\right.\\
&\left.\left.rv^{(0,1)}[t,r]\left(4v^{(0,2)}[t,r]-7v^{(2,0)}[t,r]\right)\right)+\right.\\
&\left.r\left(-7v^{(0,2)}[t,r]u^{(1,0)}[t,r]v^{(1,0)}[t,r]+\right.\right.\\
&\left.\left.u^{(0,2)}[t,r]\left(-2u^{(1,0)}[t,r]^2+5v^{(1,0)}[t,r]^2\right)+\right.\right.\\
&\left.\left.2\left(3u^{(1,0)}[t,r]^2+v^{(1,0)}[t,r]^2\right)u^{(2,0)}[t,r]+4u^{(1,0)}[t,r]v^{(1,0)}[t,r]v^{(2,0)}[t,r]\right)\right)
\end{aligned}
$$

and $\mathcal{V}$ is given by:

righthandside[[4]] * (45r^3/(4α^2))

$$
\begin{aligned}
& u[t,r]^2\left(-2v^{(0,1)}[t,r]+2rv^{(0,2)}[t,r]+5rv^{(2,0)}[t,r]\right)+\\
& ru[t,r]\left(v^{(1,0)}[t,r]\left(10u^{(1,0)}[t,r]+3ru^{(1,1)}[t,r]\right)-\right.\\
& 14ru^{(1,0)}[t,r]v^{(1,1)}[t,r]+rv^{(0,1)}[t,r]\left(4u^{(0,2)}[t,r]-7u^{(2,0)}[t,r]\right)+\\
& 2u^{(0,1)}[t,r]\left(2v^{(0,1)}[t,r]+\ 2rv^{(0,2)}[t,r]+5rv^{(2,0)}[t,r]\right)\Big)+\\
& r^2\left(2v^{(0,1)}[t,r]^3-\ v^{(0,1)}[t,r]\left(2u^{(1,0)}[t,r]^2-3ru^{(1,0)}[t,r]u^{(1,1)}[t,r]+\right.\right.\\
& 2v^{(1,0)}[t,r]\left(v^{(1,0)}[t,r]+4rv^{(1,1)}[t,r]\right)\Big)+\\
& u^{(0,1)}[t,r]\left(3rv^{(1,0)}[t,r]u^{(1,1)}[t,r]-\ 2u^{(1,0)}[t,r]\left(2v^{(1,0)}[t,r]+7rv^{(1,1)}[t,r]\right)+\right.\\
& rv^{(0,1)}[t,r]\left(4u^{(0,2)}[t,r]-7u^{(2,0)}[t,r]\right)\Big)+\\
& v^{(0,1)}[t,r]^2\left(6rv^{(0,2)}[t,r]-2rv^{(2,0)}[t,r]\right)+\\
& u^{(0,1)}[t,r]^2\left(6v^{(0,1)}[t,r]+2rv^{(0,2)}[t,r]+5rv^{(2,0)}[t,r]\right)+\\
& r\left(v^{(0,2)}[t,r]\left(5u^{(1,0)}[t,r]^2-2v^{(1,0)}[t,r]^2\right)+\right.\\
& u^{(1,0)}[t,r]v^{(1,0)}[t,r]\left(-7u^{(0,2)}[t,r]+4u^{(2,0)}[t,r]\right)+\\
& \left.2\left(u^{(1,0)}[t,r]^2+3v^{(1,0)}[t,r]^2\right)v^{(2,0)}[t,r]\right)
\end{aligned}
\tag{A.13}
$$

A.5 The Maxwellian approximation

Our next task is to check Equations (5.55) - (5.58). Introducing constants U and V (not to be confused with the functions $\mathcal{U}$ and $\mathcal{V}$ given above), we have that an elliptically polarized ingoing cylindrical wave is given by $u[t,r]$ and $v[t,r]$, where:

u[t, r]:=$\frac{Ur}{\omega}$(BesselJ[1, ωr]Cos[ωt] − BesselY[1, ωr]Sin[ωt])

v[t, r]:= $\frac{V}{\omega}$(BesselJ[0, ωr]Cos[ωt]− BesselY[0, ωr]Sin[ωt])

Note that *the function $u[t,r]$ now reverts back to denoting u $(= A_\theta)$ again, instead of $\hat{u}$.*

In order to calculate dr/dt for ingoing radial null geodesics, the equations of Section 5.1.3 require us to calculate $\frac{1}{r^2}\left((\partial_t u - \partial_r u)^2 + r^2(\partial_t v - \partial_r v)^2\right)$. Thereby we enter the lines:

FullSimplify[

$\frac{1}{r^2}$ **((D[u[t, r], t] − D[u[t, r], r])²+ r²(D[v[t, r], t] − D[v[t, r], r])²)]**

$$\begin{aligned} U^2((\text{BesselJ}[0, r\omega] + \text{BesselY}[1, r\omega])\text{Cos}[t\omega] + \\ (\text{BesselJ}[1, r\omega] - \text{BesselY}[0, r\omega])\text{Sin}[t\omega])^2 + \\ V^2((-\text{BesselJ}[1, r\omega] + \text{BesselY}[0, r\omega])\text{Cos}[t\omega] + \\ (\text{BesselJ}[0, r\omega] + \text{BesselY}[1, r\omega])\text{Sin}[t\omega])^2 \end{aligned} \tag{A.14}$$

This output (A.14) confirms Equation (5.55).

For the outgoing radial null geodesics, we need $\frac{1}{r^2}\left((\partial_t u + \partial_r u)^2 + r^2(\partial_t v + \partial_r v)^2\right)$. To this end, we enter:

FullSimplify[

$\frac{1}{r^2}$ **((D[u[t, r], t] + D[u[t, r], r])²+ r²(D[v[t, r], t] + D[v[t, r], r])²)]**

$$\begin{aligned} U^2((-\text{BesselJ}[0, r\omega] + \text{BesselY}[1, r\omega])\text{Cos}[t\omega] + \\ (\text{BesselJ}[1, r\omega] + \text{BesselY}[0, r\omega])\text{Sin}[t\omega])^2 + \\ V^2((\text{BesselJ}[1, r\omega] + \text{BesselY}[0, r\omega])\text{Cos}[t\omega] + \\ (\text{BesselJ}[0, r\omega] - \text{BesselY}[1, r\omega])\text{Sin}[t\omega])^2 \end{aligned} \tag{A.15}$$

This confirms Equation (5.56).

Henceforth, we restrict to the case of circular polarization, whereby $U = V = A =$ constant.

U*:=*A

V*:=*A

We check Equations (5.57) and (5.58) by re-entering:

FullSimplify[

$\frac{1}{r^2}\left((D[u[t,r],t]-D[u[t,r],r])^2+r^2(D[v[t,r],t]-D[v[t,r],r])^2\right)$

$$A^2\left(-\frac{4}{\pi r\omega}+\text{BesselJ}[0,r\omega]^2+\text{BesselJ}[1,r\omega]^2+\right.$$
$$\left.\text{BesselY}[0,r\omega]^2+\text{BesselY}[1,r\omega]^2\right) \tag{A.16}$$

FullSimplify[

$\frac{1}{r^2}\left((D[u[t,r],t]+D[u[t,r],r])^2+r^2(D[v[t,r],t]+D[v[t,r],r])^2\right)$

$$A^2\left(\frac{4}{\pi r\omega}+\text{BesselJ}[0,r\omega]^2+\text{BesselJ}[1,r\omega]^2+\right.$$
$$\left.\text{BesselY}[0,r\omega]^2+\text{BesselY}[1,r\omega]^2\right) \tag{A.17}$$

The outputs (A.16) and (A.17) confirm Equations (5.57) and (5.58).

Appendix B

Some additional remarks

In Section 5.3.1, we studied effective geometries corresponding to branch I of our exact solution $B + 8\alpha^2(E^2B - B^3)/45 = k/r$ (5.71), with certain restrictions on the constant E. The purpose of this appendix is to take a further look at the effective geometries of our exact solution. We do so only briefly. This appendix is intended to be read as a continuation of Section 5.3.1; we still assume that $k > 0$, and the $(+)$ and $(-)$ polarization states have the same meaning as in Section 5.3.1.

Theorem 11. *For $E = 0$, in the effective geometry of branch I corresponding to the $(+)$ polarization state, the outgoing radial null geodesics, issuing from any point where the effective geometry is defined, are never trapped.*

Proof. For the $(+)$ polarization state, with $E = 0$, Equation (5.74) gives:

$$\frac{1}{\Lambda} = \frac{495 + 24\alpha^2B^2 + \left|135 - 136\alpha^2B^2\right|}{224\alpha^2}. \tag{B.1}$$

We note that there is a particular radius r_1 such that for $r \geq r_1$, we have $B^2 \leq 135/(136\alpha^2)$, and for $r_s \leq r < r_1$, we have $135/(136\alpha^2) < B^2 \leq B_s^2$. Since $E = 0$ in the present case, we have $B_s = 15/(8\alpha^2)$.

So for $r \geq r_1$ Equation (B.1) gives:

$$\frac{1}{\Lambda}\Big|_{r\geq r_1} = \frac{45}{16\alpha^2} - \frac{1}{2}B^2. \tag{B.2}$$

Note that $1/\Lambda|_{r\geq r_1} > 0$.

Using Equation (5.80), we get that:

$$\begin{aligned}\left.\frac{dr}{dt}\right|_{\text{out, } r\geq r_1} &= \frac{-EB + \sqrt{\left(\left.\frac{1}{\Lambda}\right|_{r\geq r_1}\right)^2 - \left(\left.\frac{1}{\Lambda}\right|_{r\geq r_1}\right)(B^2 - E^2)}}{E^2 + \left.\frac{1}{\Lambda}\right|_{r\geq r_1}} \\ &= \sqrt{1 - B^2\Lambda\Big|_{r\geq r_1}}. \end{aligned} \tag{B.3}$$

For $r \geq r_1$, the value of B^2 never exceeds $135/(136\alpha^2)$ ($< B_s^2$), and we observe that this fact implies $\left.dr/dt\right|_{\text{out, } r\geq r_1} = \sqrt{1 - B^2\Lambda\Big|_{r\geq r_1}} > 0$.

In the region where $r_s \leq r < r_1$, we have:

$$\left.\frac{1}{\Lambda}\right|_{r_s\leq r<r_1} = \frac{45}{28\alpha^2} + \frac{5}{7}B^2. \tag{B.4}$$

So:

$$\left.\frac{dr}{dt}\right|_{\text{out, } r_s\leq r<r_1} = \sqrt{1 - B^2\Lambda\Big|_{r_s\leq r<r_1}}. \tag{B.5}$$

For $r_s \leq r < r_1$, the value of B^2 never exceeds B_s^2, and consequently $\left.dr/dt\right|_{\text{out, } r_s<r\leq r_1} = \sqrt{1 - B^2\Lambda\Big|_{r_s<r\leq r_1}} > 0$.

□

Theorem 12. *For $E^2 \leq \frac{45}{34\alpha^2}$, in the effective geometry of branch I corresponding to the $(-)$ polarization state, either $dr/dt_{out,\ r=r_s}$ is zero (when $E > 0$) or $dr/dt_{in,\ r=r_s}$ is zero (if $E < 0$). If $E = 0$, then both $dr/dt_{out,\ r=r_s}$ and $dr/dt_{in,\ r=r_s}$ are zero.*

Proof. Since $E^2 \leq \frac{45}{34\alpha^2}$, we have that for the $(-)$ polarization state, at $r = r_s$:

$$\left.\frac{1}{\Lambda}\right|_{r=r_s} = B_s^2. \tag{B.6}$$

Using (5.80) and (B.6), we get:

$$\left.\frac{dr}{dt}\right|_{\text{out, } r\,=\,r_s} = \frac{B_s\left(|E| - E\right)}{E^2 + B_s^2}, \tag{B.7}$$

and:

$$\left.\frac{dr}{dt}\right|_{\text{in, } r=r_s} = -\frac{B_s\left(|E|+E\right)}{E^2+B_s^2}. \tag{B.8}$$

If $E>0$, then $dr/dt\Big|_{\text{out, } r=r_s} = 0$, and $dr/dt\Big|_{\text{in, } r=r_s} < 0$. On the other hand, if $E<0$, then $dr/dt\Big|_{\text{out, } r=r_s} > 0$, and $dr/dt\Big|_{\text{in, } r=r_s} = 0$. If $E=0$, then $dr/dt\Big|_{\text{out, } r=r_s} = dr/dt\Big|_{\text{in, } r=r_s} = 0$.

□

Now let us say something about branch II. In this branch, B is an increasing function of r; it starts with the value of B_s at $r=r_s$, and increases towards the asymptotic value $\sqrt{3}B_s$ at $r=\infty$.

Theorem 13. *For $E\neq 0$, in branch II, at infinity, the radial null geodesics propagate in only one direction; towards the axis if $E>0$, away from the axis if $E<0$.*

Proof. In the limit $r\to\infty$, we have $B=\sqrt{3}B_s$, and Equation (5.74) gives:

$$\begin{aligned}\left.\frac{1}{\Lambda}\right|_{r=\infty} &= \frac{630\mp 630}{224\alpha^2}\\ &= 0 \text{ or } \frac{45}{8\alpha^2} \text{ (depending on the polarization).}\end{aligned} \tag{B.9}$$

Equation (5.80) gives, for the radial null geodesics (both "ingoing" and "outgoing"):

$$\begin{aligned}\left.\frac{dr}{dt}\right|_{r=\infty} &= \frac{-E\sqrt{E^2+\frac{45}{8\alpha^2}}\mp\sqrt{\frac{1}{\Lambda^2}-\frac{45}{\Lambda\alpha^2}}}{E^2+\frac{1}{\Lambda}}\\ &= \frac{-E\sqrt{E^2+\frac{45}{8\alpha^2}}}{E^2+\frac{1}{\Lambda}}\\ &= -\frac{\sqrt{E^2+\frac{45}{8\alpha^2}}}{E} \text{ or } -\frac{E}{\sqrt{E^2+\frac{45}{8\alpha^2}}} \text{ (depending on the polarization).}\end{aligned} \tag{B.10}$$

Both polarization states travel inwards towards the axis if $E > 0$; outwards to $r = \infty$ if $E < 0$. Note that this is consistent with Conjecture 2. We also note that, at infinity, the coordinate speeds of the two polarization states are reciprocal to one another and one polarization state propagates superluminally.

□

In branch III, the absolute value $|B|$ is an decreasing function of r; at $r = 0$ we have $|B| \to \infty$, and as $r \to \infty$, we have $|B| \to \sqrt{3}B_s$. At $r = \infty$, the effective geometry corresponding to branch III is similar the effective geometry of branch II.

Index